CONTENTS

NASA Technical Paper 1761

Mechanical Property Characterization of Borsic®/Aluminum Laminates at Room and Elevated Temperatures

Robert R. McWithey and Dick M. Royster

DECEMBER 1980

NASA

NASA Technical Paper 1761

Mechanical Property Characterization of Borsic®/Aluminum Laminates at Room and Elevated Temperatures

Robert R. McWithey and Dick M. Royster
Langley Research Center
Hampton, Virginia

National Aeronautics
and Space Administration

**Scientific and Technical
Information Branch**

1980

BLANK PAGE

BLANK PAGE

CONTENTS

SUMMARY

Six Borsic[1]/aluminum laminate orientations ($[0_6]_T$, $[90_6]_T$, $[(\pm45)_2]_S$, $[90/0/90/0]_S$, $[0/\pm45]_S$, and $[0_2/\pm45]_S$) exposed to a braze-temperature cycle were tested in tension, compression, and shear to determine stress and tangent modulus as a function of strain, maximum stress and strain, and Poisson's ratio of the laminates at room temperature, 505 K (450°F), and at an intermediate temperature of either 422 K (300°F) or 450 K (350°F). Mechanical properties in tension were determined from flat-tensile and sandwich-beam tests. Room-temperature flat-tensile tests were performed on laminates in the "as-received" condition to provide a comparison with results from specimens exposed to a braze-temperature cycle. Sandwich-beam tests were also used to determine mechanical properties in compression. Shear properties were determined from biaxially loaded, picture-frame shear specimens. The test apparatus and procedures are described and stress and tangent modulus are presented as a function of strain by using either the Ramberg-Osgood equation or a bimodular equation developed in the report. Maximum stress and strain and Poisson's ratio are presented in tables for each of the laminates.

INTRODUCTION

Recent studies (refs. 1 to 7) for supersonic-cruise vehicles demonstrated the feasibility of fabricating low-mass structural panels from diffusion-bonded 6061 aluminum alloy reinforced with silicon-carbide-coated boron filaments (Borsic/aluminum laminated composite material denoted hereinafter as Bsc/Al). Following evaluation of several joining methods (ref. 2), brazing was selected as the process with the greatest potential for fabricating efficient complex structures from Bsc/Al. Full-scale structural panels with Bsc/Al skins brazed to titanium honeycomb core were successfully designed, fabricated, and tested to meet the requirements of an upper wing panel for the NASA YF-12 airplane (refs. 3 and 7).

The material-property data used in references 1 to 7 were obtained from reference 8 or from limited data (usually one type of loading of a specific laminate) obtained during the referenced studies. Also, a literature survey has indicated that there is insufficient material-property data available for Bsc/Al laminates subjected to a braze-temperature cycle. Therefore, the present study was initiated to obtain material-property data on Bsc/Al laminates at room and elevated temperature after being subjected to a braze-temperature cycle, and to provide the type of data normally required for the design of statically loaded structures. Six Bsc/Al laminate orientations were tested by loading them to failure in tension, compression, or shear to determine tangent modulus, maximum stress and strain, and Poisson's ratio. Tensile properties were determined from flat-tensile specimens and sandwich-

---

[1]Borsic: registered trade name of United Aircraft Products, Inc.

beam specimens of the type described in reference 9. Compression properties were also determined from sandwich-beam specimens, and shear properties were determined from biaxially loaded, picture-frame specimens of the type described in reference 10. A test matrix is presented in table I that shows the Bsc/Al laminates evaluated, test temperatures, types of tests, and the number of specimens tested. In this report the specimens and techniques used are described, and the data are presented both by curves indicating stress and tangent modulus as a function of strain and by tables indicating Poisson's ratio, maximum stress, and strain.

Use of trade names or manufacturers in this report does not constitute an official endorsement of such products or manufacturers, either expressed or implied, by the National Aeronautics and Space Administration.

SYMBOLS

Measurements and calculations were made in the U.S. Customary Units. They are presented herein in the International System of Units (SI) with the equivalent values given parenthetically in the U.S. Customary Units.

A,B,N	constants in Ramberg-Osgood equation (see eq. (1))
C	constant in bimodular stress-strain equation (see eq. (2a))
E	tangent modulus in tension and compression
G	tangent modulus in shear
T	temperature
γ	shear strain
ε	normal strain
$\Delta\varepsilon$	strain over transition region defined in figure 8
ε_0	strain defined in figure 8
ε_1	strain defined in equation (2b)
μ	Poisson's ratio
σ	normal stress
τ	shear stress

Subscripts:

max	maximum

min minimum

o initial

Notation for laminate orientation:

The cross-ply angles are listed in the order of layup, separated by a slash, with the entire listing enclosed within brackets. Where there is more than one consecutive lamina at any given angle, the number of laminae at that angle is denoted by a numerical subscript within the brackets. Subscript S outside the brackets denotes symmetric; for example, $[0/\pm45]_S$ means [0/+45/-45/-45/+45/0]. Subscript T outside the brackets denotes total; for example, $[0_6]_T$ means [0/0/0/0/0/0/].

LAMINATE FABRICATION

The Bsc/Al composite sheet material was consolidated from 0.1422-mm (0.0056-in.) diameter boron fibers coated with 12.7-μm (0.0005-in.) thick silicon carbide and imbedded in a 6061 aluminum-alloy matrix. Both six- and eight-ply sheet material were consolidated by diffusion bonding at 800 K (980°F) and 28.0 MPa (4000 psi) pressure with the thickness of each ply being nominally 0.19 mm (0.0075 in.). The fiber orientation of each ply in the consolidated sheets was such that the plies were balanced and symmetrical about the center line of the sheet. Six different ply orientations were investigated and are identified in table II by ply orientation, number of plies, and the percent of fiber volume in the laminate. Note that some of the sheets have 0.127-mm (0.005-in.) thick 1100 aluminum-alloy diffusion bonded to one surface. It was shown in reference 3 that the 1100 Al surface prevents silicon from diffusing out of the braze alloy into the matrix which can cause degradation of both the matrix and fiber following brazing. The fiber-volume fractions of the laminates are lower than the optimum 48-percent fiber-volume fraction because of the aluminum-rich outer surfaces. All sheets in this investigation were consolidated by the same material supplier, Amercom, Inc.

CONFIGURATION AND FABRICATION OF TEST SPECIMENS

Flat-Tensile Specimens

The configuration of the flat-tensile specimen is shown in figure 1. The specimens were cut from the Bsc/Al sheet material by using a diamond-impregnated circular-saw blade and a feed rate of approximately 12.7 mm/min (0.5 in/min). Fiber-glass tabs were bonded to the ends of the specimens for gripping during the tests.

Sandwich-Beam Specimens

The configuration of the sandwich-beam test specimen is shown in figure 2. The test specimens were composed of a Bsc/Al composite test face sheet, a face sheet of 0.318-cm (0.125-in.) thick Ti-6Al-4V titanium alloy, and a vented

honeycomb core of Ti-3Al-2.5V titanium alloy. The core was composed of honeycomb of two different densities. The higher density core was used on the ends of the test specimen to provide shear stiffness, and the lower density core in the center test section was used to minimize the load carried by the core and thus minimize its contribution to measured face-sheet properties.

The test beams were fabricated by splicing the lower density core to the higher density core by spotwelding adjacent cell walls together. Core sizes were prepared so that either three or four test beams could be machined from one sheet of spliced material. The Ti-6Al-4V skin (sheared to the same width and length as the core), a spliced honeycomb sheet, and a 0.51-mm (0.020-in.) thick sheet of 3004 aluminum braze alloy were chemically cleaned and subsequently assembled on a fixture for brazing. The assembly was placed in a vacuum furnace which was evacuated to 1.33 mPa (1×10^{-5} torr) and heated to 908 K (1175°F). After the temperature stabilized, the assembly was heated to 950 K (1250°F) and held 5 minutes to melt the braze alloy. The furnace was then cooled to room temperature, the assembly was removed, and the honeycomb core was recleaned by vapor degreasing. A sheet of Bsc/Al was then chemically cleaned by using the procedures given in reference 2. The Bsc/Al sheet was stacked on the brazing fixture along with a 0.25-mm (0.010-in.) thick sheet of 718 aluminum braze alloy and the honeycomb-core titanium face-sheet assembly. The 1100 Al surface of the Bsc/Al sheet was adjacent to the braze alloy.

The stacked assembly was placed in the vacuum furnace, which was evacuated to 1.33 mPa (1×10^{-5} torr) and heated to 839 K (1050°F). After the temperature stabilized, the brazing furnace was quickly heated (in approximately 10 minutes) to 861 K (1090°F) and held for 5 minutes to melt the braze alloy. The assembly was then cooled rapidly (in approximately 10 minutes) to 839 K (1050°F) and then allowed to cool naturally to room temperature in the furnace. After the panel was brazed, individual test specimens 54.6 cm (21.5 in.) long and 2.54 cm (1.00 in.) wide were electrical-discharge machined from the panel and then dried, measured, and instrumented for testing.

Picture-Frame Shear Specimens

A sketch of the picture-frame shear specimen is shown in figure 3. The test specimens were sandwich panels consisting of two identical Bsc/Al cover sheets and an aluminum honeycomb core having a 5 mm (0.187 in.) cell size and a density of 128 kg/m^3 (8 lbm/ft^3). The cover sheets were fabricated by shearing the Bsc/Al sheets to size (22.86 cm (9.00 in.) square) and then by electrical-discharge machining the corner cutouts and holes along the perimeter. The holes were machined oversize so that the load would be introduced through the steel doublers and blocks. (See fig. 3.) After machining, the sheets were subjected to a temperature cycle to simulate a brazing operation. The temperature cycle was similar to that for the stacked sandwich-beam assembly and consisted of raising the sheet temperature to 839 K (1050°F) and allowing the temperature to stabilize. The sheet temperature was then rapidly raised to 866 K (1100°F) in the vacuum furnace and maintained for 10 minutes. Then, the sheet was rapidly cooled to 839 K (1050°F), and the furnace was cooled to room temperature.

The specimens were assembled by first bonding the steel blocks to the periphery of the honeycomb material. The surfaces of the blocks to be bonded to cover sheets were ground flat and parallel. The cover sheets were then bonded simultaneously to the core, steel blocks, and steel doublers at the locations shown in figure 3. Titanium corner doublers were bonded into diagonally opposite corners of the specimen to reduce local stress concentrations induced during loading. The 9602 adhesive material was used for the room-temperature specimens, and FM-34 was used for the elevated temperature specimens. The outside surfaces of the steel doublers were ground flat and parallel, and the doublers and steel blocks were drilled for attaching to the load fixture.

TEST APPARATUS AND INSTRUMENTATION

Flat-Tensile Tests

The tensile tests were conducted in a 445 kN (100 kip) hydraulic tensile test machine using templin-type grips. For the elevated-temperature tests, heat was applied to the specimen by using electric-resistance heaters and an open-ended tube furnace surrounding the specimen. The ends of the specimen protruded from the furnace for easy insertion into the grips of the testing machine. Flexible insulation was used to seal the ends of the furnace.

Room-temperature specimens were instrumented with two room-temperature strain gages mounted back to back at the center of the specimen to measure longitudinal strain. Load and strain were recorded during each test by using an X-Y recorder.

Elevated-temperature specimens were instrumented with six strain gages mounted to form two back-to-back 45° rosettes as shown in figure 1. Each strain gage was an element of a single-active-arm three-wire bridge circuit. All bridges were powered by a constant-voltage power supply, and strains were measured by using the unbalanced bridge method. Voltages from all bridge circuits were recorded on magnetic tape at regular intervals during the test. In addition, iron-constantan thermocouples (hereinafter denoted as type J thermocouples) were adhesive-bonded to the specimens near the gages to monitor specimen temperature.

Sandwich-Beam Tests

The test apparatus consisted of a hydraulic tensile test machine for room-temperature tests and an Instron test machine for elevated-temperature tests, an air-circulating oven, and a four-point loading frame. The loading frame, which is shown in figure 4 connected to the hydraulic test machine, is supported by the upper machine head. The loading frame was fabricated from high-strength steel and was designed to be several orders of magnitude stiffer than the test specimens and to maintain a constant stress in the test section. In addition, it was designed to keep the distance between load points fixed and to keep the force resultants at each load point parallel. The load-bearing surface at each loading point included the widths of the beam and was 2.03 cm (0.80 in.) wide.

A maximum beam deflection of 3.0 cm (1.2 in.) may be obtained by using this loading frame.

For elevated-temperature tests, an oven was positioned between the test-machine columns. The oven totally encloses the loading apparatus as shown in figure 5. Ports in the top and bottom of the oven allowed direct connection between the loading frame and the test machine.

Specimen instrumentation consisted of room- or elevated-temperature strain gages located near the center of each beam and oriented longitudinally and transversely to the beam axis as shown in figure 2. Strains were measured in a manner similar to that for the elevated-temperature flat-tensile tests. The applied load was measured electronically by using the test-machine load cell. Two type J thermocouples were spotwelded to the titanium face sheet to monitor the specimen temperature. Temperatures were measured by using an ice bath as the cold-junction reference temperature. Measurements were recorded on magnetic tape at regular intervals during the test.

Picture-Frame Shear Tests

The test apparatus consisted of a 445 kN (100 kip) hydraulic tensile test machine, a hydraulic cylinder with a load cell, and a loading apparatus. The specimen was loaded biaxially with the tensile load component applied vertically by using the hydraulic test machine, and with the compressive load component applied horizontally by using the hydraulic cylinder as shown in figure 6. The tensile and compressive loads were measured independently by load cells. For tests at elevated temperatures, a quartz-lamp radiator was installed on each side of the test specimen as shown in figure 7. For uniform temperatures and faster heating, the steel blocks on the elevated-temperature specimens were extended in width to allow for a 9.5-mm (0.375-in.) diameter hole to be drilled through the length of each block and cartridge heating elements inserted and energized during the test. Power to the quartz lamps and cartridge heaters was controlled separately.

The picture-frame shear specimens were instrumented as recommended in reference 10 and as shown in figure 3. Rosette-type strain gages were used to measure strain. Three type J thermocouples were used (see fig. 3) to monitor and control the temperature. Strain-load measurements were recorded on magnetic tape at regular intervals during the test, and temperatures were recorded on a 12-channel recorder.

TEST PROCEDURE

Prior to elevated-temperature tests, temperature surveys were made on each type of specimen with the appropriate heating apparatus to determine the power settings and times required to attain a nearly uniform temperature distribution over the test region. These heating conditions were subsequently used during the mechanical property tests in which temperatures were monitored at only one or two locations on the specimen.

For all tests except the room-temperature Bsc/Al flat-tensile tests, voltages from load transducers were recorded and regression analyses were used to obtain first- and second-order polynomial relations between load and voltage. These relations were programmed into the data-acquisition system along with specimen dimensions to convert load transducer output voltage into stress during a test. Maximum applied loads were obtained from load indicators on the testing machines. In addition, prior to a test all strain-gage bridge circuits were balanced at the test temperature. During a test, bridge voltage outputs were converted to strain by the data-acquisition system using the linear bridge equation. Gage factors at the test temperatures were obtained from the manufacturer's data sheets. The bridge voltage in all tests was 6 volts. For the sandwich-beam tests, strain-gage data were corrected for the effects of transverse strain on the gage. The magnitude of this correction was less than 1 percent of the strain reading of the gage.

Flat-Tensile Tests

Room-temperature tensile tests were made by using a testing-machine crosshead speed of 1.27 mm/min (0.05 in/min). Load and strain were recorded during the test by using an X-Y recorder and were subsequently converted to digital form and stored on magnetic tape.

For the elevated-temperature tensile tests, the test procedure typically consisted of clamping the specimen in the upper grips of the testing machine, positioning the furnace around the specimen, and heating the specimen to the desired temperature. Approximately 30 minutes were required to reach a test temperature of 505 K (450°F) with an additional 20 minutes required for the specimen temperature to stabilize. The lower grips were attached to the specimen after the specimen reached the test temperature. The various laminates were loaded to failure at the load rates specified in table III(a).

Sandwich-Beam Tests

Sandwich-beam tension and compression tests were made at room temperature and elevated temperature by using the initial testing-machine crosshead speeds shown in table III(b). The lower crosshead speeds allowed examination of the mechanical properties at low strain values. Crosshead speeds were increased up to 2.5 mm/min (0.1 in/min) during the test for laminates exhibiting plasticity. In all tests, loading continued until the composite failed or excessive deformation was present in the beam. Data obtained from each test included strain from the four strain gages and the applied load.

For the elevated temperature tests, a specimen instrumented with seven thermocouples was placed in the loading frame and heated in the oven to determine the temperature variation in the specimen. The temperature distribution was uniform over the beams within ±1 K (±2°F) with a heat-up time from room temperature to 505 K (450°F) of approximately 60 minutes. During a test the temperature was monitored on the titanium flange near the center and near one end of the beam.

Picture-Frame Shear Tests

The tensile and compressive load components were applied equally and simultaneously to apply shear load to the picture-frame specimen. Outputs from the load cells were recorded electronically along with the output from the strain gages. During specimen loading, load and strain were recorded by a multichannel recording system at intervals of once every 5 seconds until nonlinear behavior was observed in the load-strain data, and thereafter once every 2 seconds to specimen failure. The strain output from eight strain gages was monitored during the test to observe specimen response to load.

The testing sequence entails balancing the strain gages, loading the specimen to 4.45 kN (1000 lbf), zeroing the gages, and then proceeding to load the specimen to failure at a rate of 44.5 kN/min (10 000 lbf/min). Elevated-temperature tests were conducted at 450 K (350°F) and 505 K (450°F). The test sequence for the elevated-temperature tests involved heating the specimen to the test temperature and holding it for 20 minutes to allow the temperature to stabilize; then, the strain gages were balanced and the specimen was loaded to failure.

DATA ANALYSIS

Nonlinear stress-strain behavior was exhibited by each of the Bsc/Al laminates, and analytical expressions relating this behavior were obtained for each set of replicate tests to provide the structural analyst with a convenient method for relating stress and strain. Polynomial equations were obtained by using polynomial regression analyses and stress-strain data from replicate tests. This method was unsuitable, however, because waviness in the higher order polynomial curves did not satisfactorily represent actual material behavior. Attempts were made to define a Ramberg-Osgood equation of the form

$$\varepsilon = A\sigma + B\sigma^N \tag{1}$$

for each set of replicate tests by using a least-squares technique. This technique was successful for all laminates except those exhibiting a bimodular stress-strain behavior. (See fig. 8.) For these laminates the bimodular equation

$$\sigma = \left(\frac{E_{max} + E_{min}}{2}\right)\varepsilon - \left(\frac{E_{max} - E_{min}}{2C}\right) \ln\left[\frac{\cosh C(\varepsilon_1 - \varepsilon)}{\cosh C\varepsilon_1}\right] \tag{2a}$$

where

$$\varepsilon_1 = \varepsilon_0 + \frac{\Delta\varepsilon}{2} \tag{2b}$$

was derived and used successfully to relate the stress-strain response of the bimodular laminates. The constants E_{max}, E_{min}, ε_0, and $\Delta\varepsilon$ in equations (2a) and (2b) are graphically defined in figure 8 and were determined from plots of the stress-strain and tangent-modulus-strain data. The constant C in equation (2a) determines the width of the transition region (shown in fig. 8) in the stress-strain curve and was determined by selecting the value of C, by inspection, that best represented the stress-strain data in the transition region. The resulting Ramberg-Osgood and bimodular stress-strain curves are presented subsequently for the room-temperature and 505 K (450°F) tests of the six Bsc/Al laminates along with tangent modulus-strain curves that were obtained by differentiating the stress-strain equations. The constants defining each stress-strain curve are given in the corresponding figure in U.S. units (psi). A typical comparison between a replicate set of stress-strain data used in the analysis and the resulting Ramberg-Osgood equation is shown in figure 9(a) for the $[90_6]_T$ laminate in compression. A similar comparison with the bimodular equation is shown in figure 9(b) for the $[0/\pm45]_S$ laminate in compression.

TEST RESULTS

Test results are presented for stress, strain, tangent modulus, and Poisson's ratio. Tests were conducted at room temperature, 505 K (450°F), and at an intermediate temperature of either 422 K (300°F) or 450 K (350°F). Stress-strain data are shown for the room-temperature and 505 K (450°F) tests. Stress-strain data for the intermediate temperatures are not shown because they are similar to the room-temperature tests results.

Flat-Tensile Tests

Stress and tangent modulus as a function of strain for the six laminate orientations tested at room temperature are shown in figure 10. Specimens for each laminate were tested both in the "as-received" condition and after undergoing a temperature cycle typical of the cycle required for a brazing operation in panel fabrication to determine the effects of the braze-temperature cycle on tensile properties. The data in figure 10 indicate a nonlinear relation between stress and strain for longitudinal strains less than approximately 0.002 for all laminates. By using tables IV and V a comparison can be made of values of tangent modulus at zero and 0.002 strain and of values of maximum stress and strain between specimens tested after exposure to the braze-temperature cycle and in the "as-received" condition for each laminate. The data in tables IV and V indicate that the braze-temperature cycle had little effect on the $[0_6]_T$,

$[(\pm 45)_2]_S$, and $[0/\pm 45]_S$ laminates; decreased the maximum stress by 19 percent and the maximum strain by at least 20 percent in the $[90_6]_T$ laminate; increased the tangent modulus (at $\varepsilon = 0.002$) by 28 percent in the $[90/0/90/0]_S$ laminate; and increased the maximum stress in the $[90/0/90/0]_S$ laminate by 21 percent.

Stress-strain curves and corresponding tangent-modulus-strain curves for the six laminate orientations tested at 505 K (450°F) are shown in figure 11. The data indicate a nonlinear relation between stress and strain below a longitudinal strain of 0.002 similar to that at room temperature for all laminates except the $[0_6]_T$ laminate in which the modulus decreases at a nearly constant rate with strain. Comparisons of maximum stress and strain values at room temperature, 422 K (300°F), and 505 K (450°F) for these laminate orientations can be made from tables V and VI. The largest changes in maximum stresses between room temperature and 422 K (300°F) are a 14-percent increase in the maximum stresses of the $[90_6]_T$ and $[0_2/\pm 45]_S$ laminates. At 505 K (450°F), however, the $[90_6]_T$ laminate data indicate a 29-percent decrease in maximum stress from the value at room temperature. The values of maximum stress are shown graphically in figure 12 as a function of temperature. Large reductions in maximum strain (48 percent at 505 K (450°F)) are also indicated for the $[90_6]_T$ laminate with increasing temperature. The maximum strain in the $[0_2/\pm 45]_S$ laminate increases with increasing temperature (15 percent at 422 K (300°F) and 19 percent at 505 K (450°F)). Significantly lower tangent-modulus values (at $\varepsilon = 0.002$) were observed for all laminates except the $[0_6]_T$ laminate at 505 K (450°F). This may be caused by matrix degradation at elevated temperatures. Slight changes in Poisson's ratio are also apparent between 422 K (300°F) and 505 K (450°F) for the $[0/\pm 45]_S$ and $[0_2/\pm 45]_S$ laminates as shown in table VI. The angle between the loading axis and the principal strain axis, as determined from the gage rosette data taken at elevated temperature, was usually less than 3°.

Sandwich-Beam Tensile Tests

Room-temperature and elevated-temperature stress-strain curves and corresponding tangent-modulus-strain curves for the six laminate orientations tested are shown in figure 13. For all laminates except the $[0_6]_T$ laminate, the data indicate a nonlinear relation similar to that from the flat-tensile tests below a longitudinal strain of 0.002. Failure of the sandwich beams for the tensile tests always occurred in the composite within the test section. A summary of the tensile properties from sandwich-beam tests is given in table VII.

A comparison of room-temperature properties from flat-tensile tests (table V) with the properties from sandwich-beam tests (table VII) indicates different results for the $[90_6]_T$, $[(\pm 45)_2]_S$, and $[0/\pm 45]_S$ laminates. The results from the sandwich-beam tests for the $[90_6]_T$ laminate indicate that the tangent modulus at a strain of 0.002 increased 50 percent and the maximum stress increased 46 percent above the values obtained in the flat-tensile tests. A similar comparison for the $[0/\pm 45]_S$ laminate indicates decreases of 13 percent in maximum stress and 17 percent in maximum-strain values obtained from the sandwich-beam tests.

A comparison of room-temperature and elevated-temperature results from table VII indicates that elevated temperature had little effect on mechanical properties of the $[0_6]_T$ laminate, but the maximum stress and strain of the $[90_6]_T$ laminate were significantly degraded at an elevated temperature. In addition, the maximum stress and strain in the $[0/\pm45]_S$ laminate increased at elevated temperature. Slight changes in Poisson's ratios are also apparent between room temperature and elevated temperatures for all laminates except the $[90/0/90/0]_S$ laminate.

Comparisons of Poisson's ratios at elevated temperature from flat-tensile tests (table VI) and from table VII for each of the laminates indicate that higher values of Poisson's ratios were obtained during the flat-tensile tests. In addition, similar comparisons of the maximum stress and strain values for the $[90_6]_T$ laminate indicate a higher maximum stress, but lower maximum strain was obtained for this laminate in the sandwich-beam tests at 505 K (450°F). This occurs because higher strain rates were used for the $[90_6]_T$ laminate sandwich-beam tests at 505 K (450°F) than were used in the flat-tensile tests and, at elevated temperature, the strengths of aluminum alloys increase with an increase in strain rate. A graph of maximum-stress data as a function of temperature from the sandwich-beam tests is shown in figure 14.

The present results for the $[0_6]_T$ and $[(\pm45)_2]_S$ Bsc/Al laminates at room temperature are compared in figure 15 with similar results given in reference 11 for boron/aluminum. Figure 15 indicates that the $[0_6]_T$ boron/aluminum laminate is stronger and stiffer than the $[0_6]_T$ Bsc/Al laminate, and the $[(\pm45)_2]_S$ boron/aluminum laminate has a higher initial modulus and higher strength than the $[(\pm45)_2]_S$ Bsc/Al laminate.

Sandwich-Beam Compression Tests

Room-temperature and elevated-temperature stress-strain curves and corresponding tangent-modulus-strain curves for the six laminate orientations tested are shown in figure 16. A summary of the laminate mechanical properties from the sandwich-beam compression tests is given in table VIII. For most of the laminates the data indicate a nonlinear relation between stress and strain below a longitudinal strain of 0.002 which is similar to that for the tensile tests. Initial values of Poisson's ratio obtained from both tensile and compression sandwich-beam tests were nearly equal for a given laminate.

In all compression tests except those involving the $[(\pm45)_2]_S$ and $[90_6]_T$ laminates, beam failure occurred by fracture in the Bsc/Al face sheet either under or adjacent to one of the inner loading pads. The $[(\pm45)_2]_S$ Bsc/Al face sheets did not fracture and these tests were terminated when the center deflection of the beam reached 3.0 cm (1.2 in.) (the maximum deflection allowed by the loading apparatus). Failures in the $[90_6]_T$ Bsc/Al face sheets occurred in the test section between the inner loading points of the beam. Thus, the maximum compressive stress and strain data presented for all laminates except the $[90_6]_T$ laminate may be conservative.

Picture-Frame Shear Tests

Shear stress and tangent-shear modulus as a function of strain from the picture-frame tests at room temperature and 505 K (450°F) are shown in figure 17. A summary of the test results is given in table IX. The data in table IX indicate that short-term exposure to elevated temperature has little effect on the maximum stress and strain of the $[(\pm 45)_2]_S$ laminate. However, there is a deleterious effect on most of the mechanical properties of the remaining laminates, with the most severe effect occurring in the $[0_6]_T$ and $[90/0/90/0]_S$ laminates. The maximum shear stress was reduced 18 percent in the $[0_2/\pm 45]_S$ laminate, approximately 30 percent in the $[0/\pm 45]_S$ laminate, 40 percent in the $[0_6]_T$ laminate, and 46 percent in the $[90/0/90/0]_S$ laminate. Curves of maximum shear stress as a function of temperature are shown in figure 18.

CONCLUSIONS

Room- and elevated-temperature material properties were determined for six Borsic/aluminum (Bsc/Al) laminates after the laminates were subjected to a braze-temperature cycle. The material-property data are presented in tables and in figures indicating stress and tangent modulus as a function of strain. The following conclusions are presented:

1. Each of the six Bsc/Al laminates tested in tension, compression, and shear showed some degree of nonlinear behavior in stress as a function of strain. As expected, this nonlinearity was the least in the $[0_6]_T$ laminate in tension and compression and in the $[(\pm 45)_2]_S$ laminate in shear, and it was most apparent during initial loading (where normal strain was less than 0.002).

2. The braze-temperature cycle decreased the room-temperature tensile maximum stress and maximum strain in the $[90_6]_T$ laminate and increased the tangent modulus and maximum stress in the $[90/0/90/0]_S$ laminate. No significant changes due to the braze-temperature cycle appeared in the tensile mechanical properties of the remaining laminates.

3. The tensile properties of the $[90_6]_T$ laminate were significantly degraded at 505 K (450°F), and the maximum strains in the $[0/\pm 45]_S$ and $[0_2/\pm 45]_S$ laminates increased over their room-temperature values.

4. At elevated temperatures, higher values of Poisson's ratio were obtained from flat-tensile tests than from sandwich-beam tests in tension.

5. Short-term exposure at 505 K (450°F) reduced the shear modulus and maximum shear stress in all laminates except the $[(\pm 45)_2]_S$ laminate. The shear properties of the $[(\pm 45)_2]_S$ laminate were only slightly affected by elevated temperature.

6. Initial values of Poisson's ratio obtained from both tensile and compression sandwich-beam tests were nearly equal for a given laminate.

Langley Research Center
National Aeronautics and Space Administration
Hampton, VA 23665
December 4, 1980

REFERENCES

1. McWithey, Robert R.: Analytical Structural Efficiency Studies of Borsic/Aluminum Compression Panels. NASA TN D-8333, 1976.

2. Royster, Dick M.; Wiant, H. Ross; and McWithey, Robert R.: Effects of Fabrication and Joining Processes on Compressive Strength of Boron/Aluminum and Borsic/Aluminum Structural Panels. NASA TP-1121, 1978.

3. Bales, Thomas T.; Wiant, H. Ross; and Royster, Dick M.: Brazed Borsic/Aluminum Structural Panels. NASA TM X-3432, 1977.

4. Royster, Dick M.; McWithey, Robert R.; and Bales, Thomas T.: Fabrication and Evaluation of Brazed Titanium-Clad Borsic®/Aluminum Compression Panels. NASA TP-1573, 1980.

5. McWithey, Robert R.; Royster, Dick M.; and Ko, William L.: Compression Panel Studies for Supersonic Cruise Vehicles. NASA TP-1617, 1980.

6. Bales, Thomas T.; Hoffman, Edward L.; Payne, Lee; and Reardon, Lawrence F.: Fabrication Development and Evaluation of Advanced Titanium and Composite Structural Panels. NASA TP-1616, 1980.

7. Bales, Thomas T.; Royster, Dick M.; and McWithey, Robert R.: Fabrication and Evaluation of Brazed Titanium-Clad Borsic®/Aluminum Skin-Stringer Panels. NASA TP-1674, 1980.

8. Kreider, Kenneth G., ed.: Metallic Matrix Composites. Academic Press, Inc., c.1974.

9. Hofer, K. E., Jr.; and Rao, P. N.: A New Static Compression Fixture for Advanced Composite Materials. J. Test. & Eval., vol. 5, no. 4, July 1977, pp. 278-283.

10. Bush, Harold G.; and Weller, Tanchum: A Biaxial Method for Inplane Shear Testing. NASA TM-74070, 1978.

11. Sova, J. A.; and Poe, C. C., Jr.: Tensile Stress-Strain Behavior of Boron/Aluminum Laminates. NASA TP-1117, 1978.

TABLE I.- Bsc/Al TEST MATRIX INDICATING THE NUMBER OF SPECIMENS TESTED

(a) Flat-tensile tests

Laminate orientation	Temperature for condition -			
	As received	After exposure to a braze heating cycle		
	Room temperature	Room temperature	422K (300°F)	505 K (450°F)
$[0_6]_T$	3	3	5	4
$[90_6]_T$	3	3	4	5
$[(\pm45)_2]_S$	3	2	3	3
$[90/0/90/0]_S$	3	3	3	2
$[0/\pm45]_S$	3	3	3	3
$[0_2/\pm45]_S$	---	3	4	3

(b) Sandwich-beam tests and picture-frame shear tests

Laminate orientation	Temperature		
	Room temperature	450K (350°F)	505 K (450°F)
Sandwich-beam tensile tests			
$[0_6]_T$	3	4	3
$[90_6]_T$	3	4	3
$[(\pm45)_2]_S$	4	4	4
$[90/0/90/0]_S$	3	4	4
$[0/\pm45]_S$	4	4	4
$[0_2/\pm45]_S$	1	3	1
Sandwich-beam compression tests			
$[0_6]_T$	3	3	3
$[90_6]_T$	3	4	3
$[(\pm45)_2]_S$	4	4	3
$[90/0/90/0]_S$	3	3	3
$[0/\pm45]_S$	3	4	4
$[0_2/\pm45]_S$	2	3	1
Picture-frame shear tests			
$[0_6]_T$	2	3	3
$[(\pm45)_2]_S$	2	1	1
$[90/0/90/0]_S$	2	2	2
$[0/\pm45]_S$	2	2	1
$[0_2/\pm45]_S$	3	---	1

TABLE II.- BORSIC/ALUMINUM LAMINATES TESTED

Ply orientation, deg	Fiber-volume fraction, percent
Outer surfaces: 0.127-mm (0.005-in.) 1100 Al; 0.090-mm (0.0035-in.) 6061 Al	
$[0_6]_T$	39.1
$[90_6]_T$	40.9
$[(45\pm)_2]_S$	41.6
$[90/0/90/0]_S$	40.5
$[0/\pm45]_S$	40.0
$[0_2/\pm45]_S$	41.3
Outer surfaces: 0.090-mm (0.0035-in.) 6061 Al on both surfaces	
$[0/\pm45]_S$	41.8
$[90_6]_T$	42.4

TABLE III.- LOADING RATES AND INITIAL CROSSHEAD SPEEDS USED IN TESTS

(a) Loading rates used in elevated temperature flat-tensile tests

Laminate orientation	Loading rate, kN/min (lbf/min)
$[0_6]_T$	4.45 (1000)
$[90_6]_T$	.89 (200)
$[(\pm45)_2]_S$	1.11 (250)
$[90/0/90/0]_S$	2.67 (600)
$[0/\pm45]_S$	2.22 (500)
$[0_2/\pm45]_S$	1.78 (400)

(b) Initial testing-machine crosshead rates used in sandwich-beam tests

Laminate orientation	Crosshead rate mm/min (in/min), at -	
	Room temperature	505 K (450°F)
$[0_6]_T$	1.27 (0.05)	1.27 (0.05)
$[90_6]_T$	.51 (.02)	1.27 (.05)
$[(\pm45)_2]_S$	.51 (.02)	.51 (.02)
$[90/0/90/0]_S$	1.27 (.05)	1.27 (.05)
$[0/\pm45]_S$	1.27 (.05)	1.27 (.05)
$[0_2/\pm45]_S$	1.27 (.05)	1.27 (.05)

TABLE IV.- SUMMARY OF DATA FROM FLAT-TENSILE TESTS AT ROOM TEMPERATURE ON Bsc/Al IN THE "AS-RECEIVED" CONDITION

Laminate orientation	E at $\varepsilon = 0$, GPa (psi) (a)	E at $\varepsilon = 0.002$, GPa (psi) (a)	σ_{max}, MPa (ksi) (b)	ε_{max} (b)
$[0_6]_T$	225 (32.6×10^6)	193 (28.0×10^6)	1131 (164)	0.0057
$[90_6]_T$	157 (22.8×10^6)	11.9 (1.72×10^6)	145 (21.0)	>.010
$[(\pm 45)_2]_S$	114 (16.5×10^6)	11.3 (1.64×10^6)	174 (25.3)	>.020
$[90/0/90/0]_S$	153 (22.1×10^6)	68.3 (9.90×10^6)	452 (65.6)	.0061
$[0/\pm 45]_S$	151 (21.9×10^6)	71.0 (10.3×10^6)	478 (69.3)	>.0060

[a]From stress-strain equation.
[b]Average from replicate tests.

TABLE V.- SUMMARY OF Bsc/Al DATA FROM FLAT-TENSILE TESTS AT ROOM TEMPERATURE AFTER EXPOSURE TO A BRAZE-TEMPERATURE CYCLE

Laminate orientation	E at $\varepsilon = 0$, GPa (psi) (a)	E at $\varepsilon = 0.002$, GPa (psi) (a)	σ_{max}, MPa (ksi) (b)	ε_{max} (b)
$[0_6]_T$	209 (30.3×10^6)	187 (27.1×10^6)	1110 (161)	0.0060
$[90_6]_T$	159 (23.0×10^6)	10.3 (1.50×10^6)	119 (17.2)	.008
$[(\pm 45)_2]_S$	118 (17.1×10^6)	9.9 (1.43×10^6)	177 (25.6)	>.010
$[90/0/90/0]_S$	135 (19.5×10^6)	87 (12.6×10^6)	547 (79.4)	.0062
$[0/\pm 45]_S$	131 (19.0×10^6)	72 (10.5×10^6)	452 (65.6)	.0059
$[0_2/\pm 45]_S$	150 (21.8×10^6)	102 (14.8×10^6)	557 (80.8)	.0053

[a]From stress-strain equation.
[b]Average from replicate tests.

TABLE VI.- SUMMARY OF Bsc/Al DATA FROM FLAT-TENSILE TESTS AT ELEVATED TEMPERATURES AFTER EXPOSURE TO A BRAZE-TEMPERATURE CYCLE

(a) Mechanical properties at 422 K (300°F)

Laminate orientation	σ_{max}, MPa (ksi) (a)	ε_{max} (a)	μ_o (a)
$[0_6]_T$	1103 (160)	0.0060	0.27
$[90_6]_T$	135 (19.6)	.0055	.17
$[(\pm45)_2]_S$	182 (26.4)	.0190	.45
$[90/0/90/0]_S$	547 (79.3)	.0057	.18
$[0/\pm45]_S$	463 (67.2)	.0058	.33
$[0_2/\pm45]_S$	636 (92.2)	.0061	.32

(b) Mechanical properties at 505 K (450°F)

Laminate orientation	E at $\varepsilon = 0$, GPa (psi) (b)	E at $\varepsilon = 0.002$, GPa (psi) (b)	σ_{max}, MPa (ksi) (a)	ε_{max} (a)	μ_o (a)
$[0_6]_T$	199 (28.8 × 10^6)	179 (26.0 × 10^6)	1055 (153)	0.0061	0.28
$[90_6]_T$	81 (11.7 × 10^6)	9.3 (1.35 × 10^6)	84 (12.2)	.0042	.18
$[(\pm45)_2]_S$	77 (11.2 × 10^6)	5.2 (0.76 × 10^6)	177 (25.7)	>.015	---
$[90/0/90/0]_S$	133 (19.3 × 10^6)	77 (11.1 × 10^6)	514 (74.6)	.0061	.20
$[0/\pm45]_S$	116 (16.8 × 10^6)	60 (8.7 × 10^6)	434 (63.0)	.0067	.40
$[0_2/\pm45]_S$	143 (20.8 × 10^6)	84 (12.2 × 10^6)	594 (86.2)	.0063	.37

[a]Average from replicate tests.
[b]From stress-strain equation.

TABLE VII.- SUMMARY OF Bsc/Al LAMINATE DATA FROM SANDWICH-BEAM TENSILE TESTS

Laminate orientation	E at $\varepsilon = 0$, GPa (psi) (a)	E at $\varepsilon = 0.002$, GPa (psi) (a)	σ_{max}, MPa (ksi) (b)	ε_{max} (b)	μ_o (b)
Room temperature					
$[0_6]_T$	194 (28.1 × 10^6)	181 (26.2 × 10^6)	1027 (149)	0.0056	0.24
$[90_6]_T$	128 (18.6 × 10^6)	15.9 (2.3 × 10^6)	172 (24.9)	.0088	.14
$[(\pm45)_2]_S$	66 (9.6 × 10^6)	18 (2.6 × 10^6)	192 (27.9)	>.012	.33
$[90/0/90/0]_S$	118 (17.1 × 10^6)	96 (13.9 × 10^6)	598 (86.7)	.0063	---
$[0/\pm45]_S$	149 (21.6 × 10^6)	73 (10.6 × 10^6)	392 (56.9)	.0049	.27
$[0_2/\pm45]_S$	185 (26.8 × 10^6)	102 (14.8 × 10^6)	583 (84.6)	.0053	.25
450 K (350°F)					
$[0_6]_T$	222 (32.2 × 10^6)	201 (29.1 × 10^6)	1069 (155)	0.0055	0.22
$[90_6]_T$	120 (17.4 × 10^6)	19 (2.8 × 10^6)	132 (19.2)	.0042	.15
$[(\pm45)_2]_S$	97 (14.1 × 10^6)	15 (2.2 × 10^6)	213 (30.9)	>.012	.37
$[90/0/90/0]_S$	141 (20.4 × 10^6)	114 (16.5 × 10^6)	654 (94.9)	.0061	.14
$[0/\pm45]_S$	157 (22.8 × 10^6)	90 (13.0 × 10^6)	461 (66.8)	.0051	.31
$[0_2/\pm45]_S$	167 (24.2 × 10^6)	130 (18.8 × 10^6)	658 (95.4)	.0053	.31
505 K (450°F)					
$[0_6]_T$	216 (31.3 × 10^6)	200 (29.0 × 10^6)	1055 (153)	0.0054	0.26
$[90_6]_T$	166 (24.0 × 10^6)	---	120 (17.4)	.0021	.12
$[(\pm45)_2]_S$	93 (13.5 × 10^6)	9.0 (1.3 × 10^6)	149 (21.6)	>.009	.38
$[90/0/90/0]_S$	172 (25.0 × 10^6)	105 (15.3 × 10^6)	625 (90.7)	.0061	.14
$[0/\pm45]_S$	144 (20.9 × 10^6)	77 (11.2 × 10^6)	464 (67.3)	.0057	.30
$[0_2/\pm45]_S$	165 (24.0 × 10^6)	131 (19.0 × 10^6)	---	---	.30

[a]From stress-strain equation.
[b]Average from replicate tests.

TABLE VIII.- SUMMARY OF Bsc/Al LAMINATE DATA FROM SANDWICH-BEAM COMPRESSION TESTS

Laminate orientation	E at $\varepsilon = 0$, GPa (psi) (a)	E at $\varepsilon = 0.002$, GPa (psi) (a)	σ_{max}, MPa (ksi) (b)	ε_{max} (b)	μ_o (b)
Room temperature					
$[0_6]_T$	216 (31.4 × 10^6)	190 (27.6 × 10^6)	1689 (245)	0.0085	0.24
$[90_6]_T$	117 (17.0 × 10^6)	21 (3.0 × 10^6)	294 (42.7)	>.039	.14
$[(\pm45)_2]_S$	139 (20.1 × 10^6)	15 (2.2 × 10^6)	>265 (38.5)	>.01	.33
$[90/0/90/0]_S$	149 (21.6 × 10^6)	123 (17.8 × 10^6)	1358 (197)	.011	.17
$[0/\pm45]_S$	131 (19.0 × 10^6)	76 (11.0 × 10^6)	1744 (253)	.023	.29
$[0_2/\pm45]_S$	162 (23.5 × 10^6)	101 (14.6 × 10^6)	1558 (226)	.015	.26
450 K (350°F)					
$[0_6]_T$	190 (27.5 × 10^6)	183 (26.5 × 10^6)	1276 (185)	0.0073	0.24
$[90_6]_T$	118 (17.1 × 10^6)	24 (3.5 × 10^6)	265 (38.4)	---	.15
$[(\pm45)_2]_S$	83 (12.1 × 10^6)	17 (2.4 × 10^6)	>220 (31.9)	>.01	.37
$[90/0/90/0]_S$	108 (15.6 × 10^6)	108 (15.6 × 10^6)	855 (124)	.0085	.13
$[0/\pm45]_S$	117 (17.0 × 10^6)	78 (11.3 × 10^6)	1413 (205)	.025	.34
$[0_2/\pm45]_S$	120 (17.4 × 10^6)	106 (15.4 × 10^6)	1076 (156)	.012	.31
505 K (450°F)					
$[0_6]_T$	179 (26.0 × 10^6)	169 (24.5 × 10^6)	1193 (173)	0.0072	.22
$[90_6]_T$	113 (16.4 × 10^6)	16 (2.3 × 10^6)	200 (29.0)	---	.13
$[(\pm45)_2]_S$	76 (11.0 × 10^6)	11 (1.6 × 10^6)	>159 (23.1)	>.01	.38
$[90/0/90/0]_S$	224 (32.5 × 10^6)	101 (14.6 × 10^6)	807 (117)	.0083	.14
$[0/\pm45]_S$	105 (15.2 × 10^6)	71 (10.3 × 10^6)	1227 (178)	.023	.32
$[0_2/\pm45]_S$	115 (16.7 × 10^6)	107 (15.5 × 10^6)	938 (136)	.010	.41

[a]From stress-strain equation.
[b]Average from replicate tests.

TABLE IX.- SUMMARY OF Bsc/Al LAMINATE DATA FROM PICUTRE-FRAME SHEAR TESTS

Laminate orientation	G at $\gamma = 0$, GPa (psi) (a)	G at $\gamma = 0.002$, GPa (psi) (a)	τ_{max}, MPa (ksi) (b)	γ_{max} (b)
Room temperature				
$[0_6]_T$	37 (5.3×10^6)	8.3 (1.2×10^6)	105 (15.2)	>0.03
$[(\pm 45)_2]_S$	134 (19.4×10^6)	55 (8.0×10^6)	312 (45.3)	.0056
$[90/0/90/0]_S$	33 (4.8×10^6)	7.6 (1.1×10^6)	112 (16.3)	> .03
$[0/\pm 45]_S$	63 (9.16×10^6)	43 (6.2×10^6)	319 (46.3)	.0077
$[0_2/\pm 45]_S$	108 (15.6×10^6)	33 (4.8×10^6)	251 (36.4)	.0091
450 K (350°F)				
$[0_6]_T$	16 (2.3×10^6)	9.0 (1.3×10^6)	83 (12.1)	>0.03
$[(\pm 45)_2]_S$	81 (11.7×10^6)	46 (6.7×10^6)	---	---
$[90/0/90/0]_S$	49 (7.1×10^6)	4.4 (0.64×10^6)	80 (11.6)	>.026
$[0/\pm 45]_S$	110 (15.9×10^6)	39 (5.7×10^6)	259 (37.5)	.0068
505 K (450°F)				
$[0_6]_T$	13 (1.9×10^6)	6.9 (1.0×10^6)	63 (9.2)	>0.03
$[(\pm 45)_2]_S$	61 (8.8×10^6)	46 (6.6×10^6)	284 (41.2)	.0059
$[90/0/90/0]_S$	23 (3.3×10^6)	3.7 (0.54×10^6)	61 (8.8)	>.026
$[0/\pm 45]_S$	77 (11.1×10^6)	36 (5.2×10^6)	228 (33.0)	.0064
$[0_2/\pm 45]_S$	46 (6.7×10^6)	26 (3.8×10^6)	205 (29.8)	.0097

[a]From stress-strain equation.
[b]Average from replicate tests.

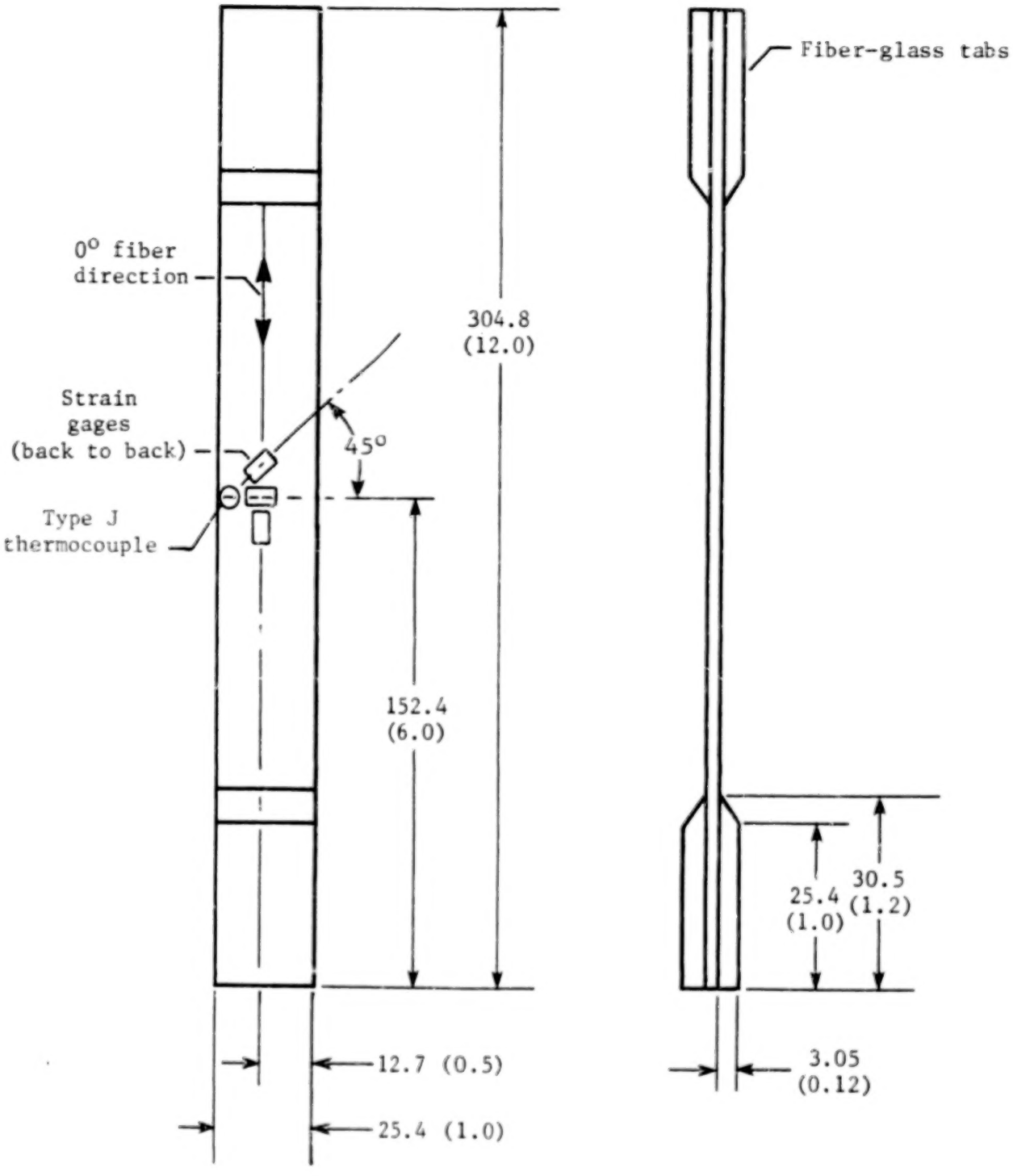

Figure 1.- Configuration and instrumentation of flat-tensile specimen. Dimensions are given in millimeters (inches).

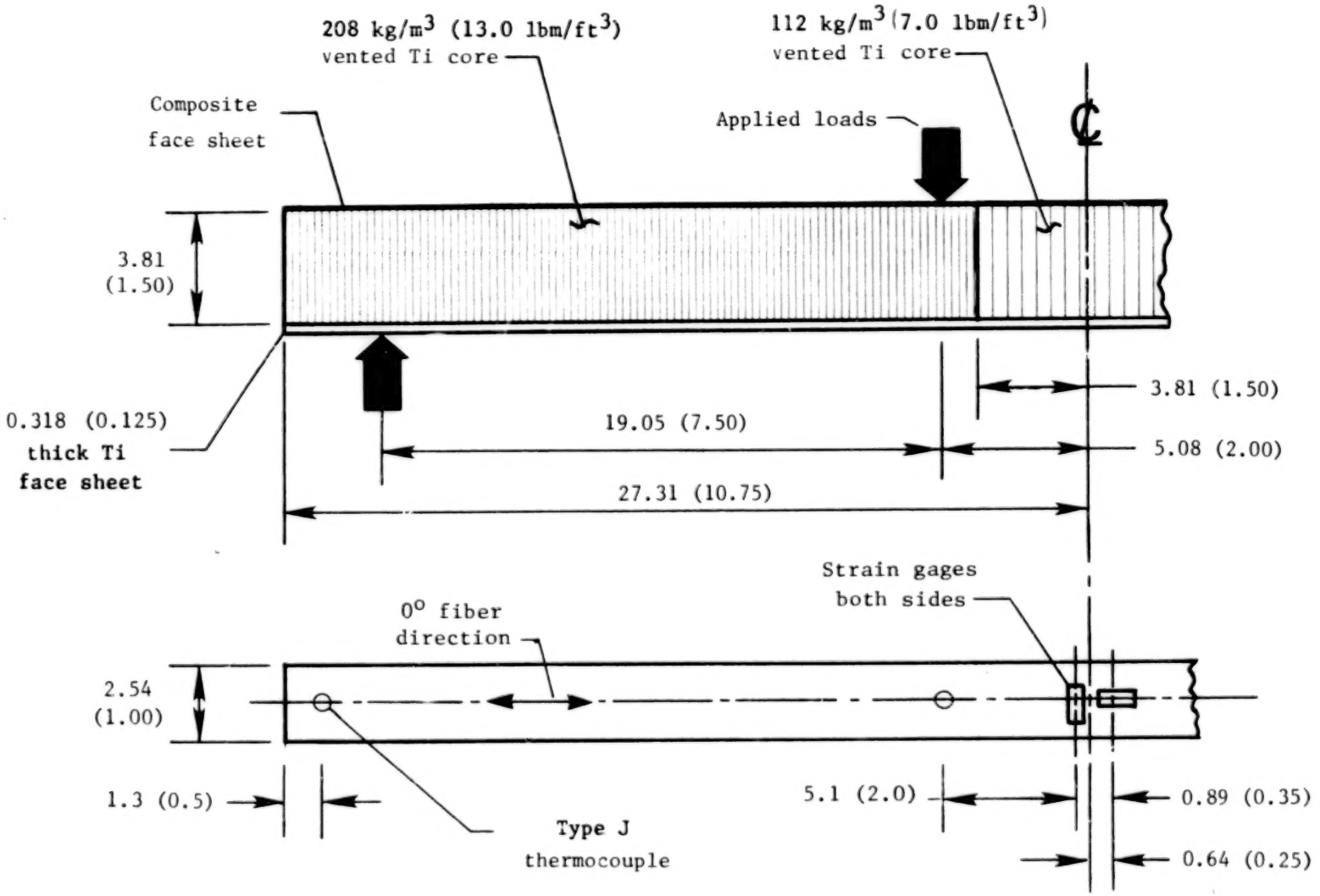

Figure 2.- Configuration of sandwich-beam test specimen. Dimensions are given in centimeters (inches) unless otherwise stated.

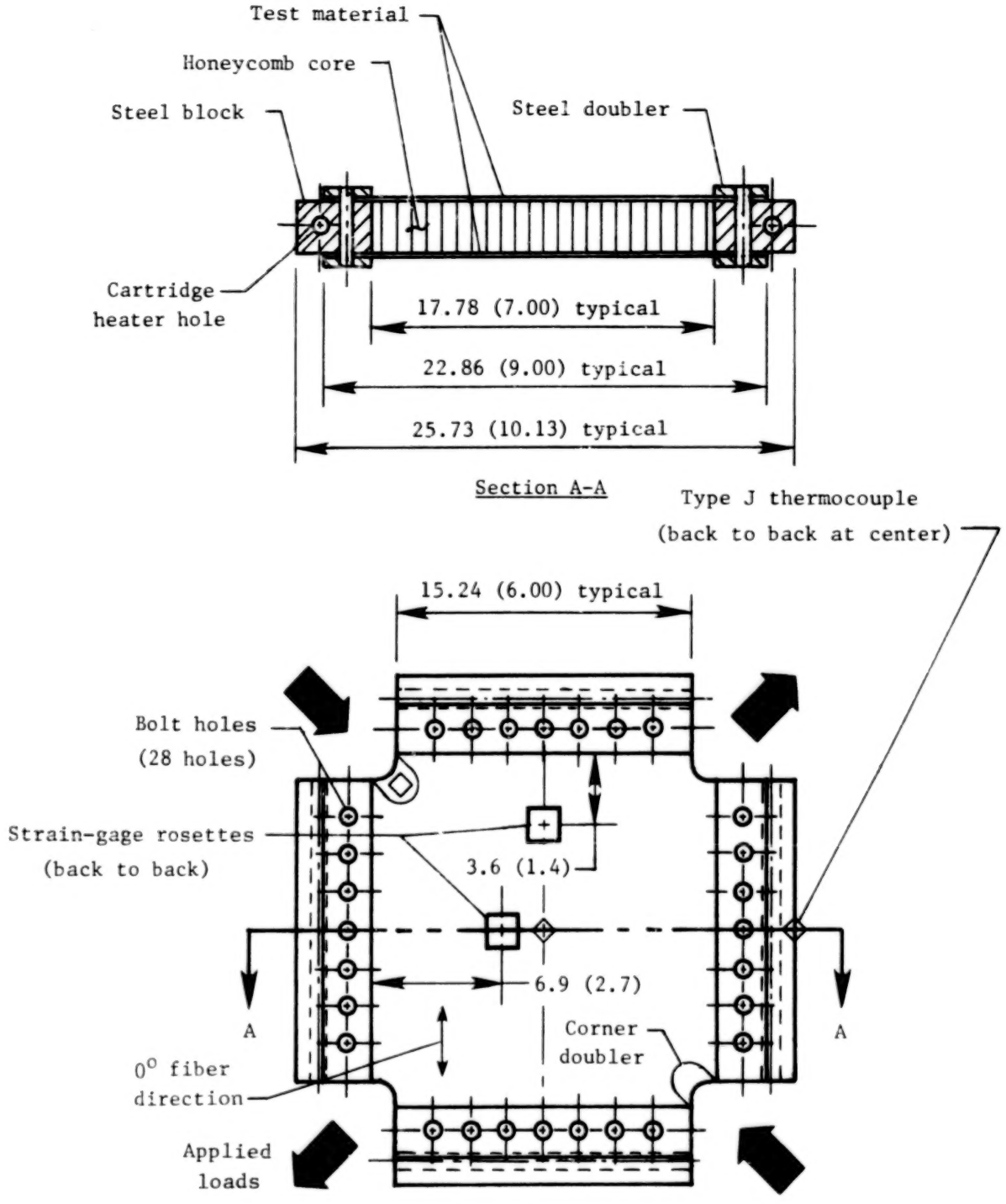

Figure 3.- Configuration of picture-frame shear specimen. Dimensions are given in centimeters (inches).

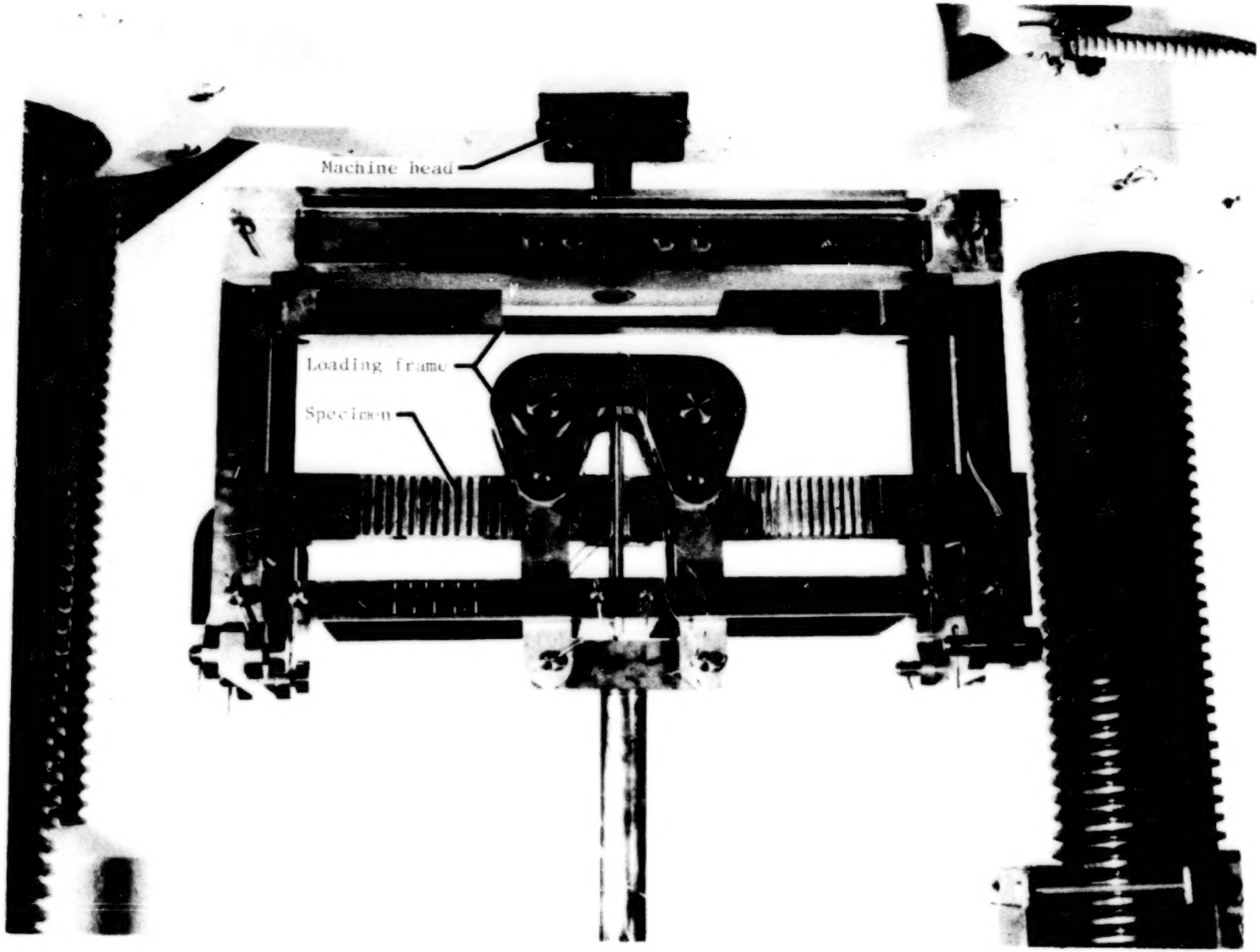

L-76-5489

Figure 4.- Loading apparatus used in sandwich-beam tests.

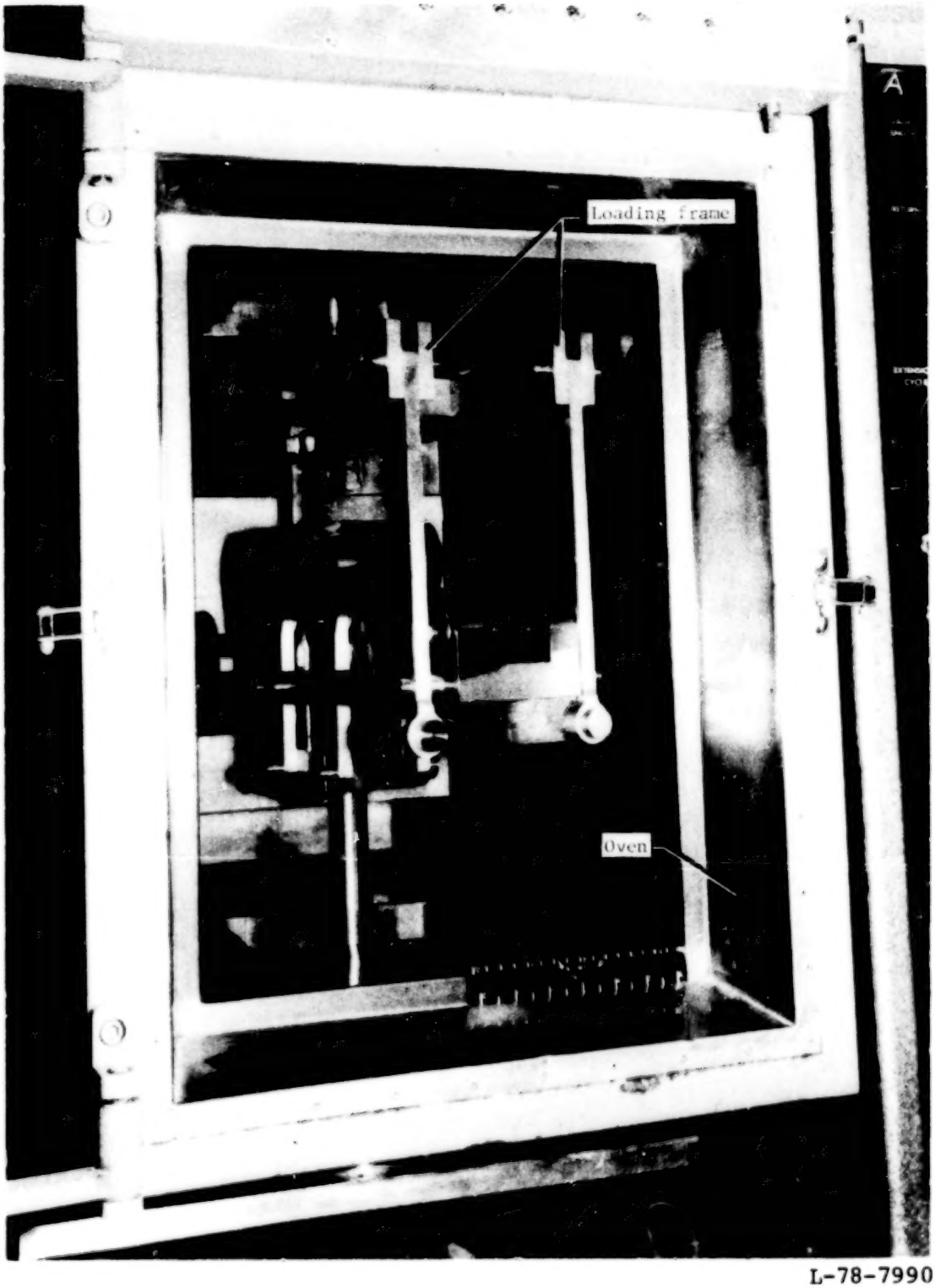

L-78-7990

Figure 5.- Assembled heating and loading apparatus used in sandwich-beam tests.

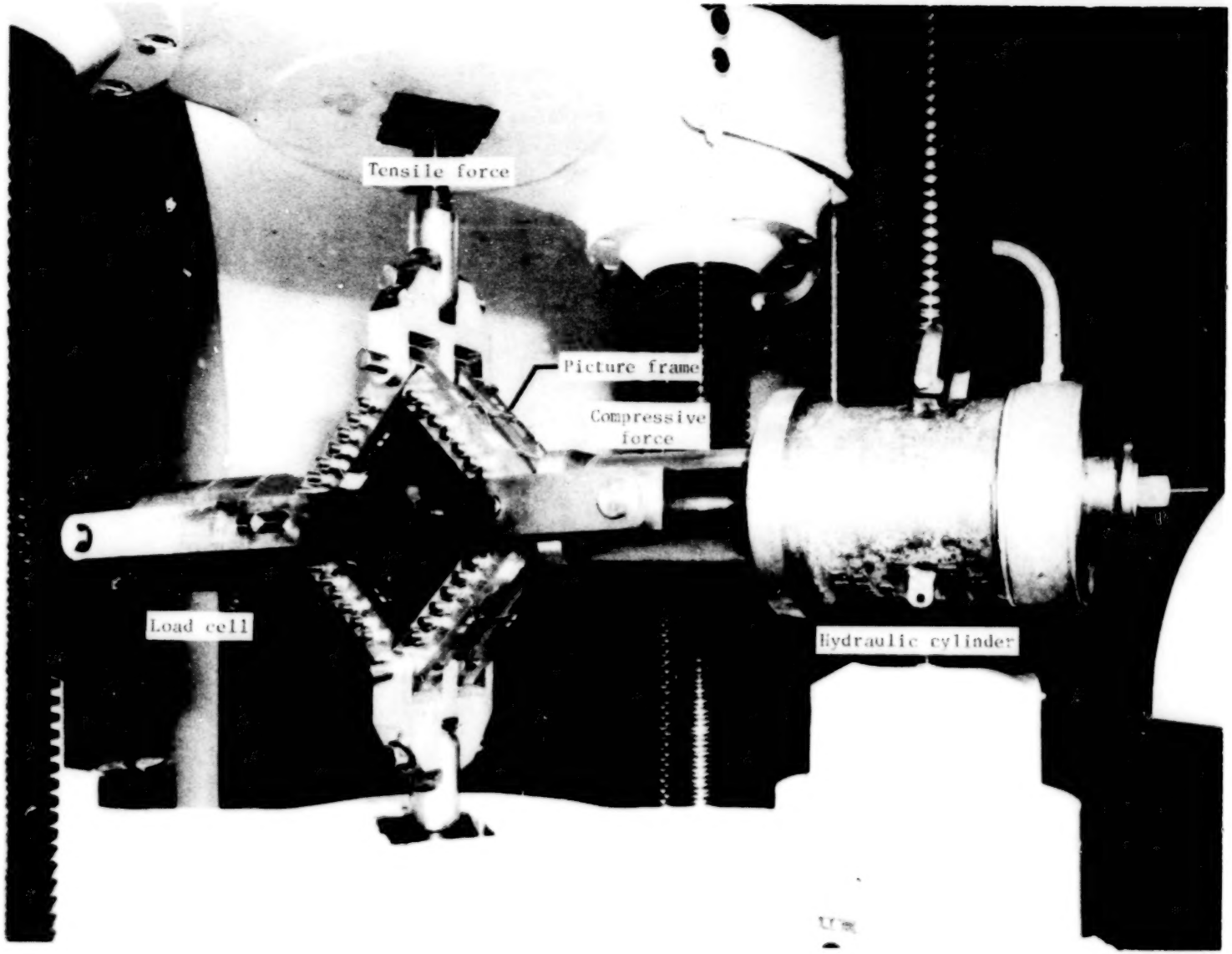

L-73-3882

Figure 6.- Loading apparatus used in picture-frame shear tests.

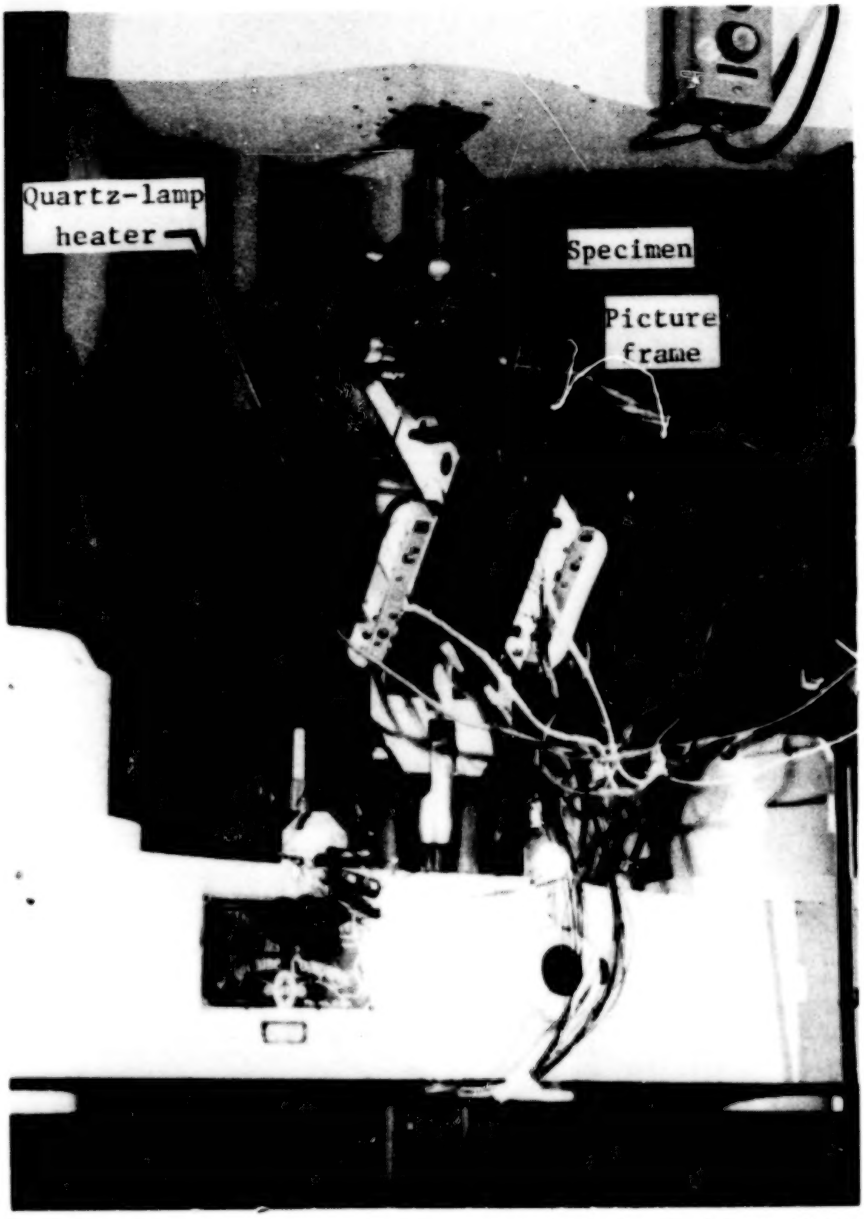

L-75-7170

Figure 7.- Heating apparatus used in picture-frame shear tests.

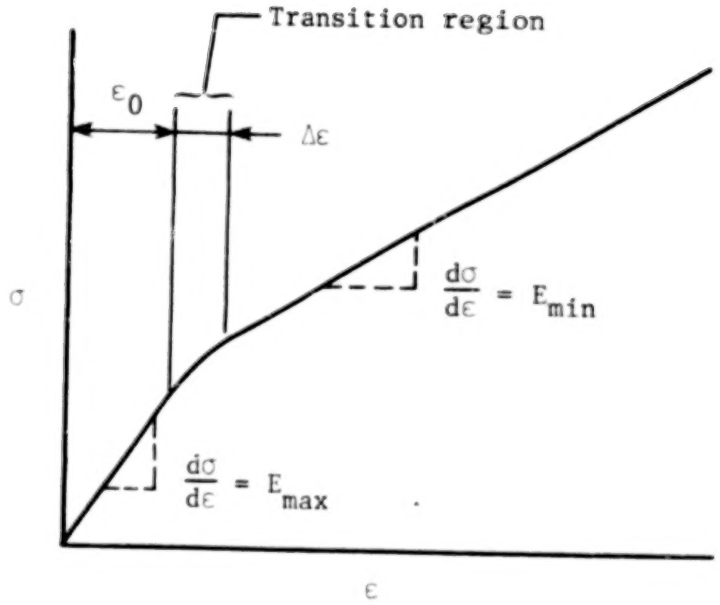

Figure 8.- Stress-strain curve for bimodular material.

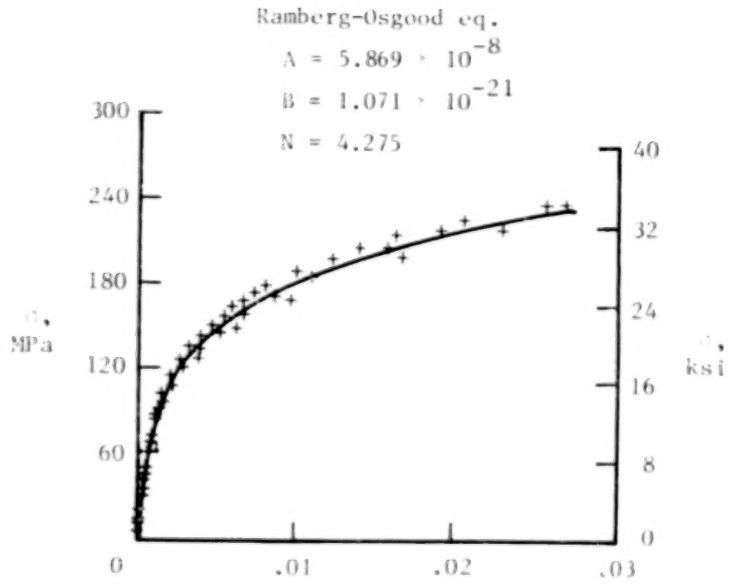

(a) $[90_6]_T$ laminate in compression.

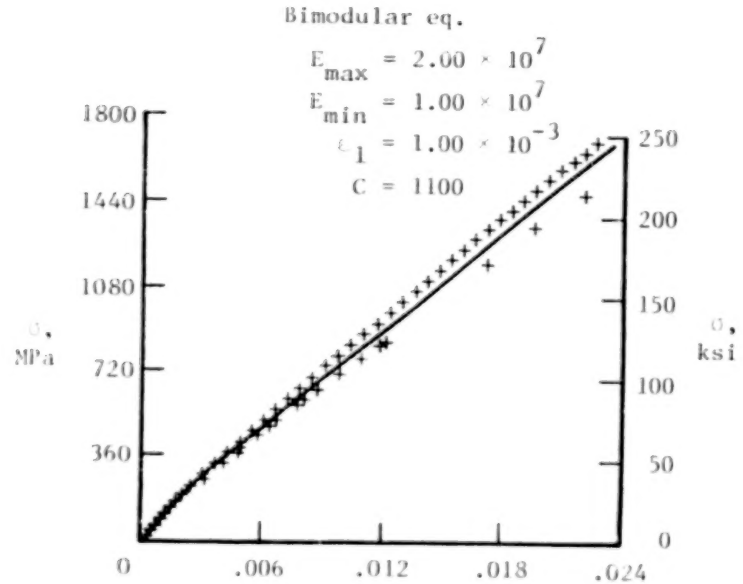

(b) $[0/\pm45]_S$ laminate in compression.

Figure 9.- Typical comparisons between stress-strain data and analytical results.

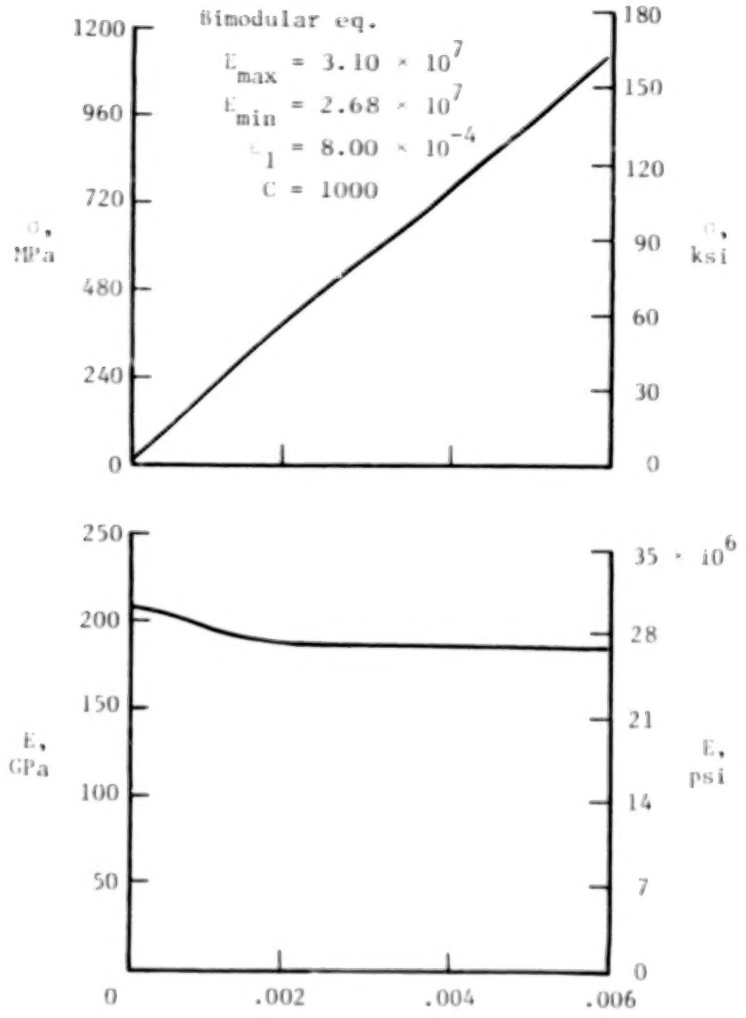

(a) $[0_6]_T$ laminate after exposure to a braze-temperature cycle.

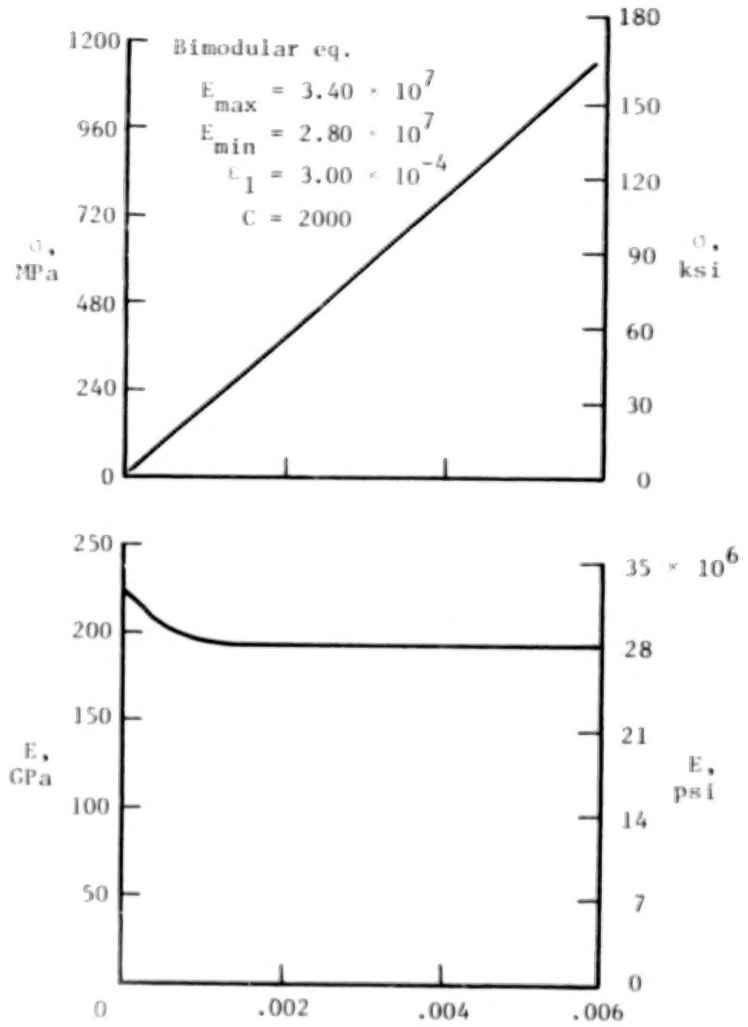

(b) $[0_6]_T$ laminate in "as-received" condition.

Figure 10.- Stress and tangent modulus as a function of strain from room-temperature flat-tensile tests on Bsc/Al laminates.

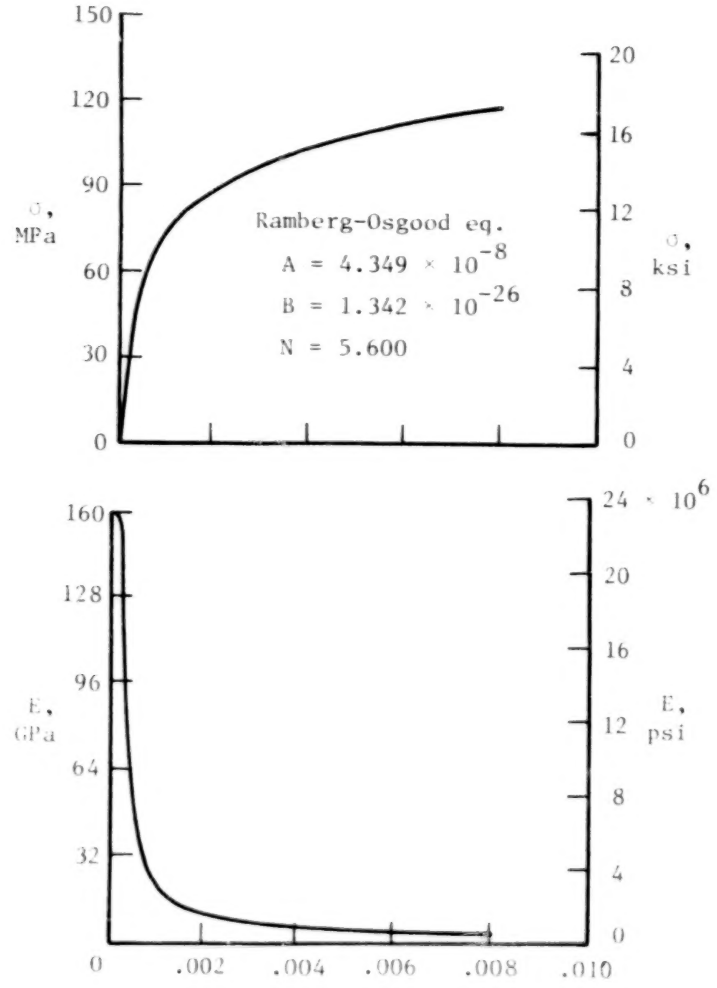

(c) $[90_6]_T$ laminate after exposure to a braze-temperature cycle.

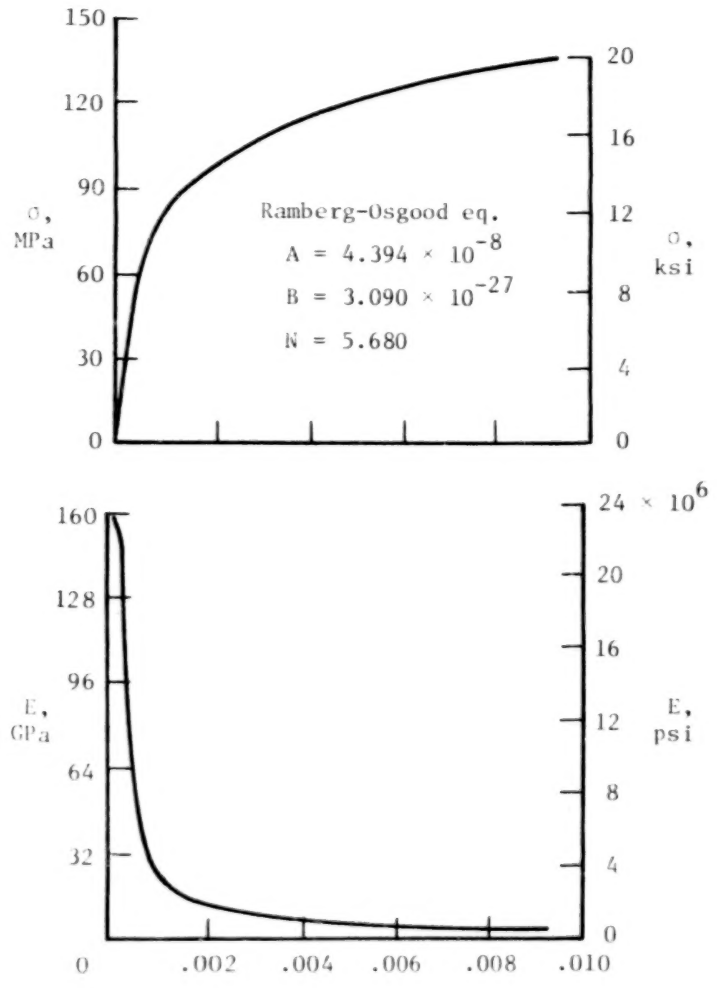

(d) $[90_6]_T$ laminate in "as-received" condition.

Figure 10.- Continued.

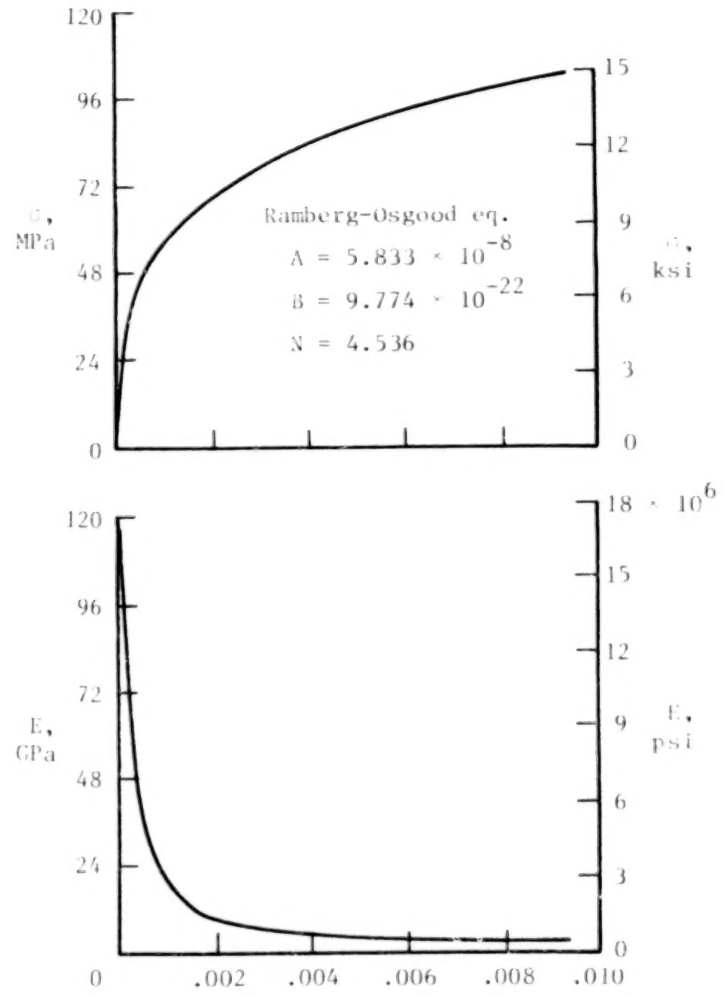

(e) $[(\pm 45)_2]_S$ laminate after exposure to a braze-temperature cycle.

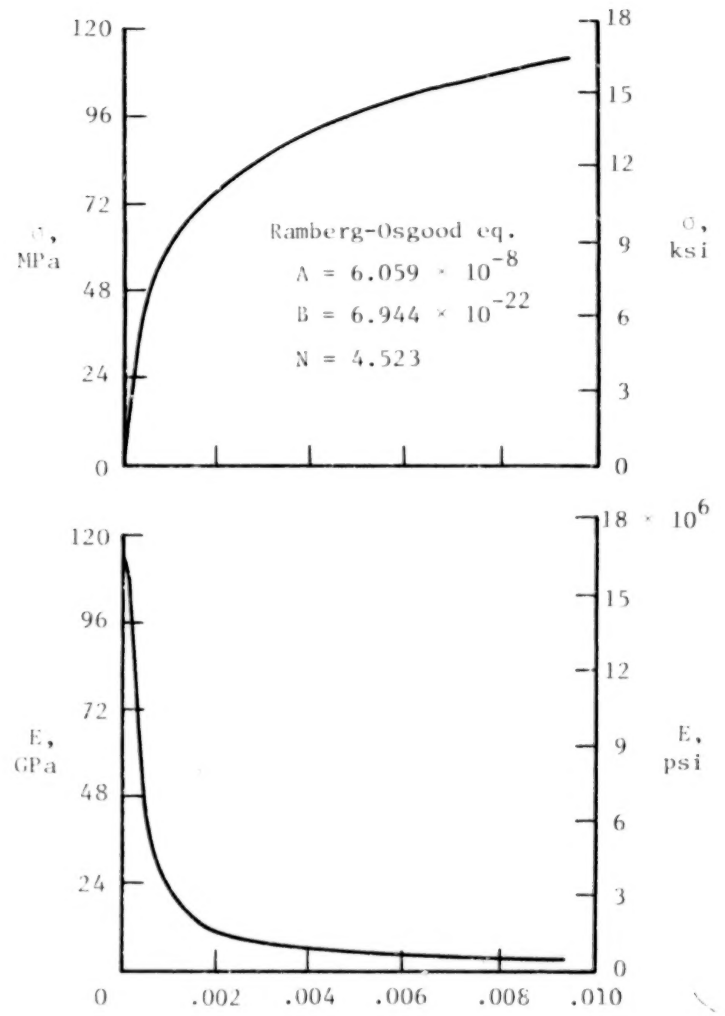

(f) $[(\pm 45)_2]_S$ laminate in "as-received" condition.

Figure 10.- Continued.

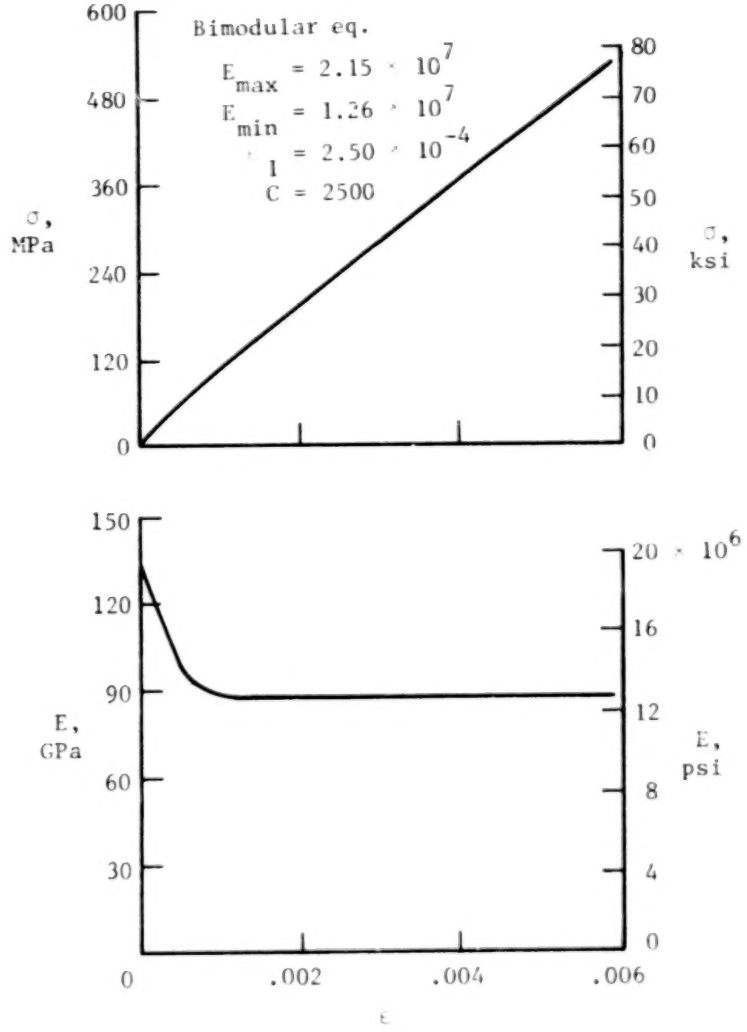

(g) $[90/0/90/0]_S$ laminate after exposure to a braze-temperature cycle.

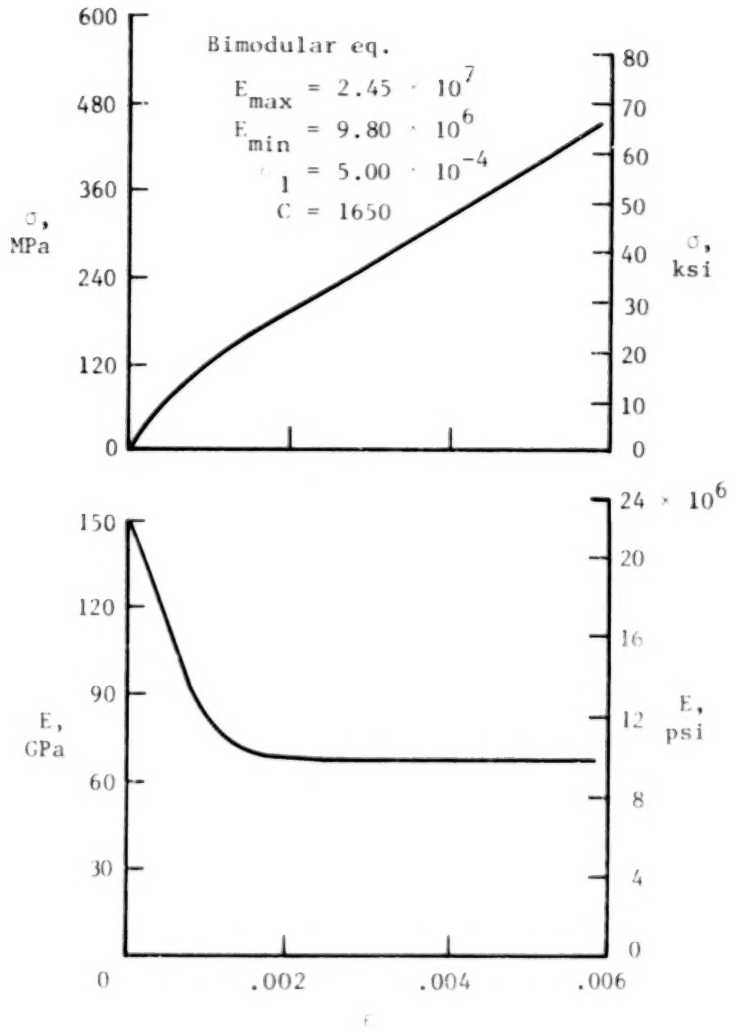

(h) $[90/0/90/0]_S$ laminate in "as-received" condition.

Figure 10.- Continued.

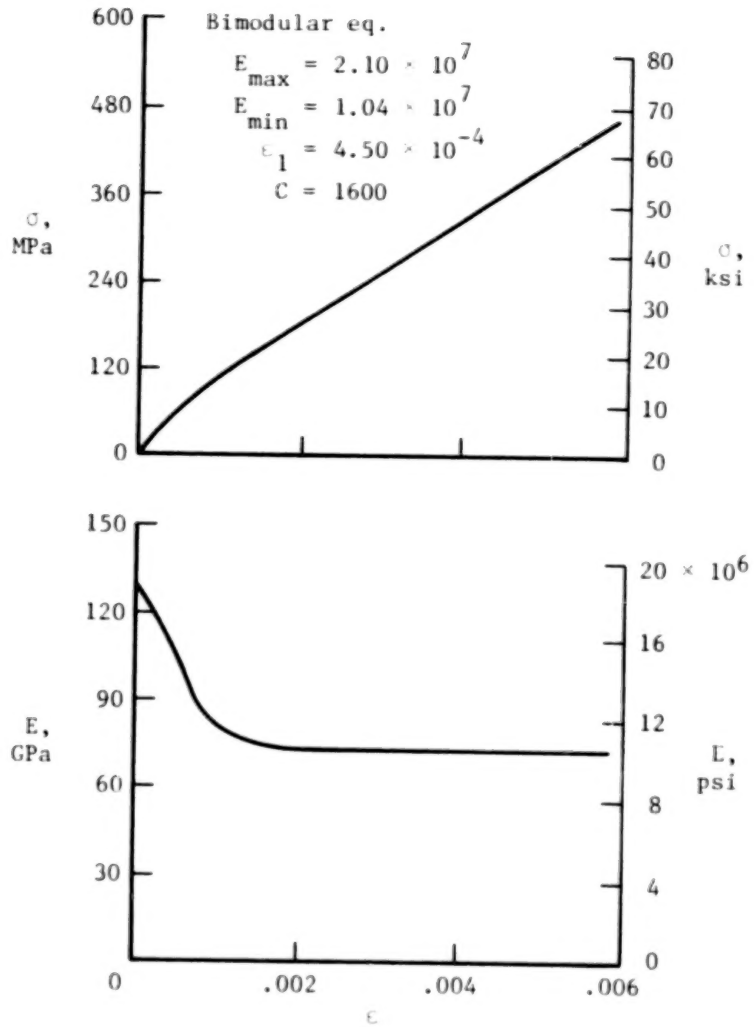

(i) $[0/\pm45]_S$ laminate after exposure to a braze-temperature cycle.

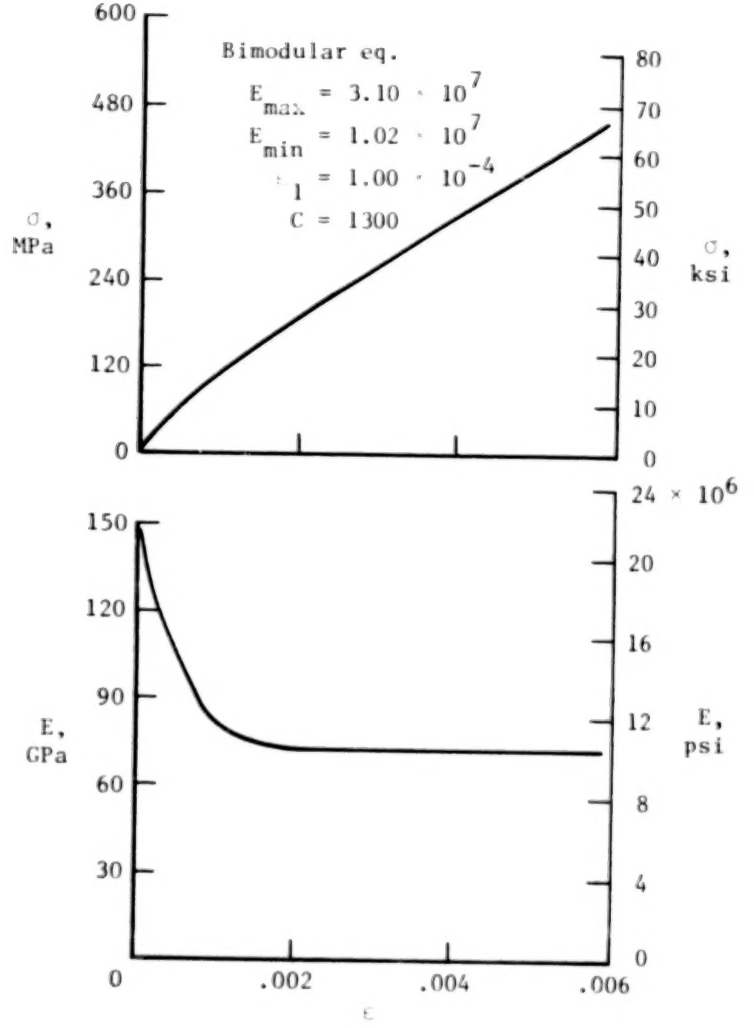

(j) $[0/\pm45]_S$ laminate in "as-received" condition.

Figure 10.- Continued.

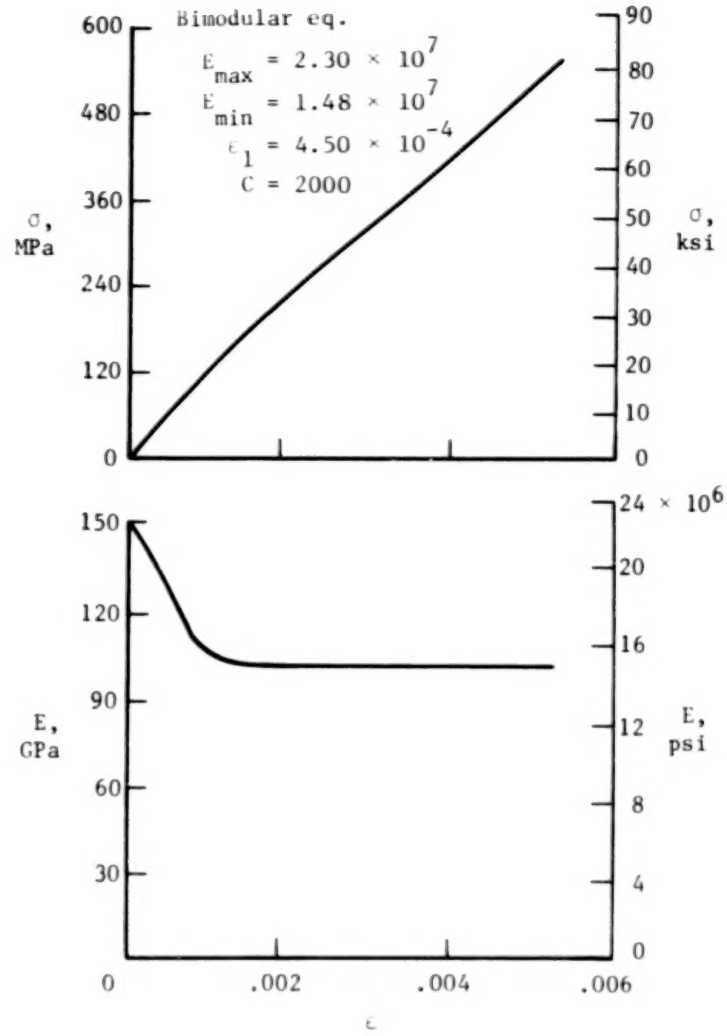

(k) $[0_2/\pm 45]_S$ laminate after exposure to a braze-temperature cycle.

Figure 10.- Concluded.

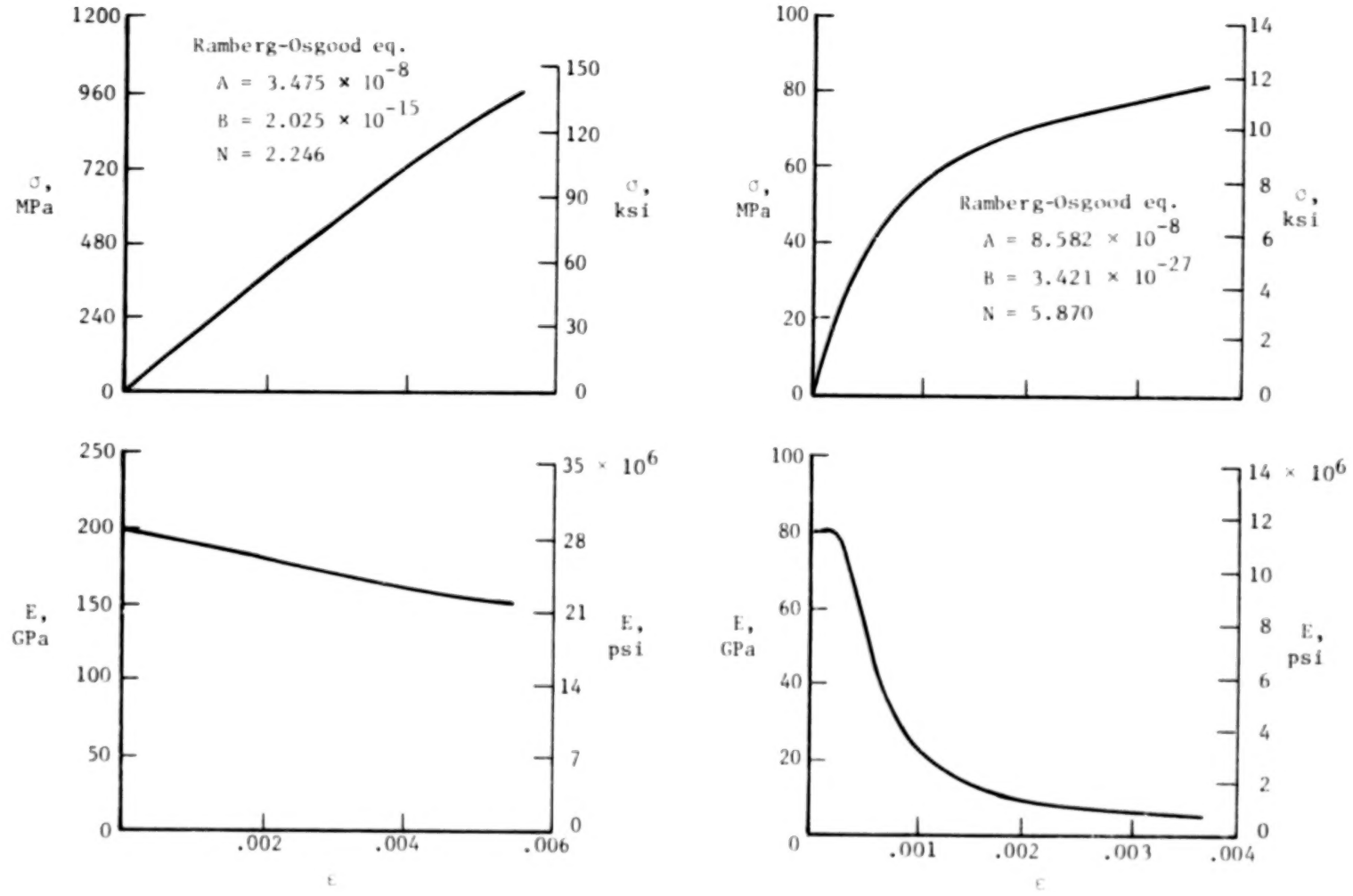

(a) $[0_6]_T$ laminate.

(b) $[90_6]_T$ laminate.

Figure 11.- Stress tangent modulus as a function of strain from flat-tensile tests at 505 K (450°F) on Bsc/Al laminates..

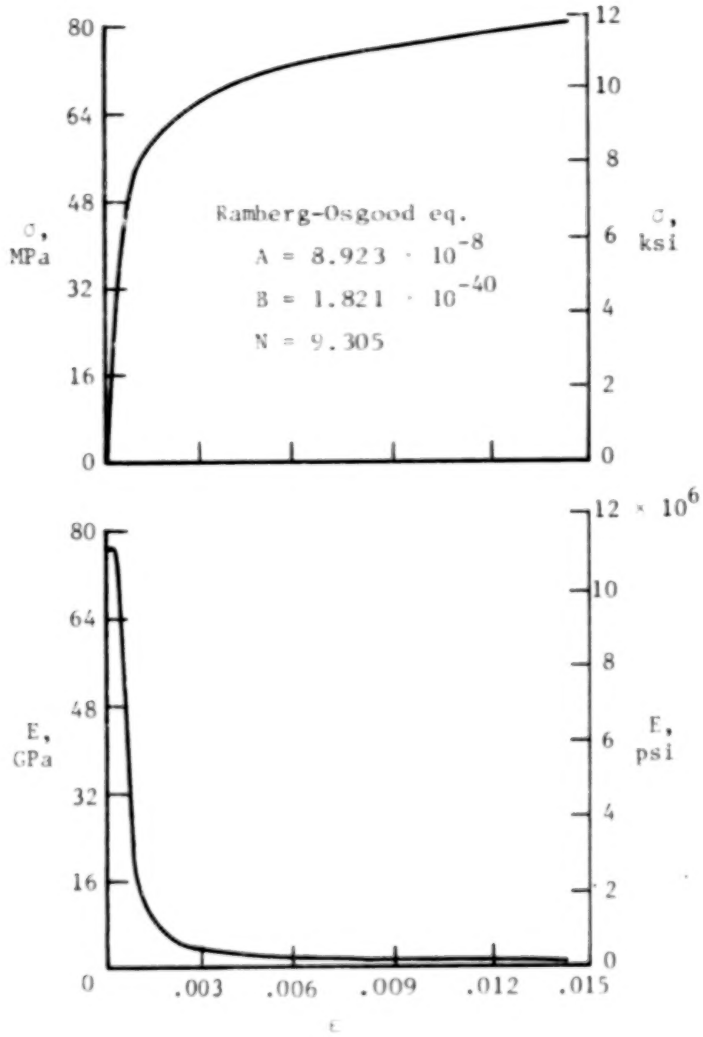

(c) $[(\pm 45)_2]_S$ laminate.

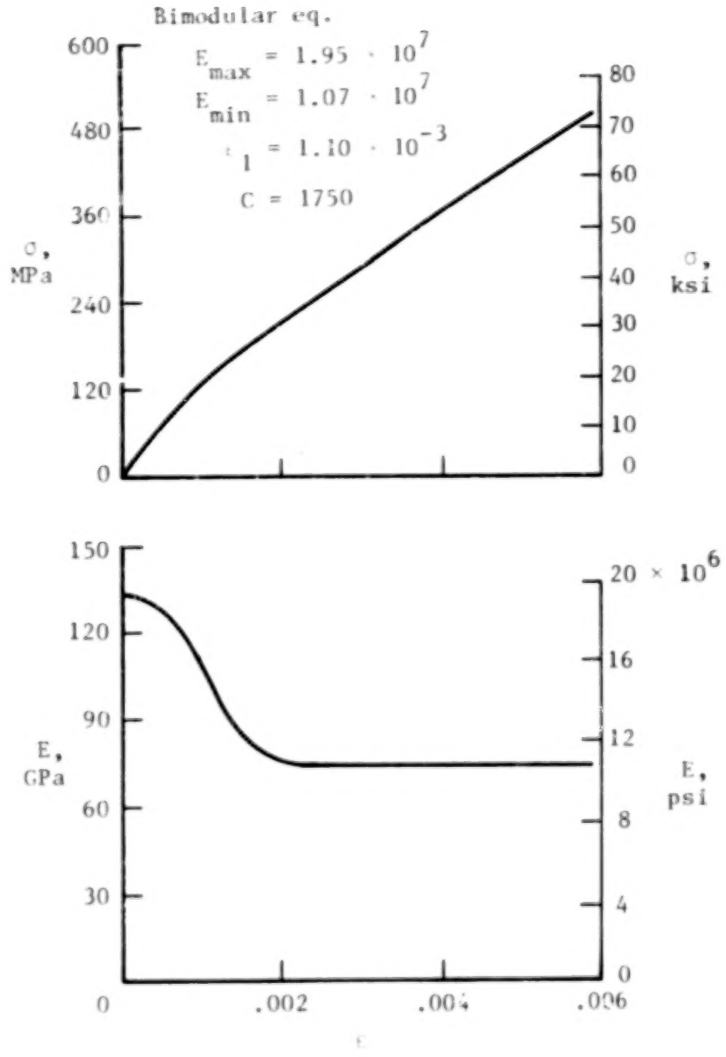

(d) $[90/0/90/0]_S$ laminate.

Figure 11.- Continued.

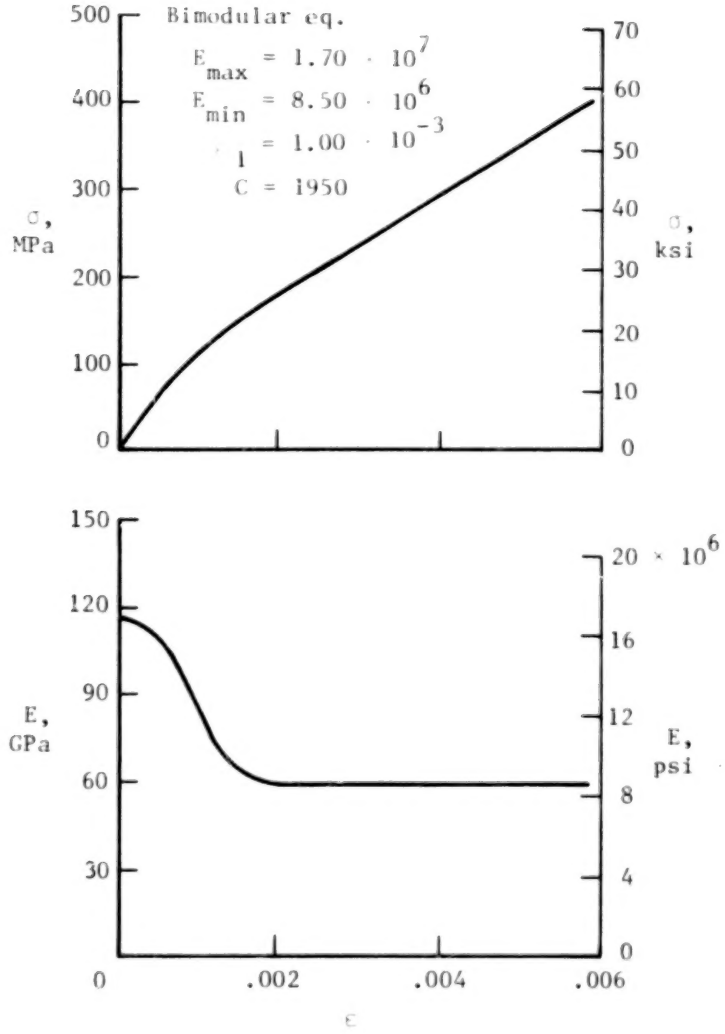

(e) $[0/\pm45]_S$ laminate.

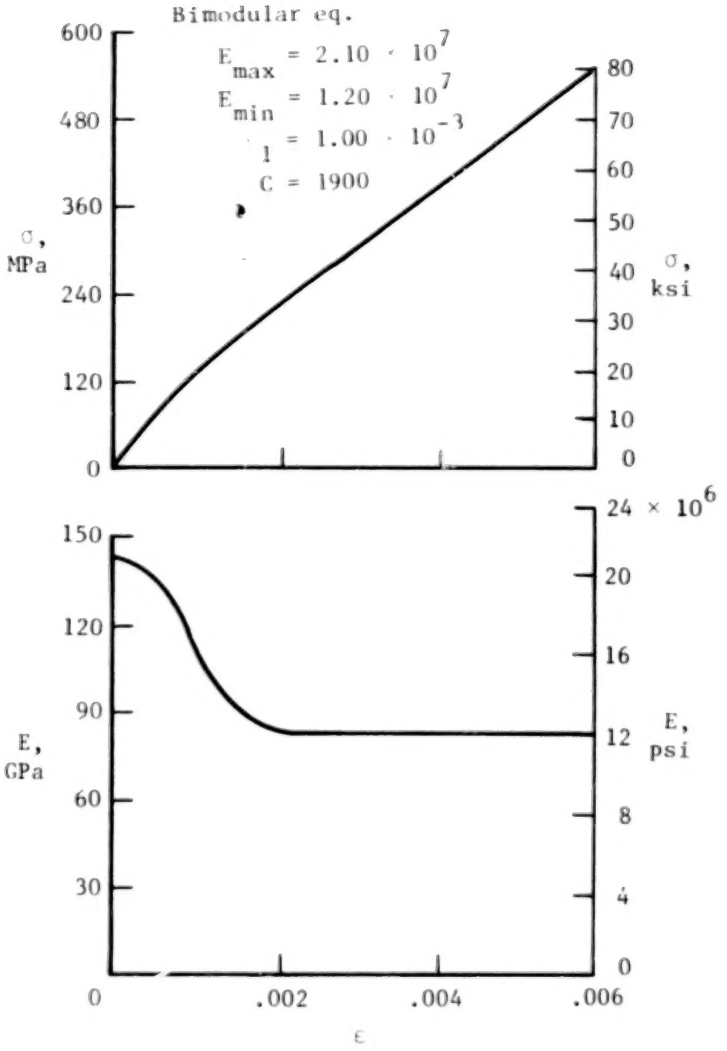

(f) $[0_2/\pm45]_S$ laminate.

Figure 11.- Concluded.

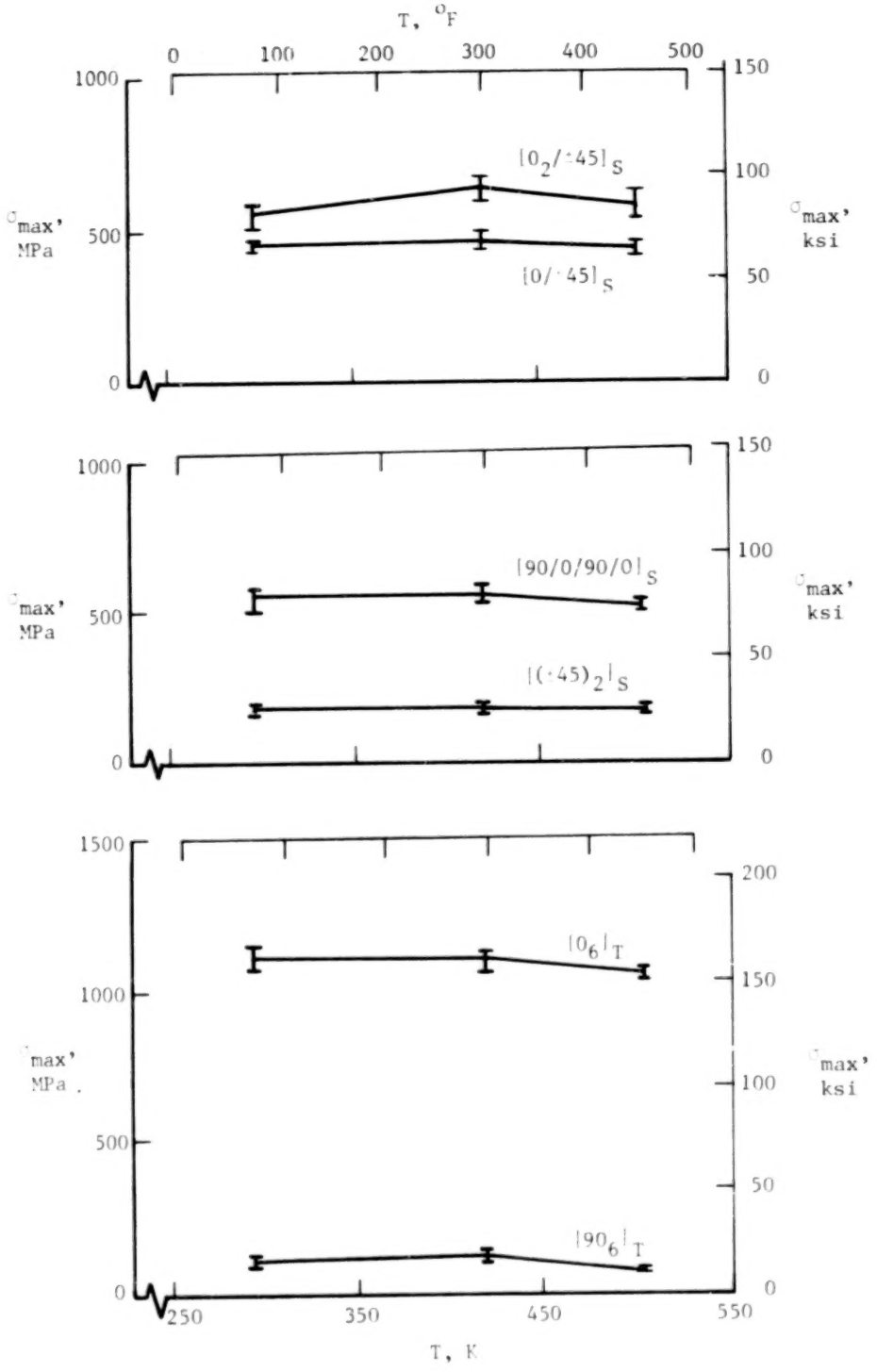

Figure 12.- Maximum tensile stress as a function of temperature from flat-tensile tests after exposure to braze-temperature cycle.

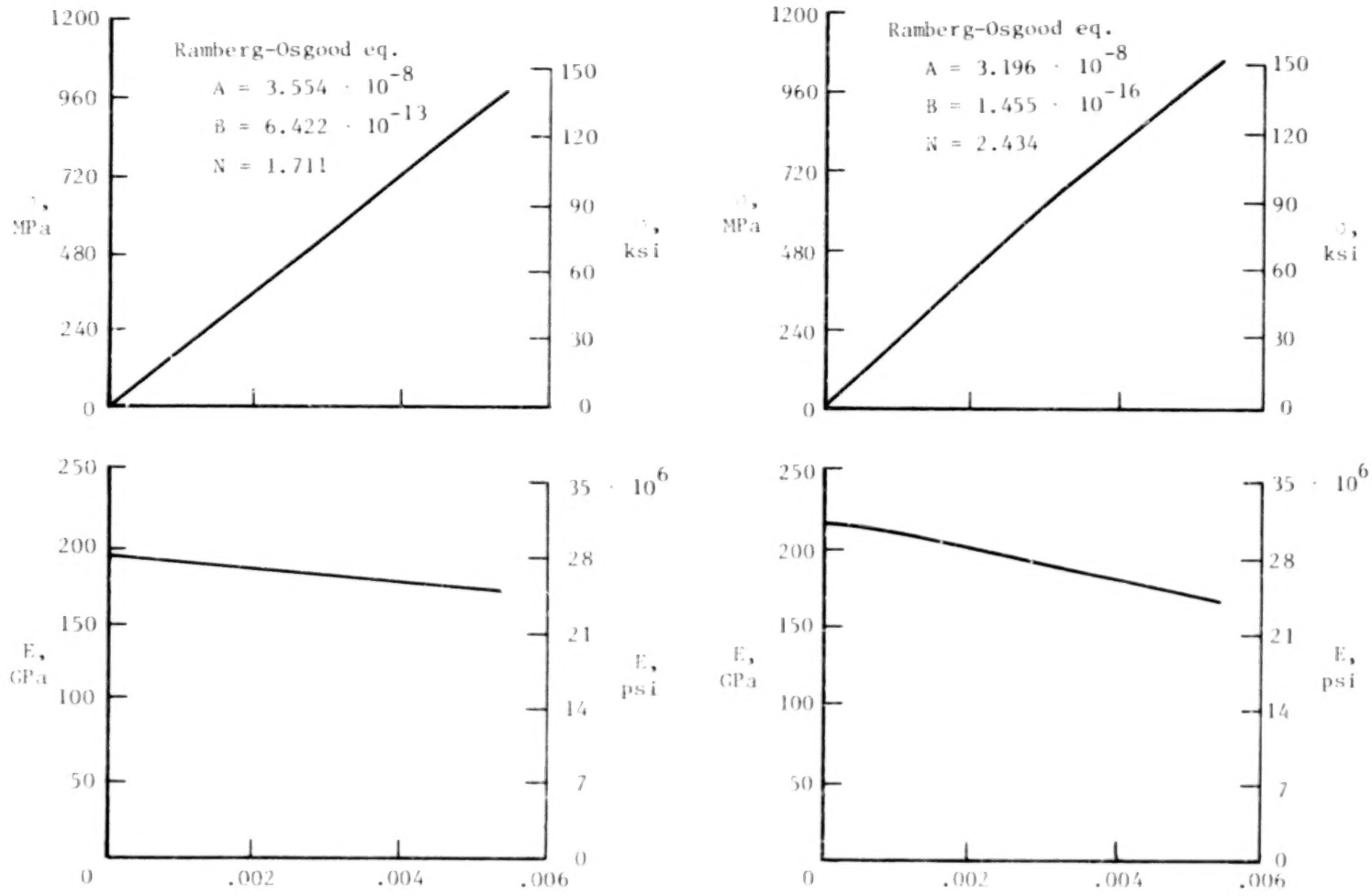

(a) $[0_6]_T$ laminate at room temperature.

(b) $[0_6]_T$ laminate at 505 K (450°F).

Figure 13.- Stress and tangent modulus as a function of strain from sandwich-beam tests on Bsc/Al laminates in tension.

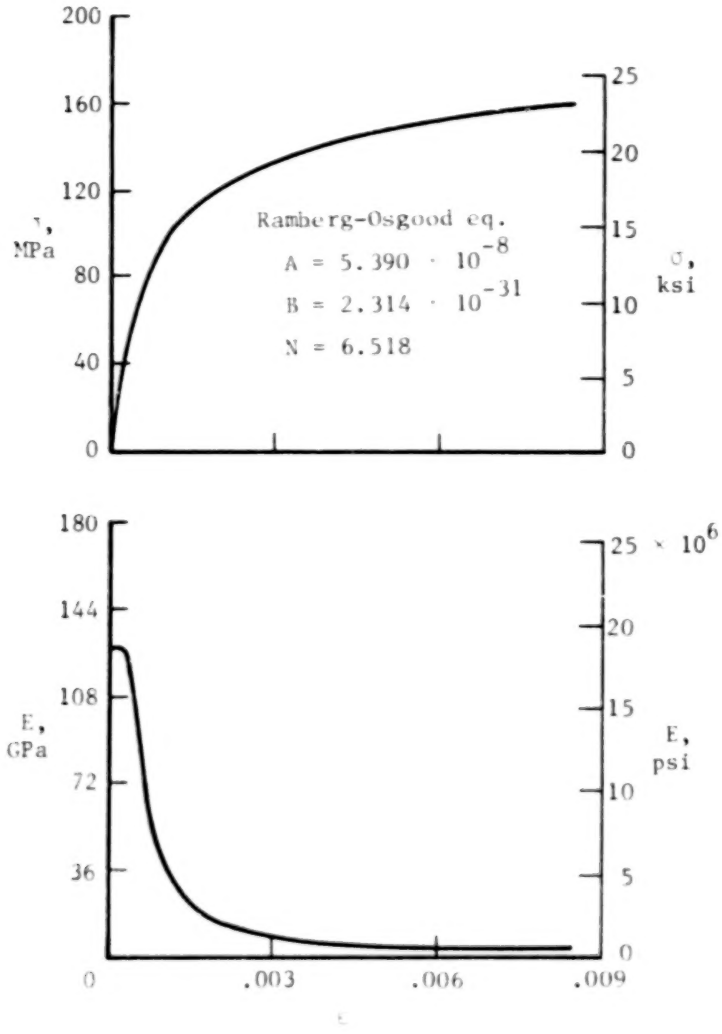

(c) $[90_6]_T$ laminate at room temperature.

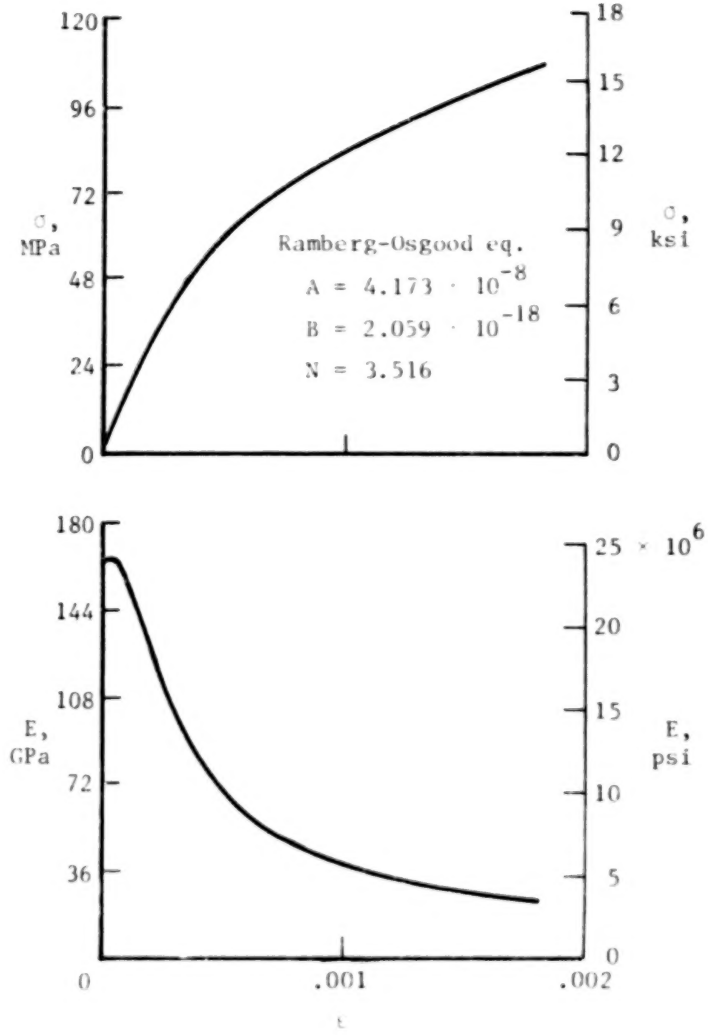

(d) $[90_6]_T$ laminate at 505 K (450°F).

Figure 13.- Continued.

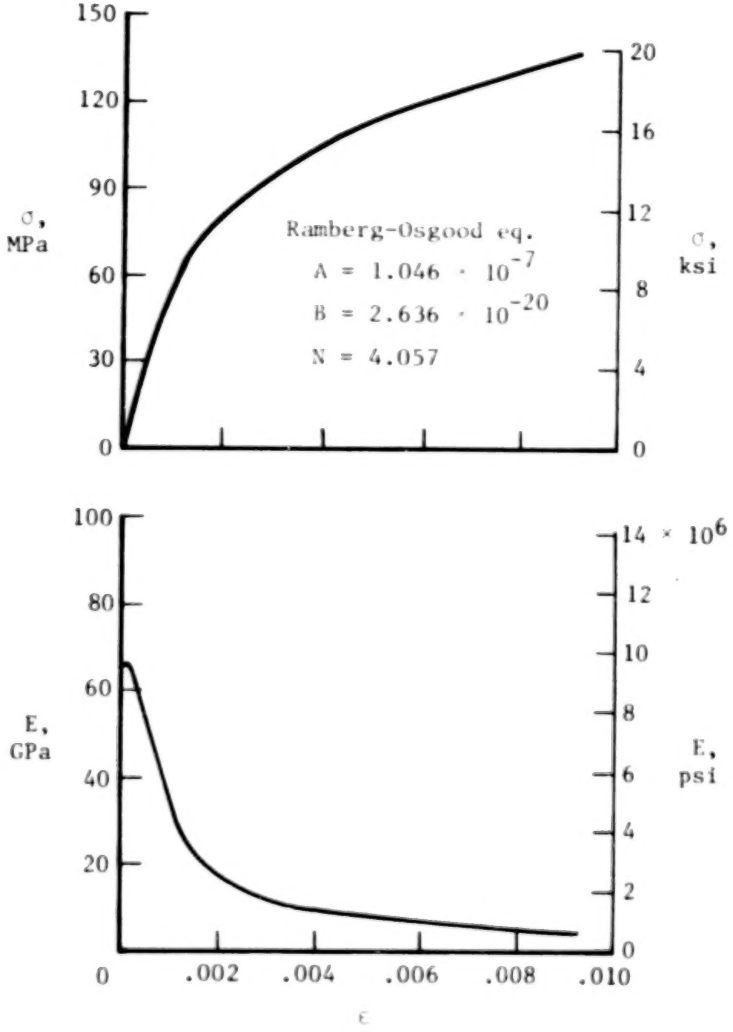

(e) $[(\pm 45)_2]_S$ laminate at room temperature.

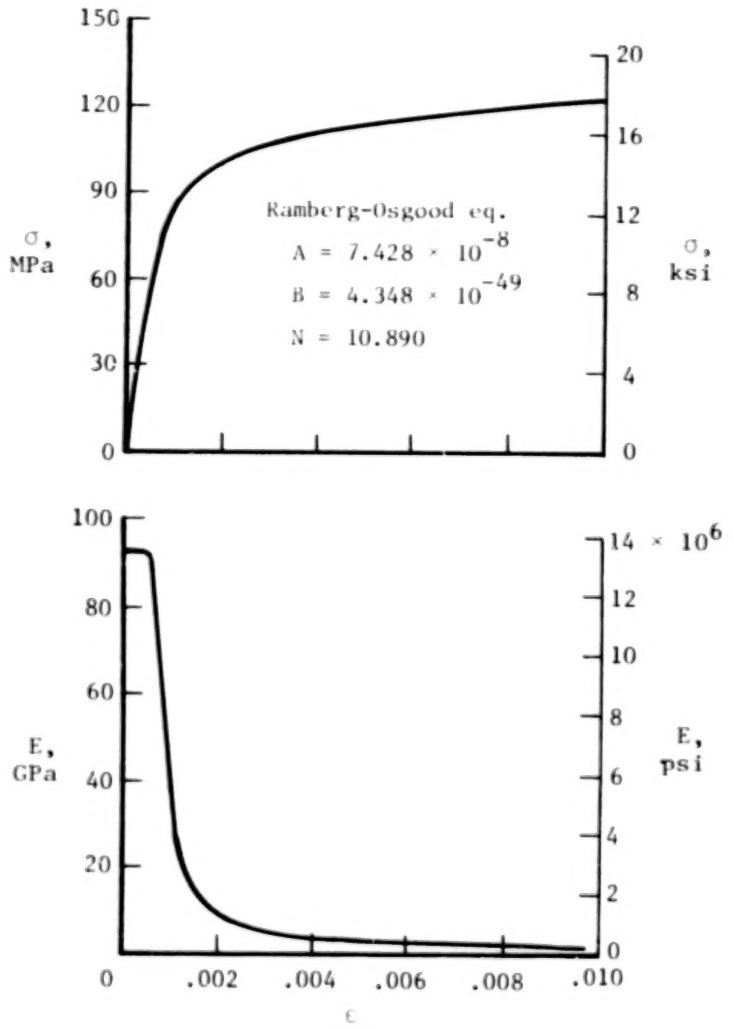

(f) $[(\pm 45)_2]_S$ laminate at 505 K (450°F).

Figure 13.- Continued.

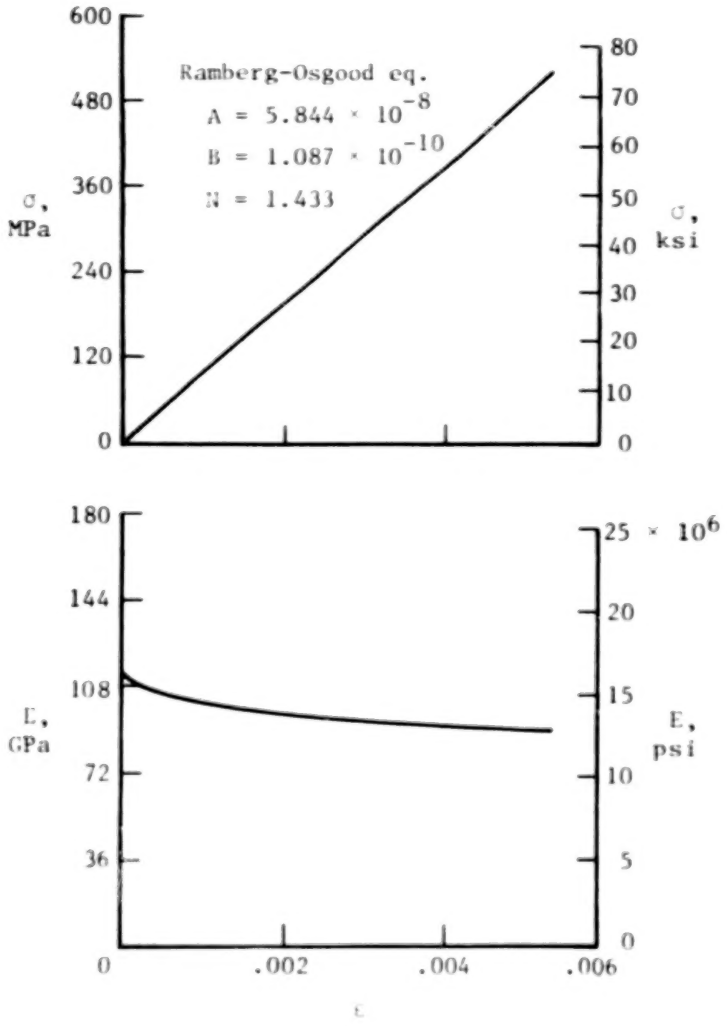

(g) $[90/0/90/0]_S$ laminate at room temperature.

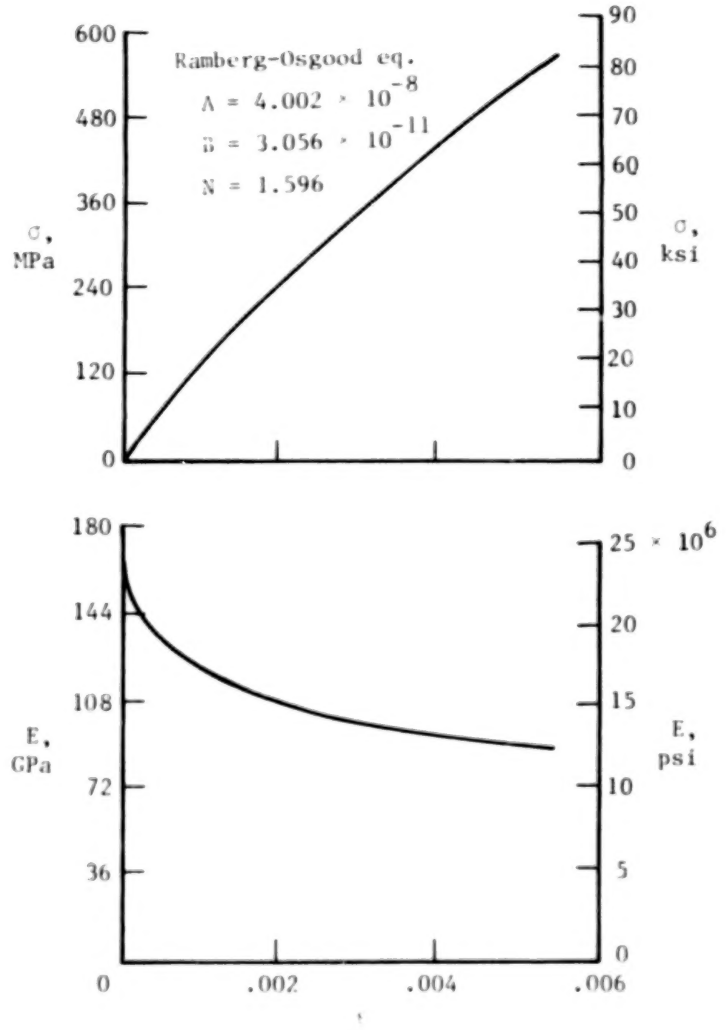

(h) $[90/0/90/0]_S$ laminate at 505 K (450°F).

Figure 13.- Continued.

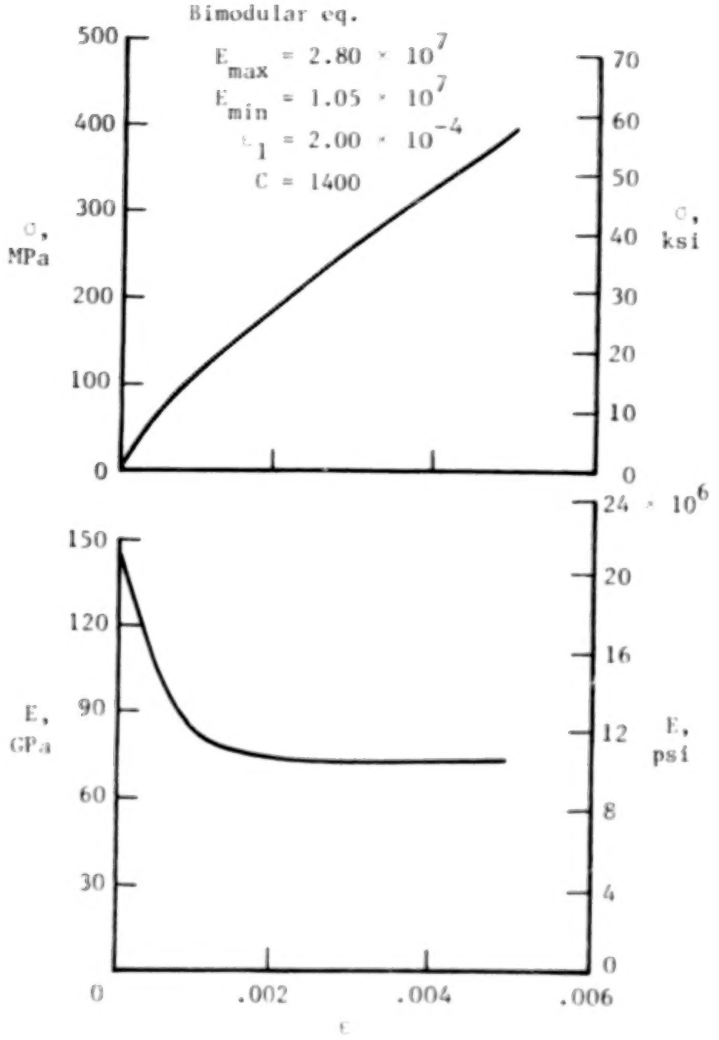

(i) $[0/\pm45]_S$ laminate at room temperature.

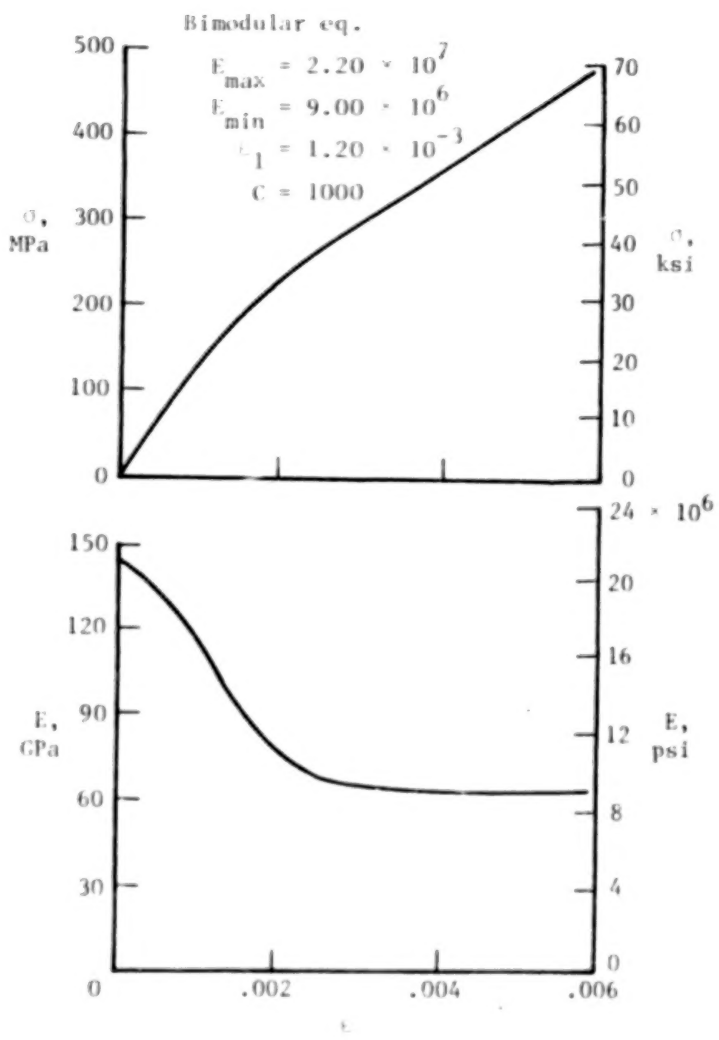

(j) $[0/\pm45]_S$ laminate at 505 K (450°F).

Figure 13.- Continued.

BLANK PAGE

BLANK PAGE

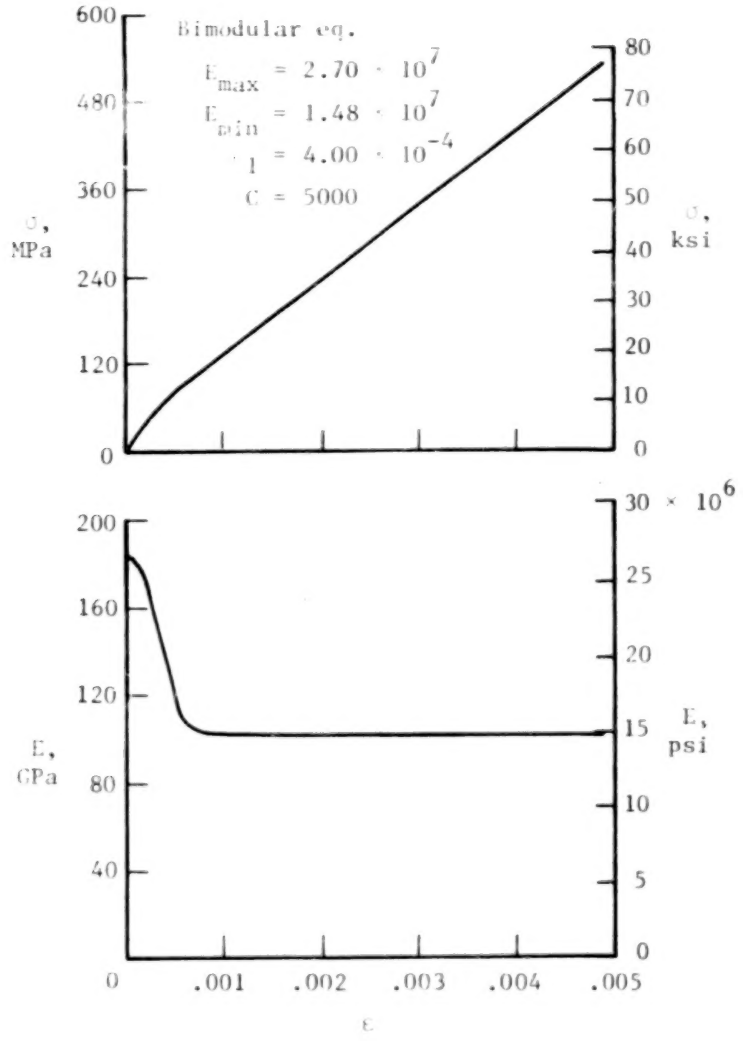

(k) $[0_2/\pm45]_S$ laminate at room temperature.

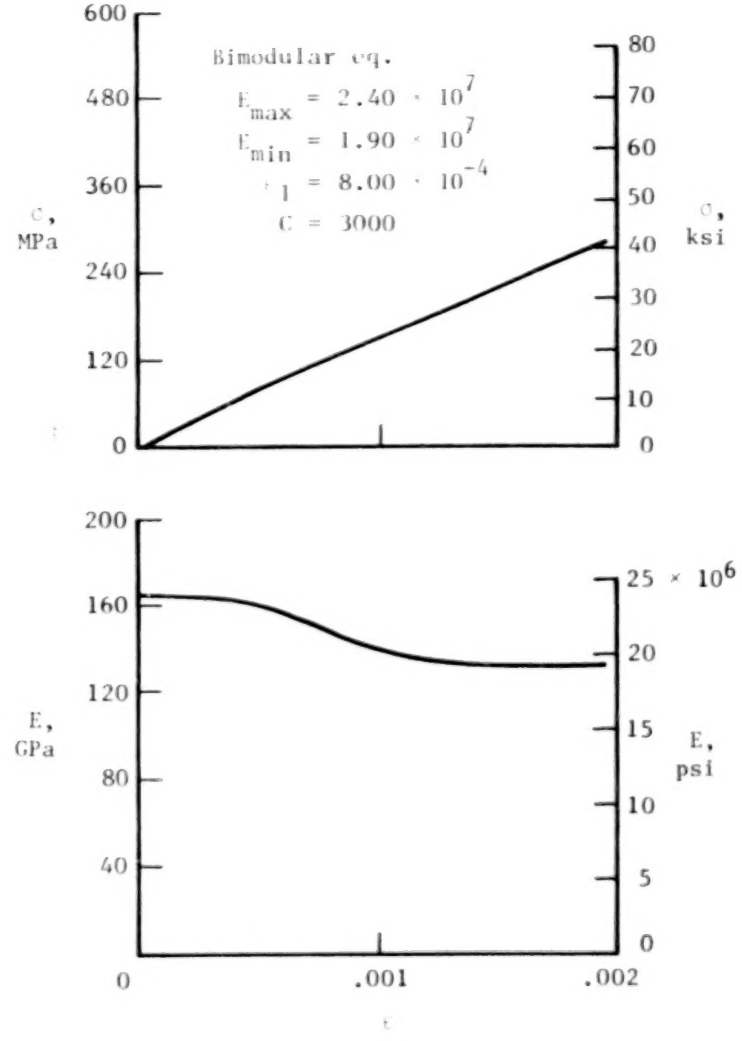

(l) $[0_2/\pm45]_S$ laminate at 505 K (450°F).

Figure 13.- Concluded.

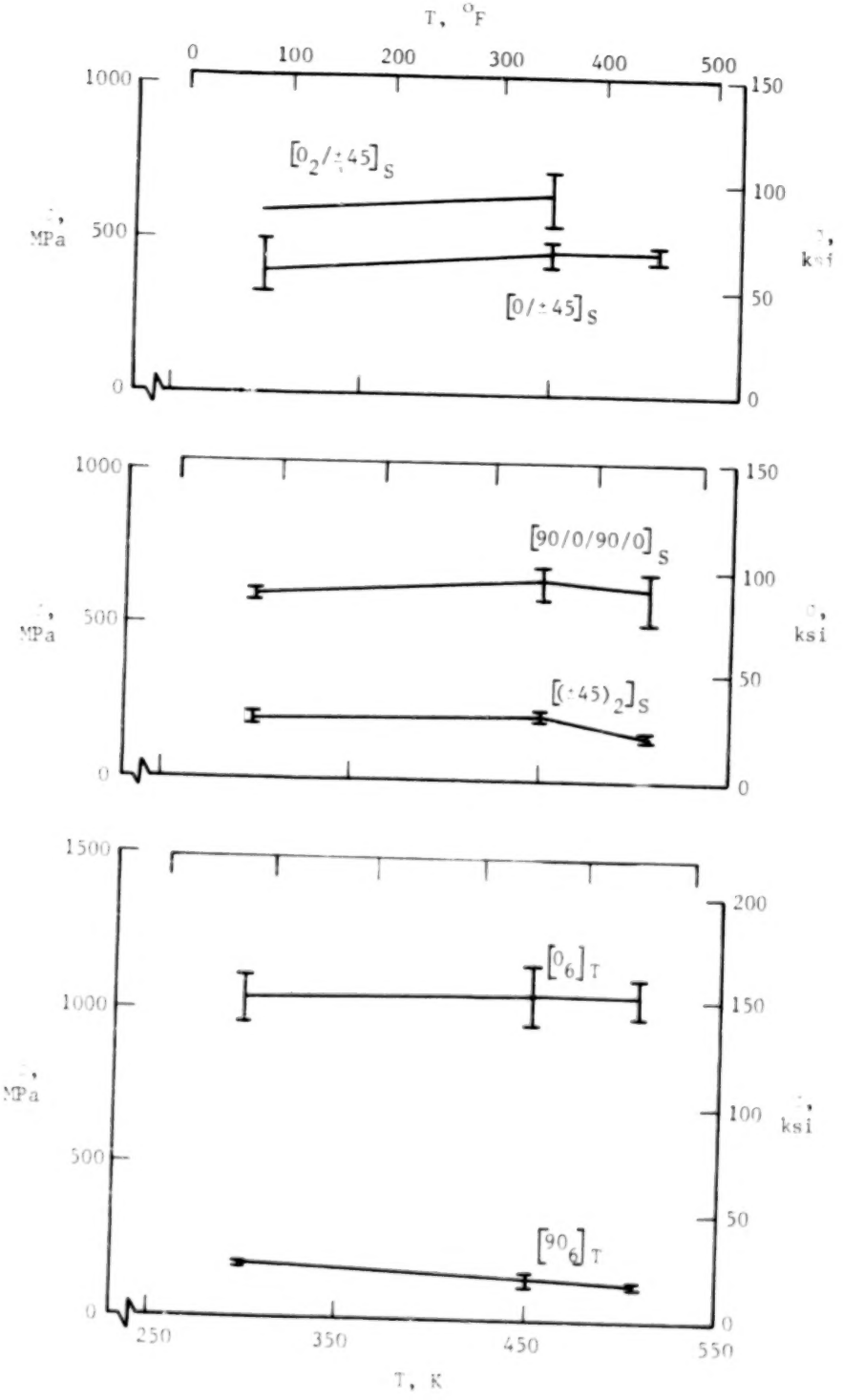

Figure 14.- Maximum tensile stress as a function of temperature from sandwich-beam tests.

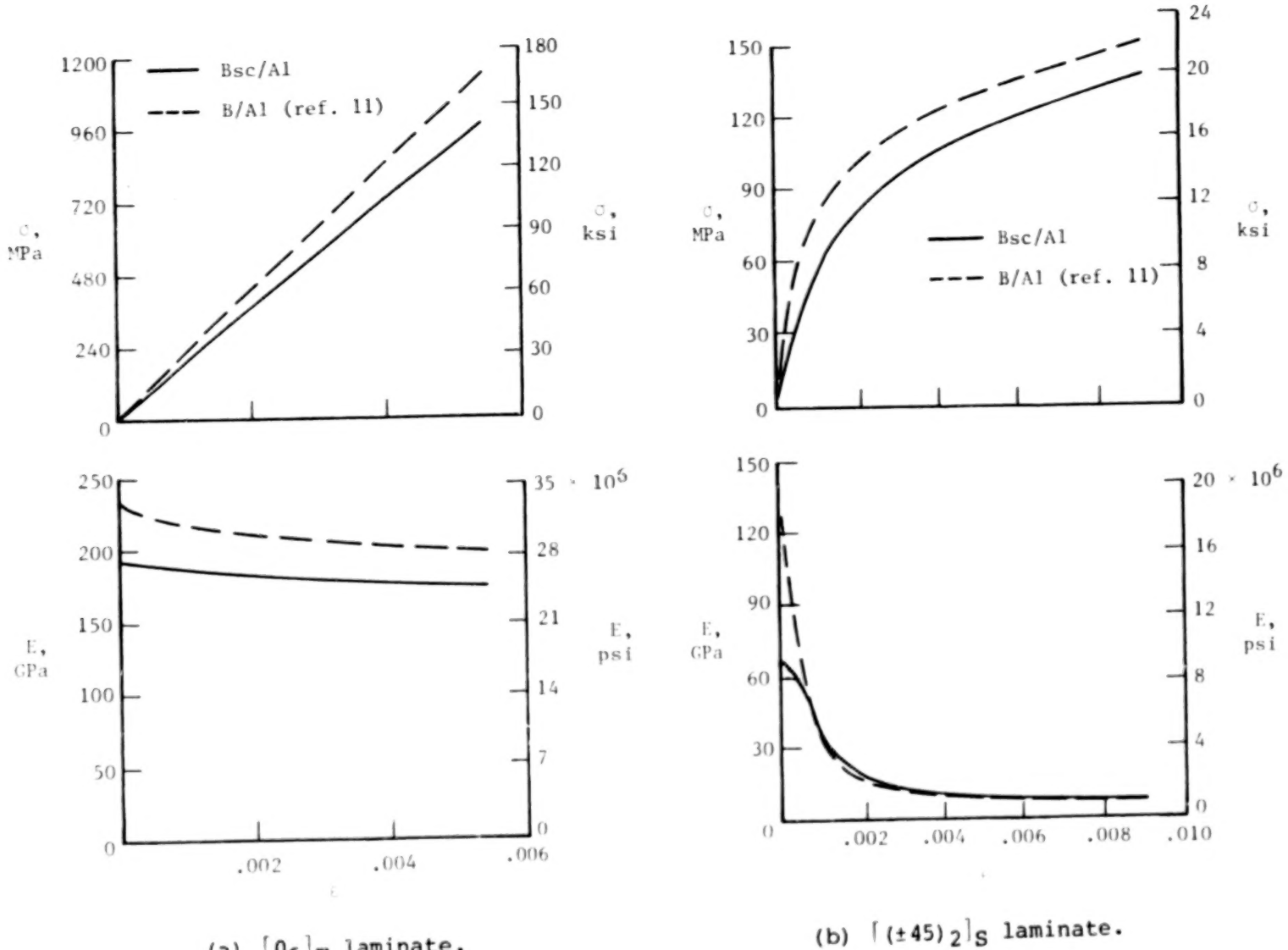

(a) $[0_6]_T$ laminate.

(b) $[(\pm 45)_2]_S$ laminate.

Figure 15.- Comparison between behavior of boron/aluminum and Bsc/Al laminate properties at room temperature.

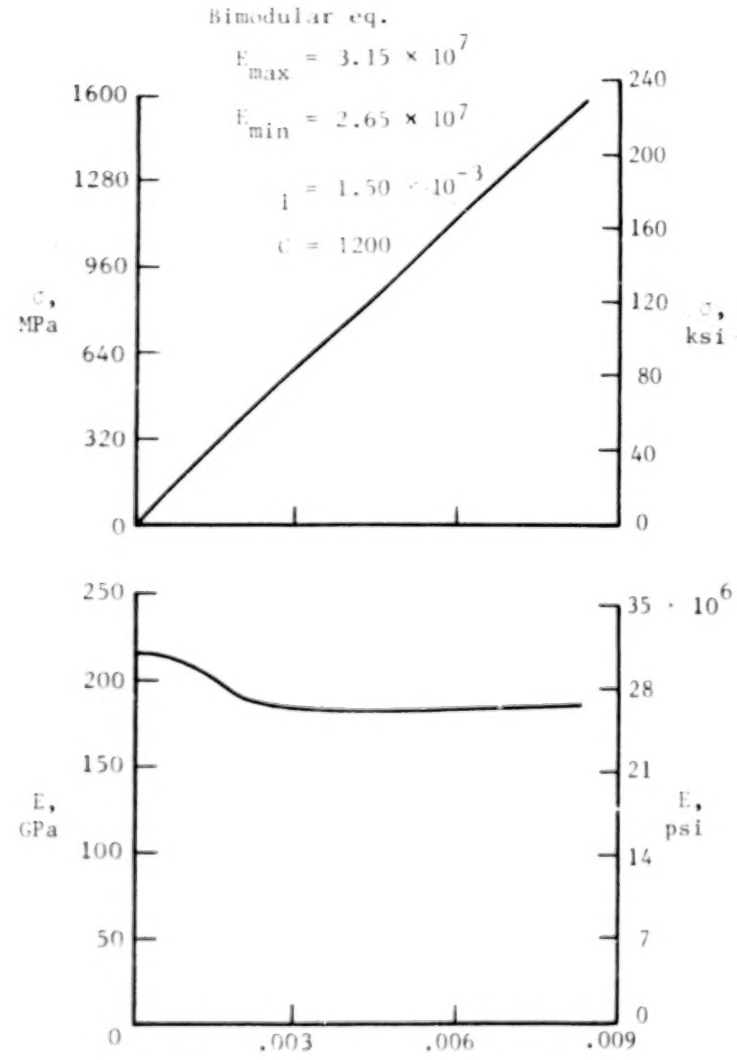

(a) $[0_6]_T$ laminate at room temperature.

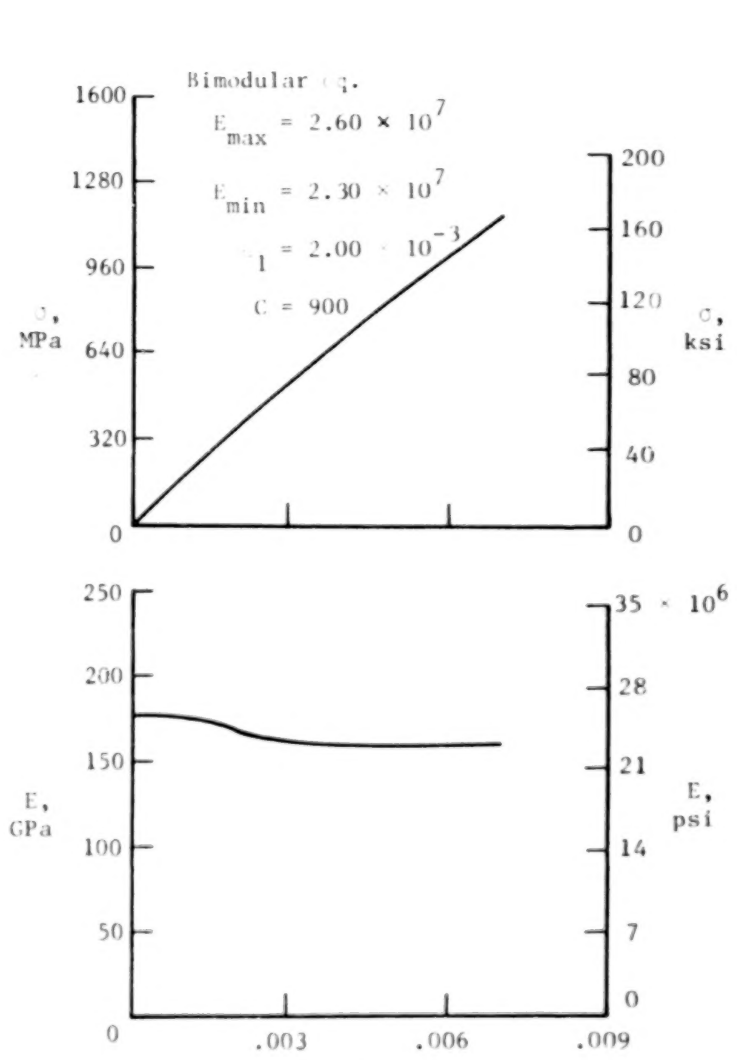

(b) $[0_6]_T$ laminate at 505 K (450°F).

Figure 16.- Stress and tangent modulus as a function of strain from sandwich-beam tests on Bsc/Al laminates in compression.

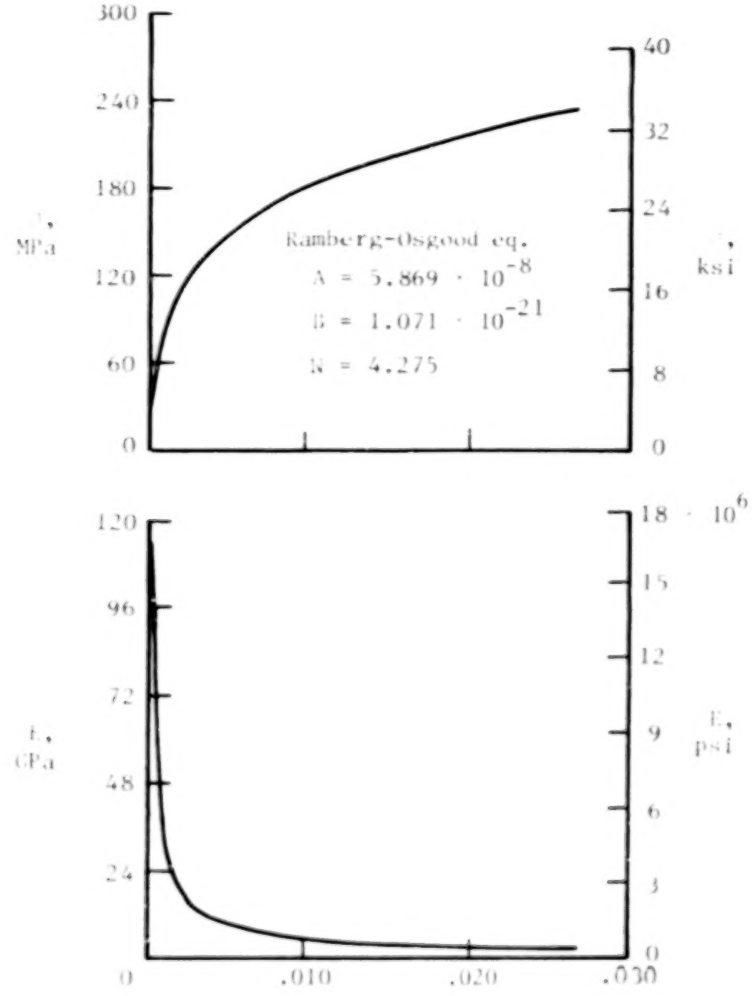

(c) $[90_6]_T$ laminate at room temperature.

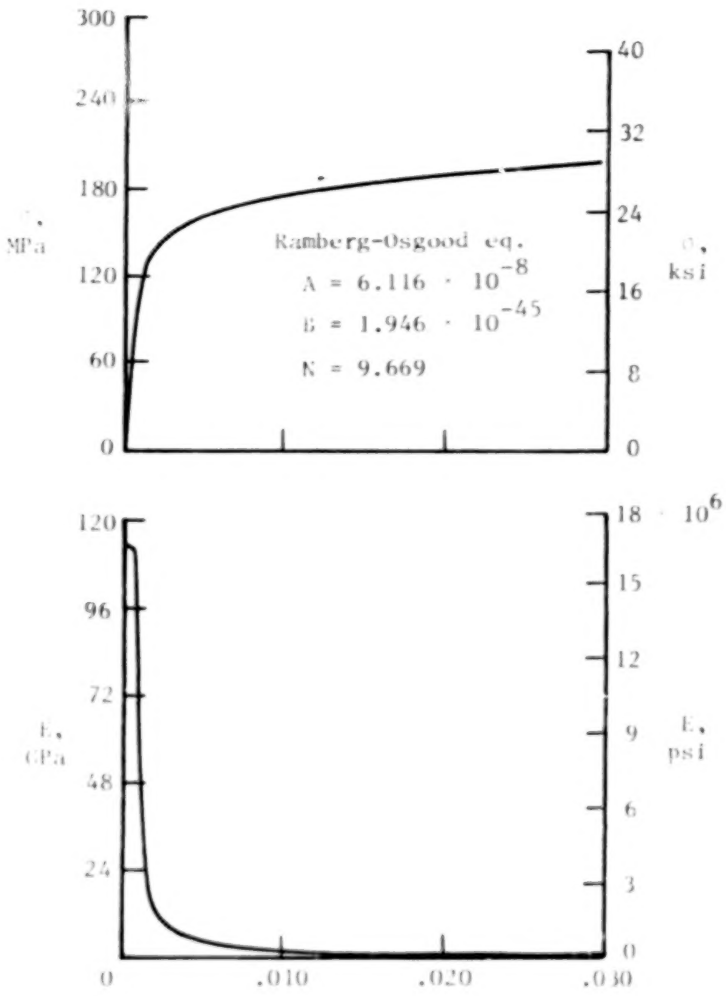

(d) $[90_6]_T$ laminate at 505 K (450°F).

Figure 16.- Continued.

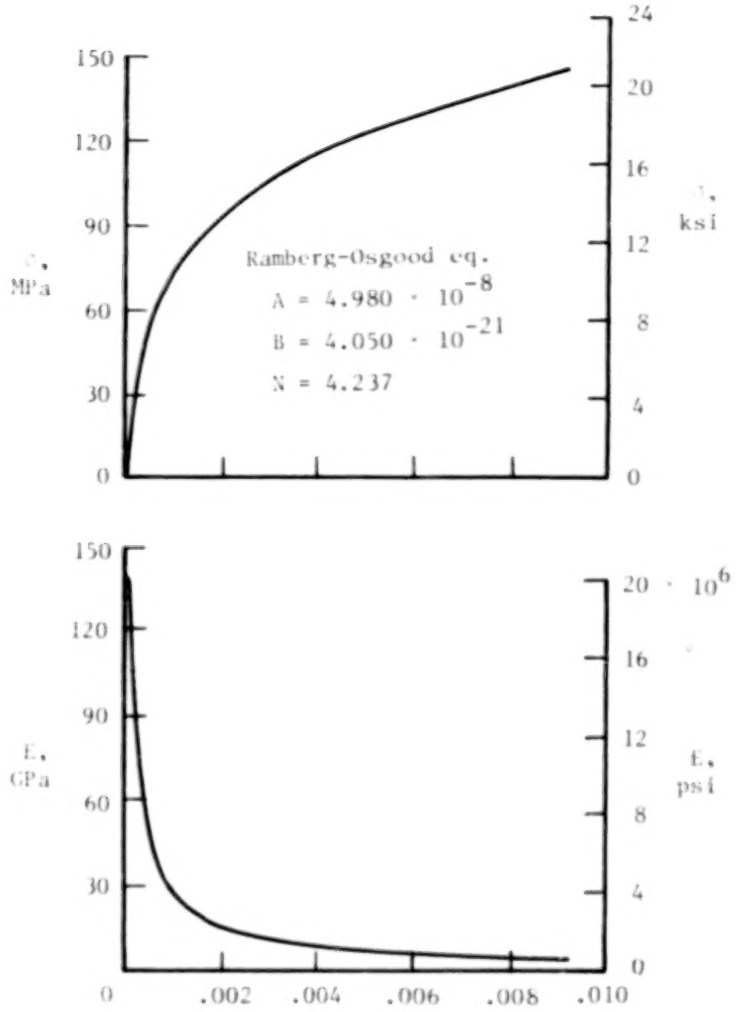

(e) $[(\pm 45)_2]_S$ laminate at room temperature.

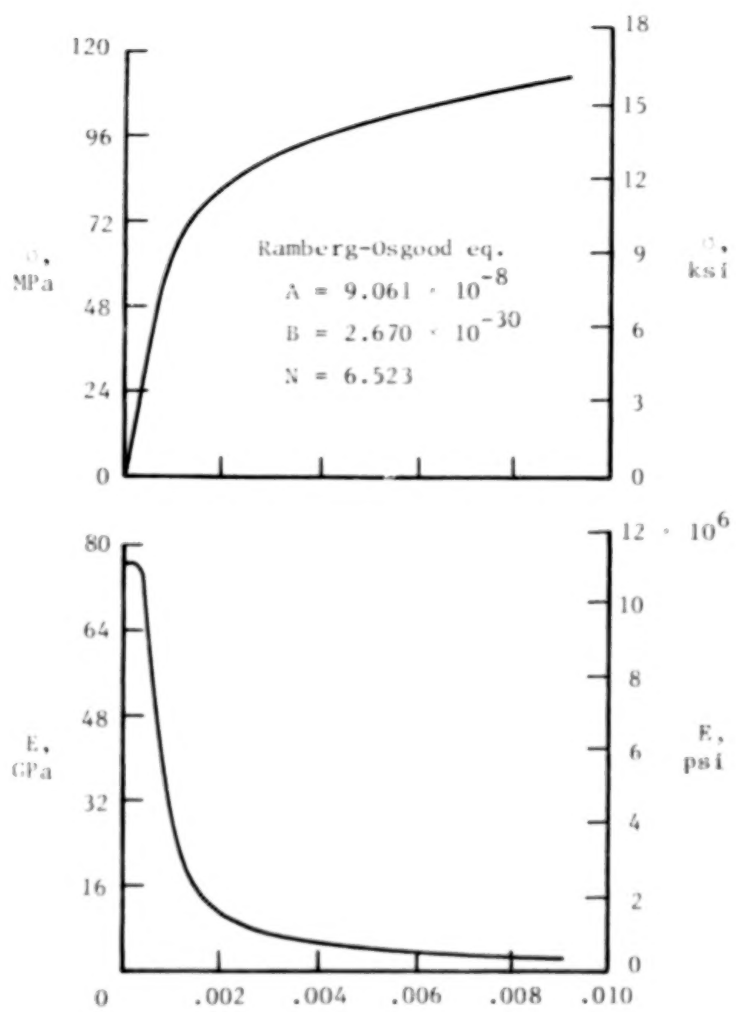

(f) $[(\pm 45)_2]_S$ laminate at 505 K (450°F).

Figure 16.- Continued.

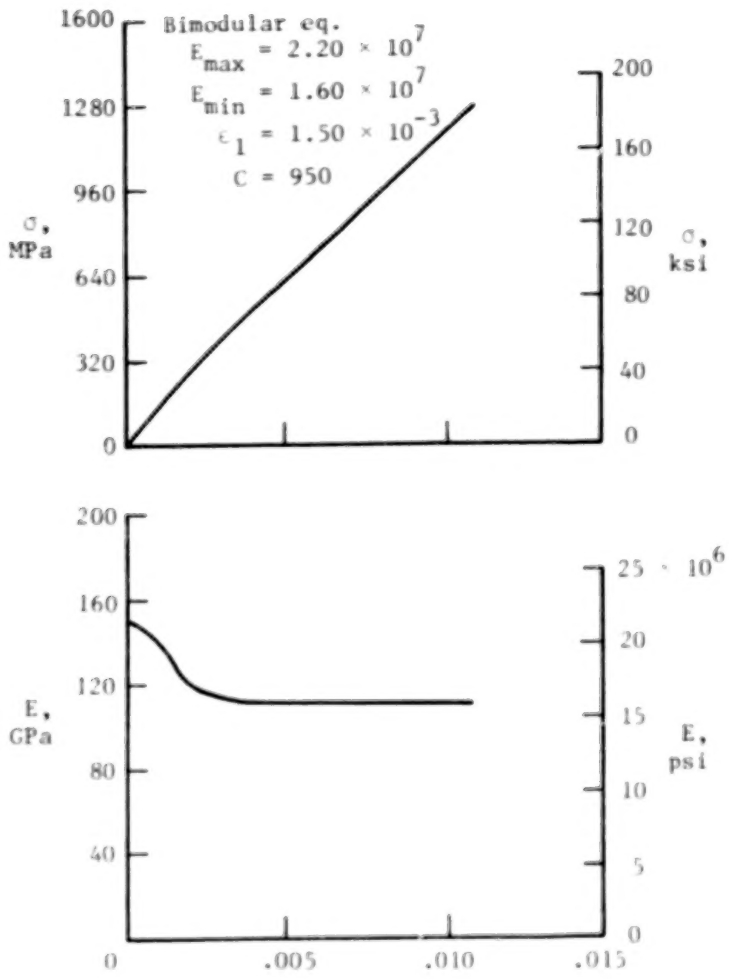

(g) $[90/0/90/0]_S$ laminate at room temperature.

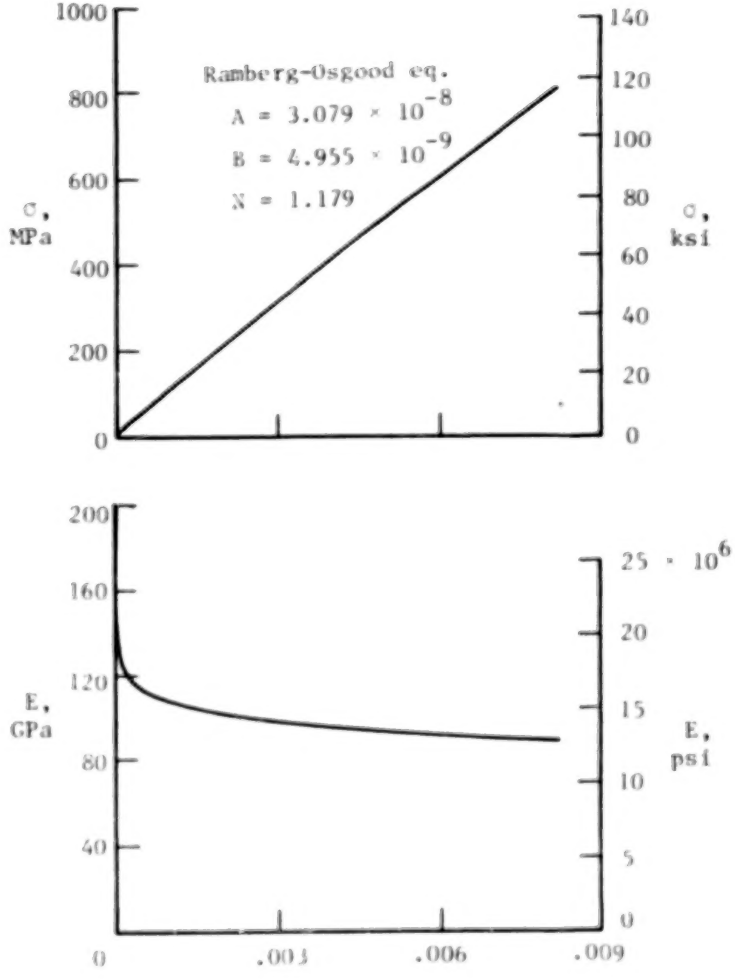

(h) $[90/0/90/0]_S$ laminate at 505 K (450°F).

Figure 16.- Continued.

BLANK PAGE

BLANK PAGE

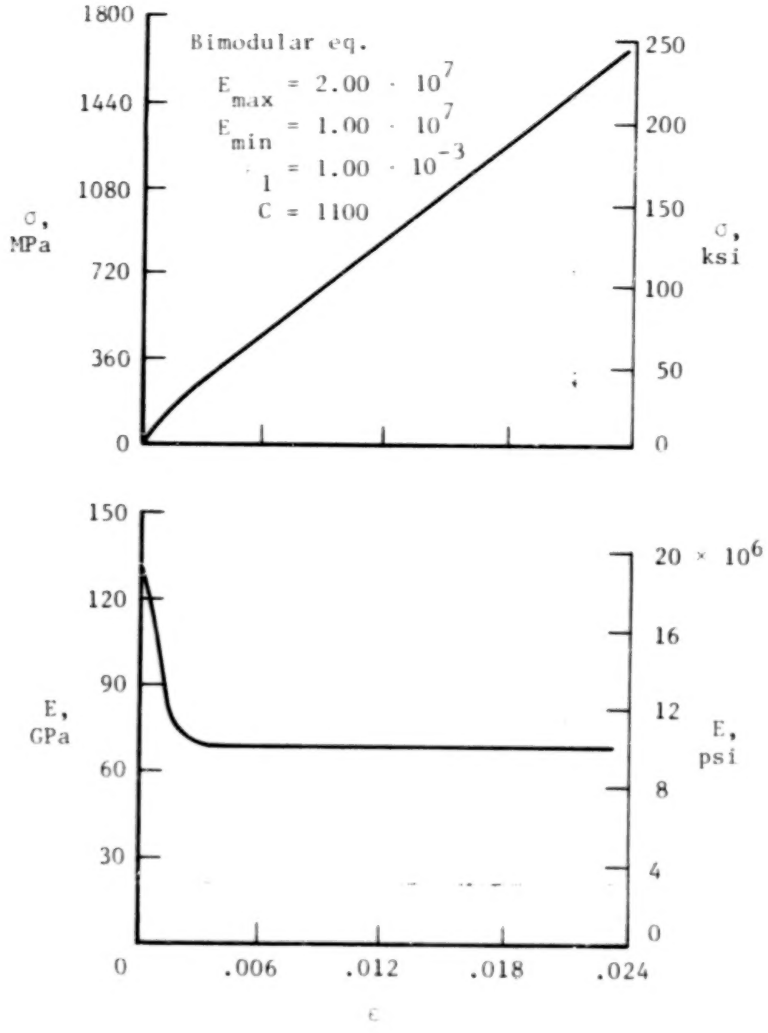

(i) $[0/\pm45]_S$ laminate at room temperature.

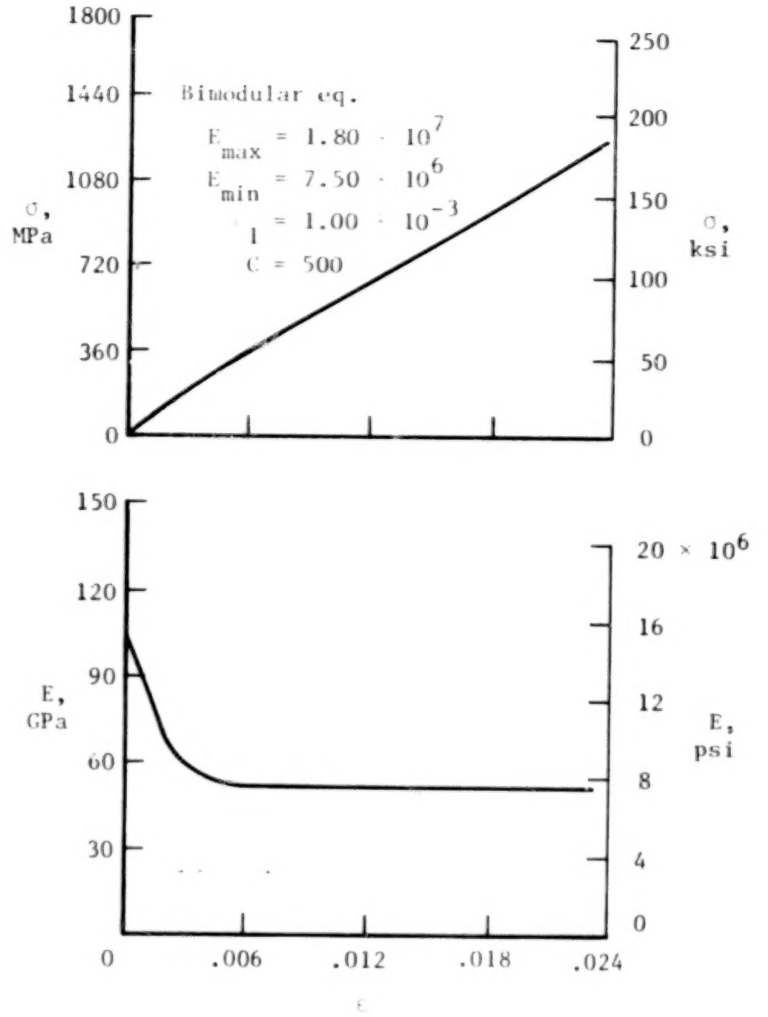

(j) $[0/\pm45]_S$ laminate at 505 K (450°F).

Figure 16.- Continued.

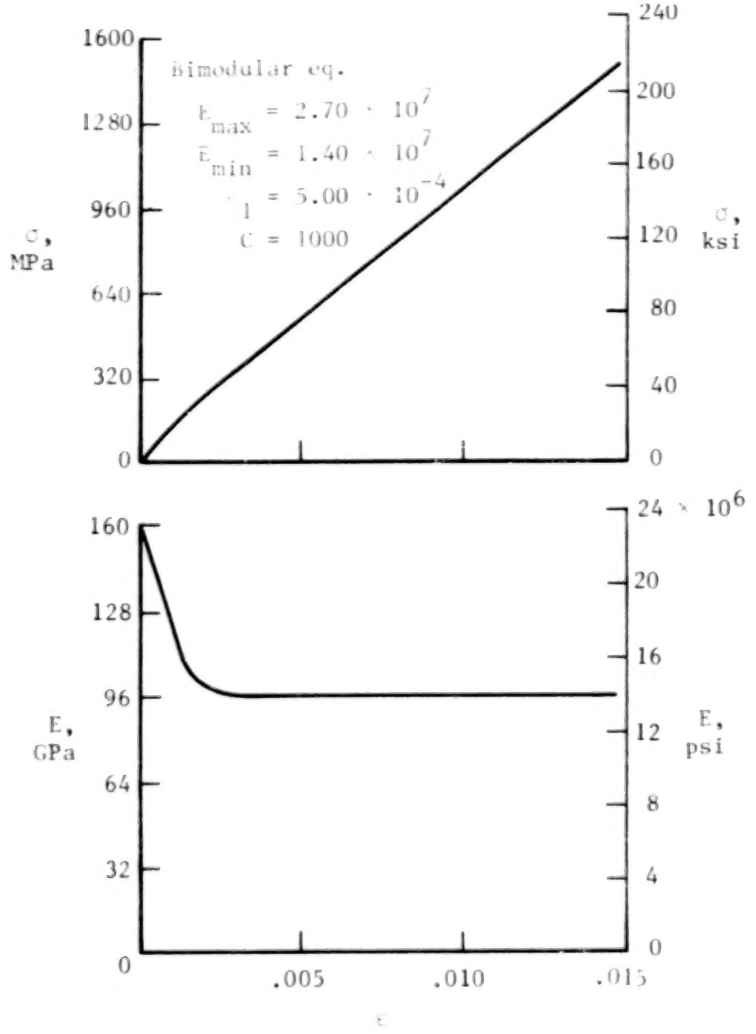

(k) $[0_2/\pm45]_S$ laminate at room temperature.

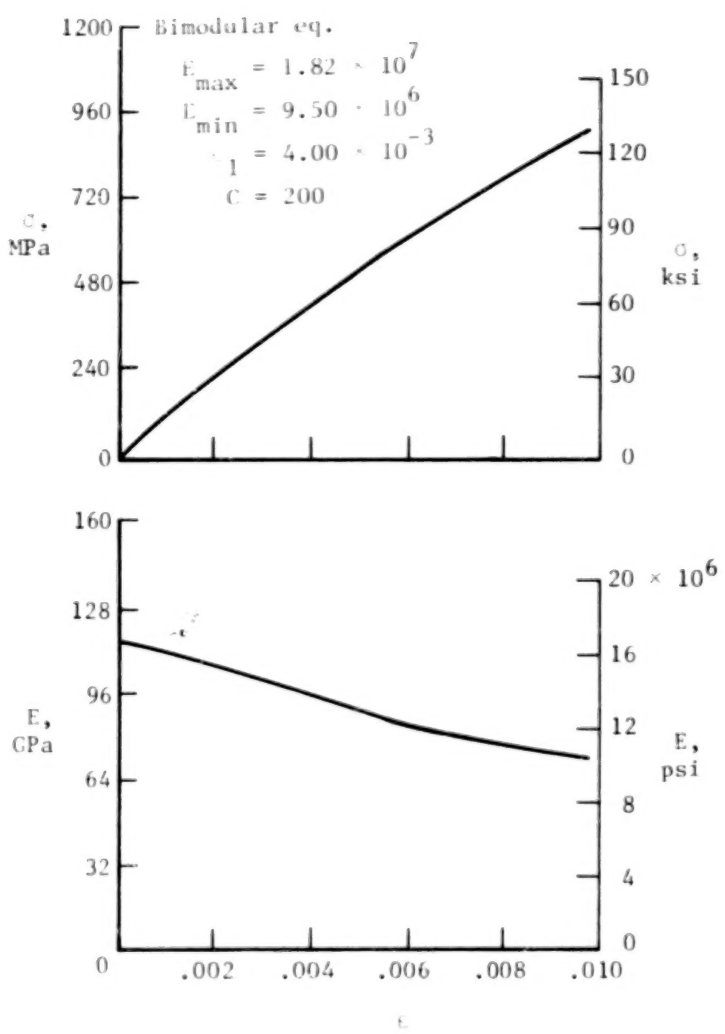

(l) $[0_2/\pm45]_S$ laminate at 505 K (450°F).

Figure 16.- Concluded.

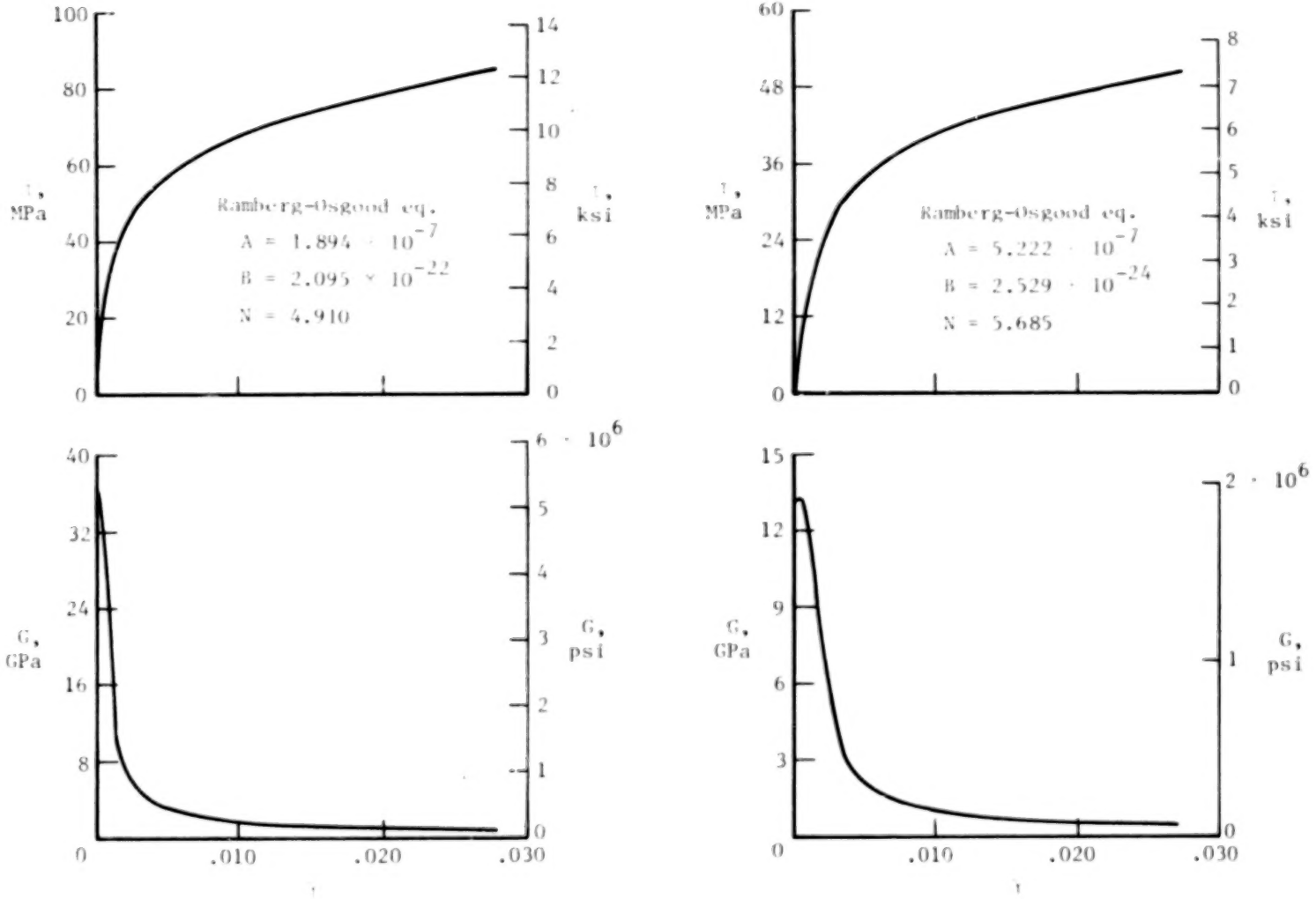

(a) $[0_6]_T$ laminate at room temperature.

(b) $[0_6]_T$ laminate at 505 K (450°F).

Figure 17.- Stress and tangent modulus as a function of strain from picture-frame shear tests on Bsc/Al laminates.

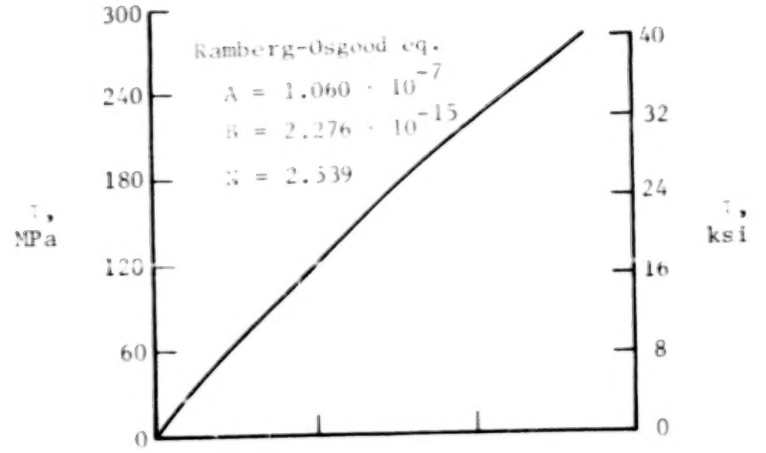

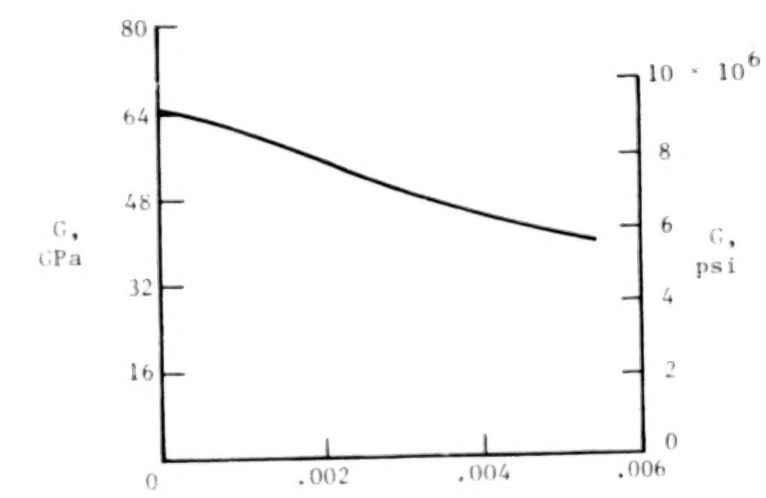

(c) $[(\pm 45)_2]_S$ at room temperature.

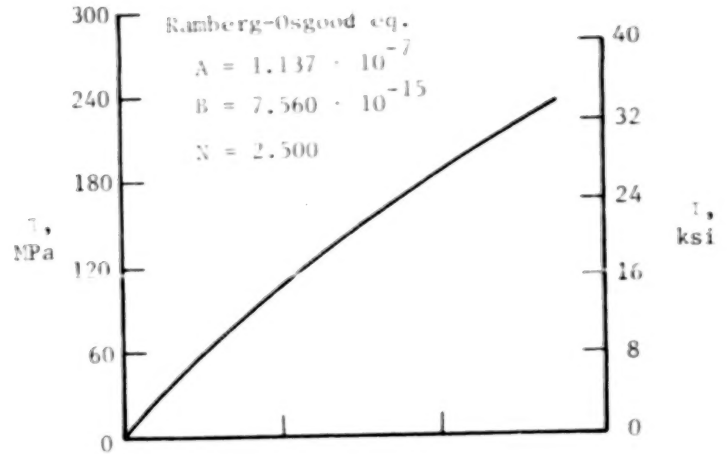

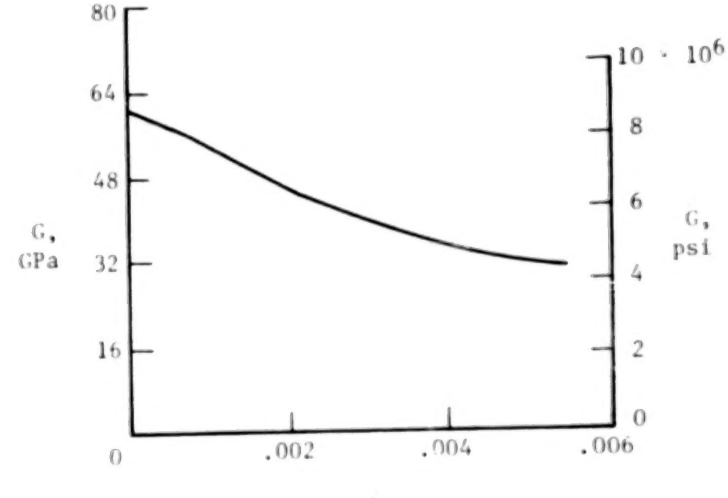

(d) $[(\pm 45)_2]_S$ at 505 K (450°F).

Figure 17.- Continued.

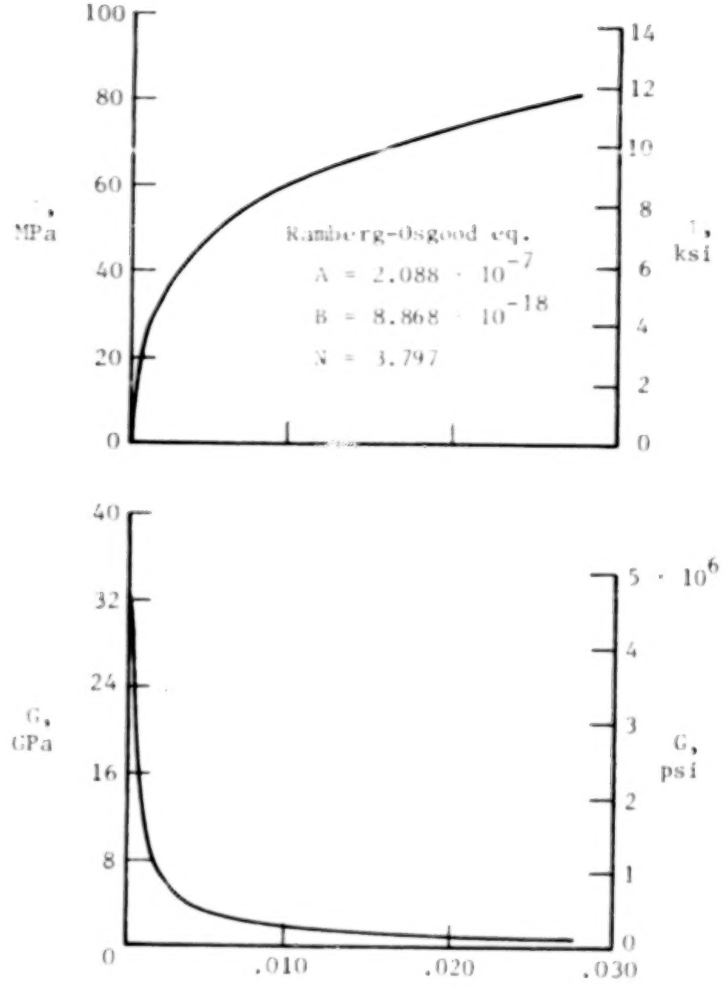

(e) $[90/0/90/0]_S$ laminate at room temperature.

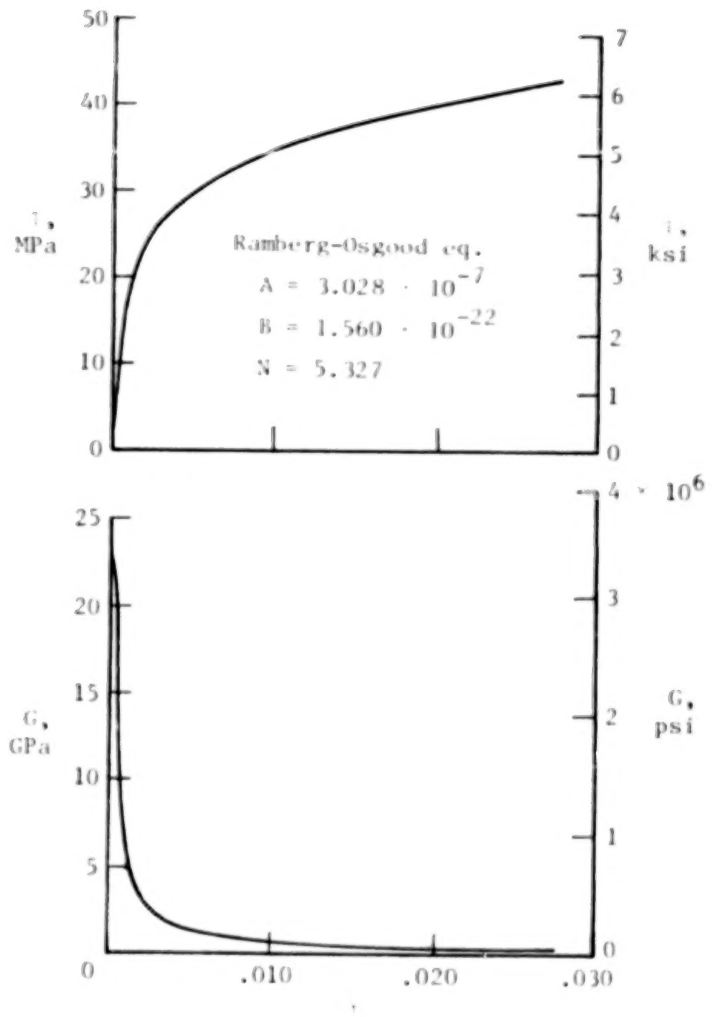

(f) $[90/0/90/0]_S$ laminate at 505 K (450°F).

Figure 17.- Continued.

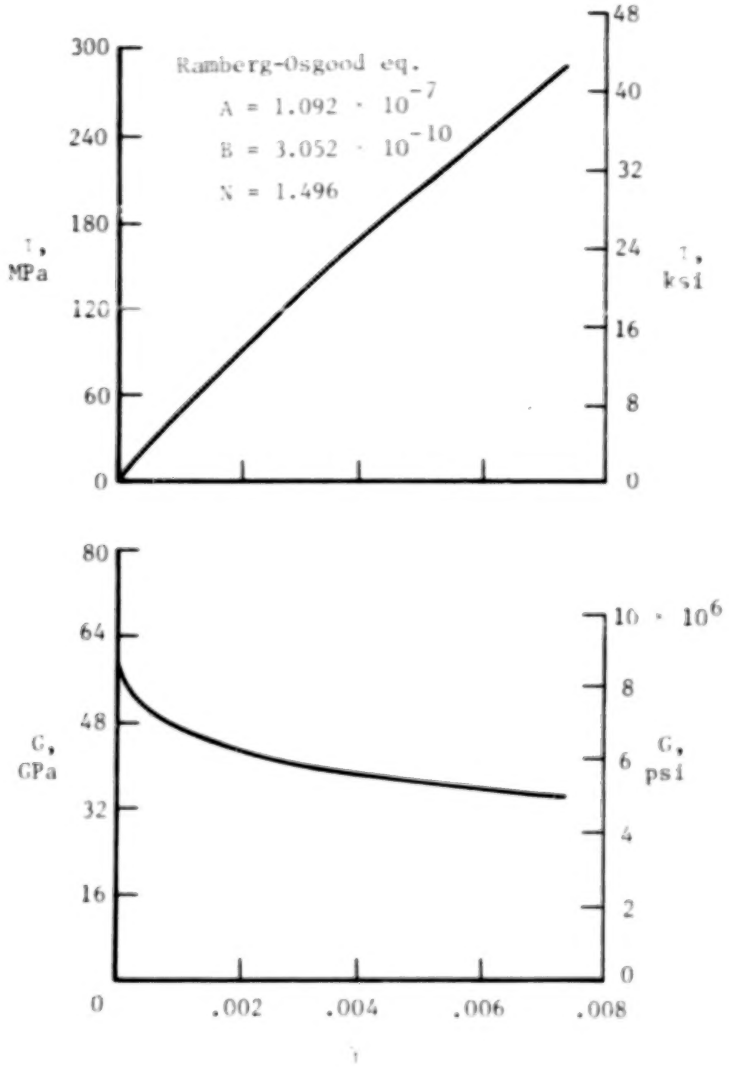

(g) $[0/\pm45]_S$ laminate at room temperature.

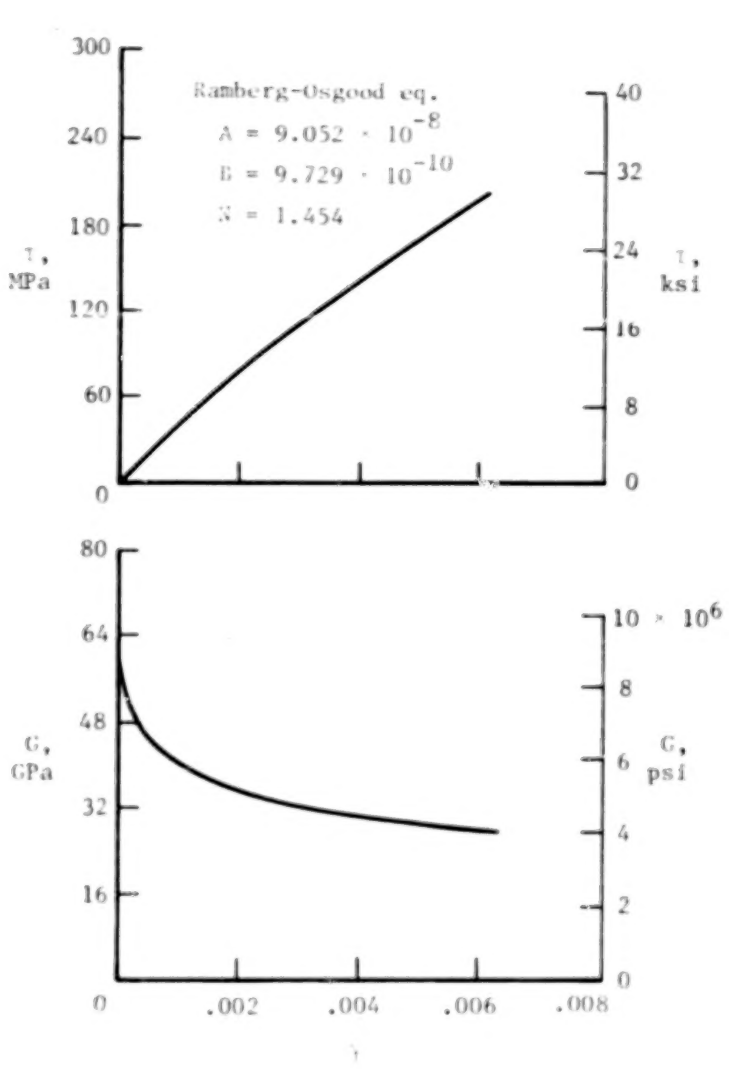

(h) $[0/\pm45]_S$ laminate at 505 K (450°F).

Figure 17.- Continued.

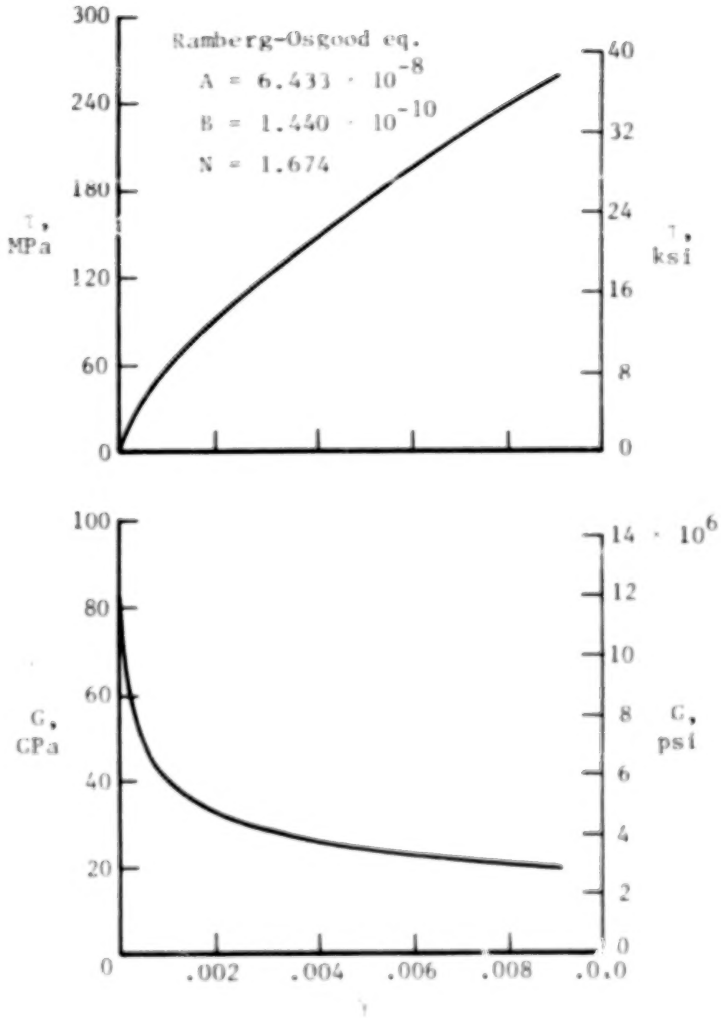

(i) $[0_2/\pm45]_S$ laminate at room temperature.

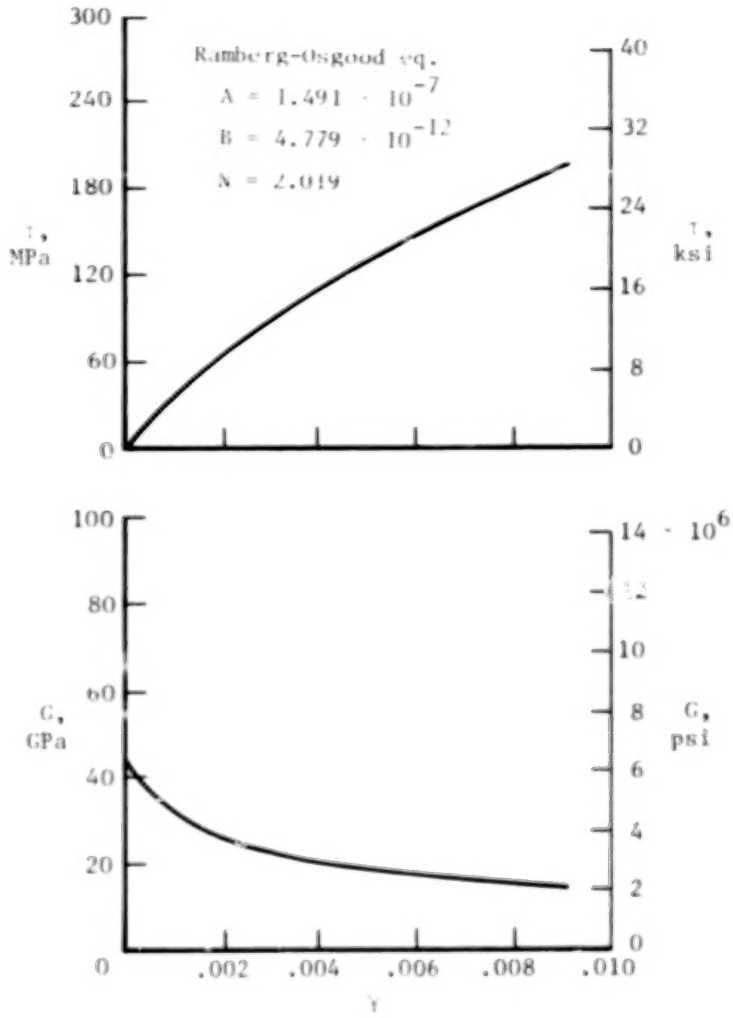

(j) $[0_2/\pm45]_S$ laminate at 505 K (450°F).

Figure 17.- Concluded.

CONTENTS

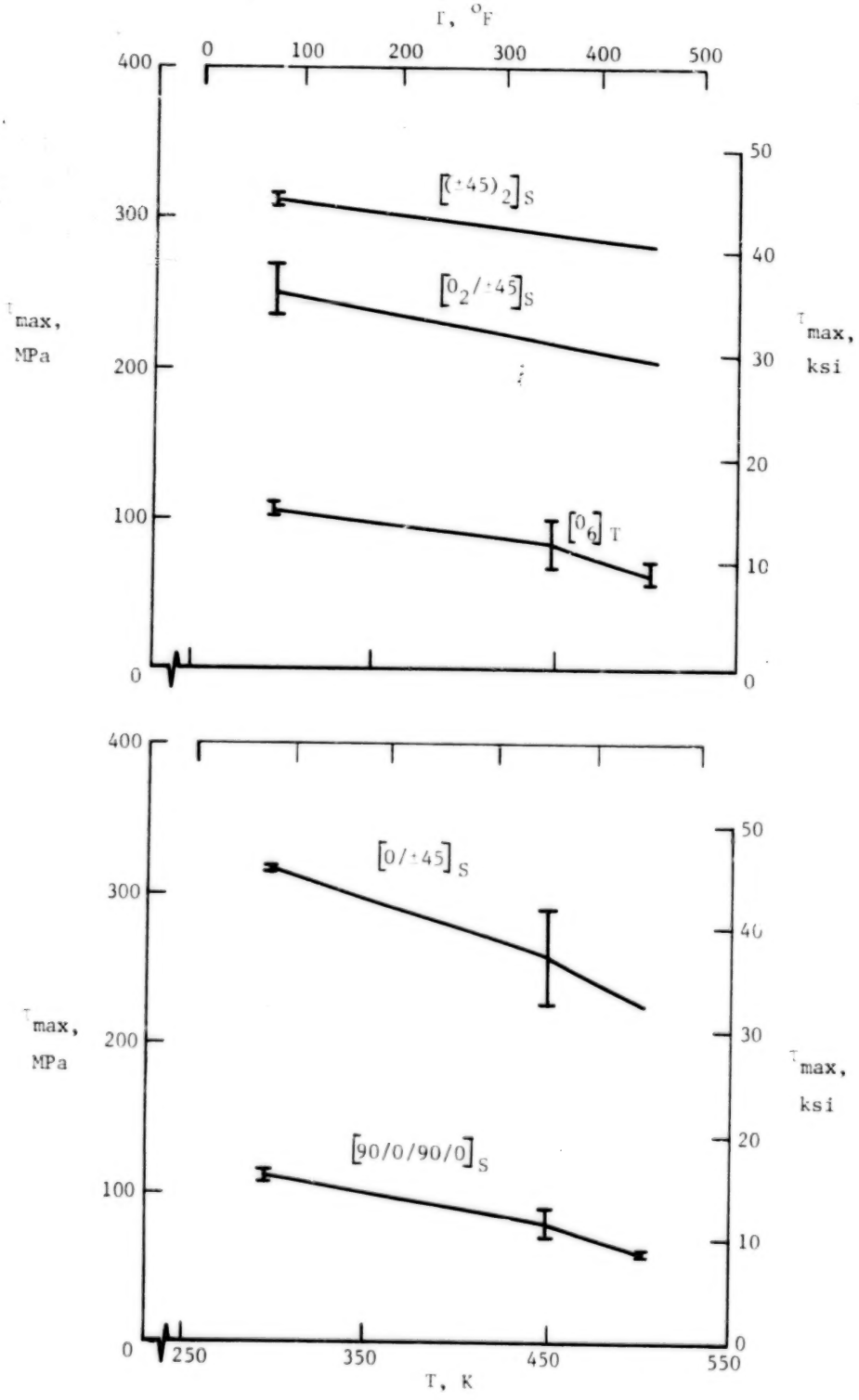

Figure 18.- Maximum shear stress as a function of temperature from picture-frame shear tests.

1. Report No. NASA TP-1761	2. Government Accession No.	3. Recipient's Catalog No.
4. Title and Subtitle MECHANICAL PROPERTY CHARACTERIZATION OF BORSIC®/ ALUMINUM LAMINATES AT ROOM AND ELEVATED TEMPERATURES		5. Report Date December 1980 6. Performing Organization Code 533-01-13-06
7. Author(s) Robert R. McWithey and Dick M. Royster		8. Performing Organization Report No. L-13763 10. Work Unit No.
9. Performing Organization Name and Address NASA Langley Research Center Hampton, VA 23665		11. Contract or Grant No. 13. Type of Report and Period Covered Technical Paper
12. Sponsoring Agency Name and Address National Aeronautics and Space Administration Washington, DC 20546		14. Sponsoring Agency Code

15. Supplementary Notes

16. Abstract

Six Borsic®/aluminum laminate orientations ($[0_6]_T$, $[90_6]_T$, $[(\pm 45)_2]_S$, $[90/0/90/0]_S$, $[0/\pm 45]_S$, and $[0_2/\pm 45]_S$) exposed to a braze-temperature cycle were tested in tension, compression, and shear to determine tangent modulus, maximum stress and strain, and Poisson's ratio of the laminates at room and elevated temperatures. Mechanical properties in tension were determined from flat-tensile and sandwich-beam tests. Room-temperature flat-tensile tests were performed on laminates in the "as-received" condition to compare with specimens exposed to a braze-temperature cycle. Sandwich-beam tests were also used to determine mechanical properties in compression. Shear properties were determined from biaxially loaded, picture-frame shear specimens. Test results are presented by using functional relations between stress and strain and tangent modulus and strain, and in tables by indicating maximum stress and strain and Poisson's ratio.

17. Key Words (Suggested by Author(s))

Composite materials
Borsic/aluminum
Material properties
Stress-strain curves
Elevated temperature
Braze-temperature cycle

18. Distribution Statement

Unclassified - Unlimited

Subject Category 24

19. Security Classif. (of this report)	20. Security Classif. (of this page)	21. No. of Pages	22. Price
Unclassified	Unclassified	63	A04

For sale by the National Technical Information Service, Springfield, Virginia 22161

NASA-Langley, 1980

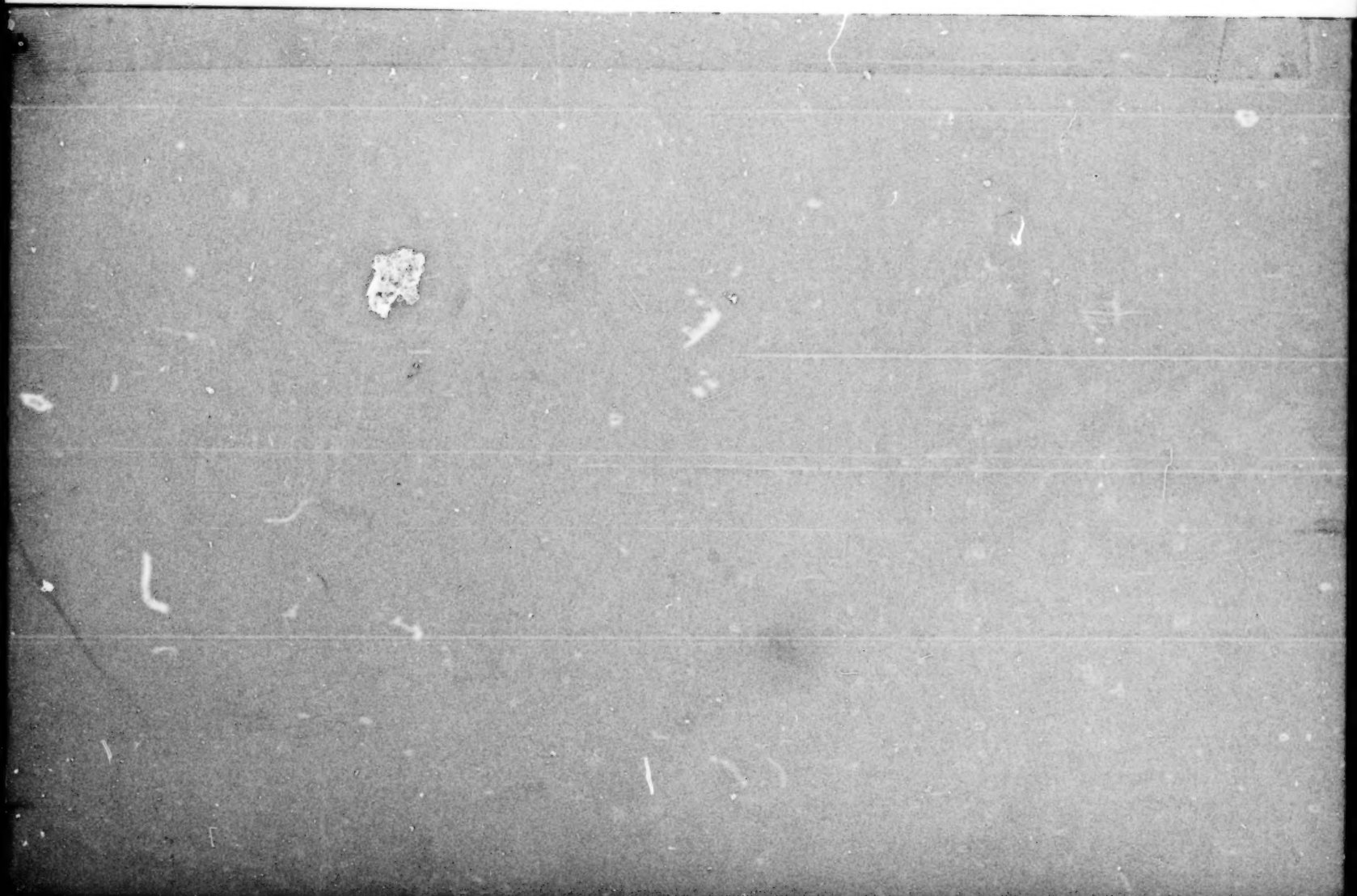

END

February 27, 1981